Development of a small molecule BAG1 inhibitor for estrogen receptor positive breast cancer therapy

Zur Erlangung des akademischen Grades eines

DOKTORS DER NATURWISSENSCHAFTEN

(Dr. rer. nat.)

von der KIT-Fakultät für Chemie und Biowissenschaften

des Karlsruher Instituts für Technologie (KIT)

genehmigte

DISSERTATION

von

Mengwu Pan, M.Sc.

aus Hubei, China

1. Referent: apl. Prof. Dr. Andrew Cato

2. Referent: Prof. Dr. Martin Bastmeyer

Tag der mündlichen Prüfung: 24.10.2022

Erklärung

Eidesstattliche Erklärung Hiermit erkläre ich, dass ich diese Dissertation eigenständig angefertigt habe. Ich habe nur die angegebenen Quellen und Hilfsmittel verwendent und mich keener unzulässigen Hilfe Dritter bedient. Wörtlich oder inhaltlich übernommenes Gedankengut als solches gekennzeichnet. Die Satzung des Karlsruher Instituts für Technologie (KIT) zur Sicherung guter wissenschaftlicher Praxis habe ich in die gültigen Fassung beachtet. Ich versichere außer- dem, dass diese Arbeit in gleicher oder ähnlicher Form noch keiner Prüfungsbehörde vorgelegt wurde.

Datum: _____ Unterschrift: _____

ABSTRACT

Breast cancer is one of the most frequently diagnosed cancer in women. It is estimated that one in eight women would potentially develop invasive breast cancer over the course of their lifetime. The largest breast cancer subgroup known is defined by estrogen receptor-positivity (ER^+). Multiple ER-directed hormone therapies have therefore been developed and are still being actively used clinically for the treatment of breast cancer. However, accumulated evidence demonstrate that hormone therapies inevitably trigger hormone resistance and there is tumor remission in up to 20% of the treated patients. To overcome the hormone resistance, novel therapies targeting the ER through hormone-independent mechanisms are required. One of these mechanisms is through the cochaperone BAG1 that is highly expressed in ER^+ breast cancers and plays a role in the activation of ER signaling pathway in breast tumor progression. Thus, targeting BAG1 would represents a novel indirect strategy for targeting the ER in the treatment of breast cancer. In my work, a compound with an imidazopyridine-based scaffold termed X15695 was identified as a selective BAG1 inhibitor. This compound exerted a potent growth inhibitory effect on ER^+ breast cancer cells and was superior to tamoxifen used in adjuvant therapy in combination with the chemotherapeutic drug Doxorubicin. X15695 worked similarly to the classical ER selective down-regulator fulvestrant in promoting ER degradation. Genome-wide transcriptomic data identified X15695 as an inhibitor of ER signaling pathway in ER^+ breast cancer cells. Additionally, X15695 activated p53 signaling pathway via two independent mechanisms: i), promoted nuclear accumulation of p53 via disruption of a cytoplasmic mortalin-p53 complex; ii), released nuclear p53 from p53-ER complex for the activation of downstream targets. Furthermore, X15695 inhibited cell cycle progression and induced cell apoptosis of ER^+ breast cancers cells. X15695 was also shown to be a potent proliferation inhibitor of tamoxifen resistant ER^+ breast cancer cells, which provides strong evidence for this compound to overcome therapy-induced hormone resistance.

Zusammenfassung

Brustkrebs gehört zu den am Häufigsten diagnostizierten Krebsarten bei Frauen. Schätzungsweise erkrankt jede achte Frau im Laufe ihres Lebens an invasivem Brustkrebs. Die größte Untergruppe von Mammakarzinomen ist gekennzeichnet durch die Expression des Estrogen-Rezeptors (ER). Daher wurde eine Vielzahl von Hormontherapien, die gegen den ER gerichtet sind, entwickelt, welche bis heute zur Behandlung von Brustkrebs in der Klinik verwendet werden. Allerdings führen diese Therapien unausweichlich zu einer Hormonresistenz und so treten Tumor-Rezidive in rund 20% der behandelten Patienten auf. Die Entwicklung neuartiger Therapien, die die ER-Aktivität durch andere Mechanismen hemmen ist daher von großer medizinischer Bedeutung, um Hormonresistenzen zu überwinden. Eine potentielle, neuartige Strategie hierzu stellt die Inhibierung des Cochaperons BAG1 dar, welches in ER-positiven (ER^+) Brustkrebszellen hoch exprimiert wird und eine wichtige Rolle in der Aktivierung von ER-Signalwegen während der Brustkrebsprogression spielt. In dieser Arbeit wurde eine Substanz mit einer Imidazopyridin-basierten Grundstruktur, X15695, als selektiver BAG1 Inhibitor identifiziert. Diese Substanz zeigte einen starken wachstumshemmenden Effekt in ER^+-Brustkrebszellen, sowie eine bessere inhibitorische Wirkung als Tamoxifen, ein in der adjuvanten Therapie in Kombination mit dem Chemotherapeutikum Doxorubicin eingesetzter Estrogenrezeptormodulator. Weiterhin fördert X15695 die Degradation des ER ähnlich dem klassischen ER Inhibitor Fulvestrant. Genom-weite Transkriptionsanalysen identifzierten X15695 als einen Inhibitor des ER-Signalwegs in ER^+-Brustkrebszellen. Zusätzliche aktiviert X15695 den p53 Signalweg durch zwei unabhängige Mechanismen: i) Förderung der nukleären Akkumulation von p53 durch Auflösen des cytoplasmatischen Mortalin-p53 Komplexes; ii) Freigabe von p53 aus dem p53-ER Komplex zur Aktivierung entsprechender Zielgene. Weiterhein inhibiert X15695 die Zellzyklus-Progression und induziert Apoptose von ER^+-Brustkrebszellen. Außerdem war X15695 in der Lage die Proliferation von Tamoxifen-resistenten ER^+-Brustkrebszellen zu inhibieren. Diese Ergebnisse liefern starke Hinweise darauf, dass X15695 für die Behandlung therapie-resistenter Brustkrebspatienten weiterentwickelt werden könnte.

Acknowledgement

It is my belief that a PhD career cannot define who I am but it will extensively shape who I am going to be. The past four years of my life have rapidly been changed by events going down and up again. Those changes, I believe, have positively promoted my personal development. As tree growth requires sunlight and water, my personal PhD life also requires massive input in terms of time and efforts, which are enormous demands on the people around me. Therefore, I would like to thank them for their understanding and support.

Andrew Cato is a great and kind mentor who supervised me to finish this work. He started to this supervision after I have struggled for over two and half years. Although the time we spent together is short, the wisdom and kindness he showed me will live with me indefinitely. I cannot image how much pressure he must have faced to help me finish my PhD as I had zero background knowledge to start this work. I can vividly recall the many occasions he sent me reading materials and discussions we had over and over again to help me familiarize myself with the research topic. Certainly, I cannot forget the nights, the weekends, the holidays and even his vacations that he sacrificed to supervise my work. It is his unlimited supervision that eventually helped get me this far. As a supervisor, he is more like a friend who never considers my questions and thoughts as a sort of challenge to his authority. Instead, he always patiently explained and clarified the subject to me. These personalities of his have absolutely influenced on me and directed me to be a better person. I just feel lucky to have had him as my supervisor.

Martin Bastmeyer is my official supervisor who took responsibility of me. He is a man of honor who willing to stepped in when I was struggling as a PhD student. I am extremely grateful to him for taking responsibility of me as my supervisor. His kindness motivated me and gave me a second chance to purse my academic dream. I hope I have not let him down.

Nicholas Simon Foulkes is a member of my thesis advisory committee who gave me fully support and helped me out of my difficult situation. He is a good person and is open to all students who have difficult issues and is willing to help them out. I am grateful for his goodness.

Olivier Kassel is another member of my thesis advisory committee who was there all the time and supported me from the first to the last year of my PhD career. He is kind, good-humored and a knowledgeable person who gave me a lot of academic advice, especially for a better understanding of statistical analysis. I thank him for his supervision.

Carsten Weiss is also a member of my thesis advisory committee. He is a warmhearted person who actively participated in discussion my work and offered a lot of useful and constructive advice. I thank him for his supervision.

Christine Blattner was my former supervisor. I thank her time for the two and half years.

Valeria Solozobova, Nane Kuznik and Jutta Stober are the colleagues in our laboratory. They are all very nice persons who helped me so much. We are a good team in the Cato laboratory and I enjoyed my time working with them.

Donald John Trump was the 45th president of the United States. I am never his fan but I must thank him for his motivating speech “never ever give up” that he gave to the graduates of Liberty University. There was a period of time that I had to listen to his “never ever give up” speech every day before I got to bed at night and woke up in the morning. I thank him for his speech for stopping me give up.

Walter Burn is a 70 years old grandpa who became my landlord during the corona pandemic. There was a time that I was financially broken and ate three to five potatoes per day to survive for more than a month. Mr. Burn offered me the lowest rent in Karlsruhe and frequently feed me with his home-made cakes. I never like sweet food but I am grateful for his kindness.

China Scholarship Council is the organization that funded my PhD. I could not have finished my PhD without their financial support. I am grateful that they decided to continuing my funding after I was stuck in China for several months due to the pandemic.

Cailing is my fiancée who has been waiting for me for more than 5 years. There was a dark time that I was emotionally a broken person on occasions I almost ruined myself. It was she who put me together. She never gave up on me. I am so lucky to have her.

I thank my family for their unconditional love and support even though they do not understand why I spend so many years being a student compare to others with my age who already have become parents and are financially independent.

There are certainly lots of other nice persons such as Lennart Hilbert, Yvonne Heneka, Christina Bauer and Zita Gonda etc. at our institute who helped me a lot over the last four years. Although I cannot list them all by names here, I do thank them all in my heart. I am very honored to have been around with so many incredible people. Thank you all!

Finally, to those who are temporarily in a difficult and worse situation but still have dreams, I would like to share several sentences from the speech of Donald J. Trump: “There will be times in your life you'll want to quit. You'll want to go home perhaps to that wonderful mother that's sitting back there watching you and say: “Mom, I can't do it. I can't do it.” Just never quit. Go back home and tell mom, dad, I can do it, I can do it. I will do it. You're going to be successful. I've seen so many brilliant people, they gave up in life, they were totally brilliant, they were top of their class, they were the best students, they were the best of everything. They gave up. I've seen others who really didn't have that talent or that ability and they're among the most successful people today in the world because they never quit and they never gave up. So just remember that never stop fighting for what you believe in and for the people who care about you”.

Table of content

List of figures

List of Tables

Abbreviations

%(v/v)	percent volume per volume
%(w/v)	percent weight per volume
ADP/ATP	adenosine diphosphate/adenosine triphosphate
AF-1	activation function-1
AF-2	activation function-2
APS	ammonium persulfate
AIs	aromatase inhibitors
AR	androgen receptor
BAG-1	Bcl-2 associated athanogene 1
BSA	bovine serum albumin
BRCA1/2	breast cancer type 1 susceptibility protein 1/2
CSCs	cancer stem cells
CEA	carcinoembryonic antigen
cDNA	complementary DNA
DBD	DNA-binding domain
DMEM	Dulbecco's Modified Eagle's Medium
DMSO	dimethyl sulfoxide
DD	dimerization domain
DFS	disease-free survival
E2	17-β-estradiol
EDTA	ethylenediaminetetraacetic acid
EMT	Epithelial to mesenchymal transition
EtOH	Ethanol

ER (+)	estrogen receptor (positive)
FBS	fetal bovine serum
GR	glucocorticoid receptor
HER2	human epidermal growth receptor 2
HSPs	Heat shock proteins
IGF1R	insulin-like growth factor 1 receptor
IARC	International agency for research on cancer
KDa	Kilodalton
LBD	ligand binding domain
MAPK	mitogen-activated protein kinase
MR	mineralocorticoid receptor
NLS	nuclear localization sequence
NTD	N-terminal Domain
NF-κB	nuclear factor kappa B
NSAIs	non-steroidal aromatase inhibitors
NCOA1	nuclear receptor co-activator 1
NCOR1	nuclear receptor co-repressor 1
OS	overall survival
OHT	4-hydroxytamoxifen
PBS	phosphate buffered saline
PCR	polymerase chain reaction
PMSF	phenylmethylsulphonyl fluoride
PAI-1	plasminogen activator inhibitor type 1
PR	progesterone receptor
PROTACs	proteolysis targeting chimeras

qRT-PCR	quantitative Real-Time PCR
RPMI	Roswell Park Memorial Institute
RTKs	receptor tyrosine kinases
RAR	retinoic acid receptor
SDS	sodium dodecyl sulfate
SAIS	steroidal aromatase inhibitors
SP1	stimulating protein-1
SERMs	selective estrogen receptor modulators
SERDs	selective estrogen receptor down-regulators
TEMED	Tetramethyl ethylene diamine
ULD	ubiquitin-like domain
uPA	Urokinase plasminogen activator
VDR	Vitamin D receptor
WHO	World health organization

Chapter 1: Introduction

1.1 Breast cancer

1.1.1 Statistics of breast cancer

Cancer has been subsisting with mankind as long as we are existed. Meanwhile, thousands of years combating cancer has made us understanding it better. As a major health threat to mankind, the mortality rate of cancer all over the world has significantly increased. An investigation of global cancer burden estimated that 8.8 million cancer patients died in the year 2004, while by 2018, the estimated cancer deaths increased to 9.5 million. Even worse, by the year 2030, an estimated 17 million people would die from cancer (Bray et al., 2018).

Breast cancer is by far the most frequently diagnosed cancer among women with an estimated 1.7 million new cases in year 2012 (Donepudi et al., 2014). About one in eight women would develop invasive breast cancer over the course of their lifetime. According to the world health organization (WHO) International agency for research on cancer (IARC) statistics 2012, the proportion of breast cancer incidence among continents are 70.08% in Europe, 57.5% in Oceania, 37.5% in Asia and 28.66% in Africa (Torre et al., 2016). So far, breast cancer has become the most common cause of death from cancer both in the developing and developed countries.

1.1.2 Classification and markers for breast cancer

1.1.2.1 Classification of breast cancer

Breast cancer is initially a hormone-dependent cancer and like most cancers, it is a heterogeneous disease with different molecular subtypes. Traditionally, breast cancers were classified by immunohistochemistry markers such as estrogen receptor (ER), progesterone receptor (PR), human epidermal growth receptor 2 (HER2) and Ki67 (Perou et al., 2000). Recently, a groundbreaking work classified breast cancer into five major intrinsic subtypes: Luminal-A breast cancer, Luminal-B breast cancer, HER2(human epidermal growth factor)-enriched breast cancer, triple negative (ER negative, PR negative and HER2 negative) basal-like breast cancer and normal-like tumors (Perou et al., 2000). Both Luminal-A and Luminal-B breast cancer are typically hormone receptor positive and form more than 90% of hormone receptor positive, HER2 negative tumors. To be more specific, Luminal A defines ER positive (ER+), PR ≥ 20%, HER2 negative, Ki67<14%, and if available, “low” recurrence risk based on gene-based assay; while Luminal B tumors are ER+, HER2 negative, and at least one of the following: Ki67 ≥ 20%, PR<20%,

and if available, “high” recurrence risk based on multi-gene expression assay (Goldhirsch et al., 2013). HER2 enriched breast cancer and triple negative basal-like breast cancer define roughly 15% and of breast cancer patients, and are frequently associated with aggressive disease and poor outcomes (Cheang et al., 2008; Figueroa-Magalhães et al., 2014).

1.1.2.2 Molecular markers of breast cancer

Molecular markers are extremely important for diagnosis, treatment and prognosis of cancers. Molecular markers for breast cancer can be generally categorized into tissue markers, genetic markers and serum markers.

Tissue markers for breast cancer mainly includes estrogen receptor (ER), progesterone receptor (PR), human epidermal growth factor 2(HER2), ki67, Urokinase plasminogen activator (uPA), plasminogen activator inhibitor type 1 (PAI-1), cathepsin D and p53 [Review: (Donepudi et al., 2014)]. ER and PR are the commonly used predictive and prognostic markers to determine whether the patients can be treated with hormone therapy (Ravdin et al., 1992). Therefore, ER and PR levels should be determined for all breast cancer patients. HER2 is a prognostic marker to identity patients who can be treated with anthracycline-based adjuvant chemotherapy and this marker also needs to be determined in all breast cancer patients (Gennari et al., 2008). Ki67 is a useful marker to assess cancer cell proliferation. However, this marker is not recommended for routine use in clinical management of breast cancer due to the lack of standardized procedure for Ki67 assessment as well as the persistence of several issues of Ki67 assay interpretation and clinical utility (Penault-Llorca and Radosevic-Robin, 2017). uPA and PAI-1 are optional markers for measurement of breast cancer patients. These two markers could be used to identify lymph node-negative patients who will not benefit from adjuvant chemotherapy (Jänicke et al., 2001). Cathepsin D is a prognostic marker which is validated by meta-analysis for lymph node-negative breast cancer only. So far, applications for clinical use of this marker has not been made because of conflicted outcomes (Ferrandina et al., 1997; Ravdin et al., 1994). Several studies have demonstrated that the risk of recurrence and death increases 50% or more if p53 functions are abrogated (Elledge and Allred, 1998). Therefore, p53 serves as a predictive and prognostic marker in breast cancer patients in majority of wild type p53 breast cancer.

Genetic markers of breast cancer are more frequently focused on mutations of BRCA1 (Breast cancer type 1 susceptibility protein) and BRCA2 (Breast cancer type 2 susceptibility protein). Germline mutations of BRCA1 or BRCA2 genes are strong predictors of breast and/or ovarian cancer development. The available evidence indicate that the mutations of these two genes in

breast cancer contribute nearly 40% to 80% to the chances of developing breast cancer (Fackenthal and Olopade, 2007). Recently breast cancer patient who do not have mutations in BRCA1 and BRCA2 have instead been found to have mutations in MSH2 (mutS homolog 2) leading to the proposition that mutations in this gene could serve as novel markers for the diagnosis of breast cancer (Wu et al., 2019).

Serum markers for breast cancer include MUC-1 (mucin-1) family proteins such as CA15.3, BR27.29, carcinoembryonic antigen (CEA), cytokeratin and oncoproteins such as HER2, c-erB-2 and cytokeratin. Clinically, combinations of one of the MUN-1 family proteins and CEA are the recommended serum marker panel in diagnosing patients with breast cancer diagnosis. Patients with high level of serum markers are thought to have unsuspected metastatic disease (Dnistrian et al., 1991).

To date, a wide range of other molecular markers have been identified for the diagnosis and prognosis of breast cancers. However, fewer markers are actually used in the clinical due to lack of sensitivity and selectivity. By far, ER, PR, HER2 are mandatory for all newly diagnosed breast cancer patients, Ki67, uPA and PAI-1 are optional according to the treatment decisions.

1.1.3 Estrogen receptor in ER^+ breast cancer

About 70% of breast cancers express ER and are classified as estrogen receptor positive (ER^+) breast cancers. Generally, one speaks of ER^+ breast cancer when more than 1% of the total cells examined are positively stained for ER. The tumor progression of ER^+ breast cancer relies on estrogen signaling. Estrogen belongs to the family of organic compounds knows as steroids, include estrone, estradiol, estriol and estretrol. As 17-β-estradiol (E2) is the main component of this class of hormones, the terms E2 and estrogen will be used synonymously in this thesis to refer to this class of hormones. Estrogens exert their function through binding to the ER, which is the key protein that activates transcriptional processes and/or signaling events in the control of gene expression and behaviors in ER^+ breast cancer cells (Fuentes and Silveyra, 2019). There are two kinds of estrogen receptors, estrogen receptor α (ERα) and estrogen receptor β(ERβ). ERα and ERβ are encoded by ESR1 and ESR2 genes localized on chromosome 6 and chromosome 14, respectively. Both ERα and ERβ have 6 functional domains (A-F). Domains A/B and F are variable and share less than 20% amino acids identify. Domain C is almost identical with 97% amino acid identify, while domain D and E share 36% and 56% amino acid identity, respectively (Yaşar et al., 2017). Domain A/B make up the N-terminus of the receptors and contain activation function 1 (AF-1). Domain C is the DNA binding domain and plays essential role in chromatin

accessibility. Domain D is known as the hinge region and it connects the N-terminal region of the receptor (domains A-C) with the C-terminal region (domains E-F) (Green et al., 1986; Kumar et al., 1987); Domain E is also known as the ligand binding domain (LBD) and mediates binding of the chaperones. This domain contains a transactivation function 2 (AF-2), a ligand-dependent dimerization function and an additional NLS. The function of Domain F is so far unclear. However recent studies report that it governs a tissue-specific 4-hydroxytamoxifen-mediated transcriptional activity of ERα (Αραο ανδ Κοραχη, 2018) (Figure 1.1).

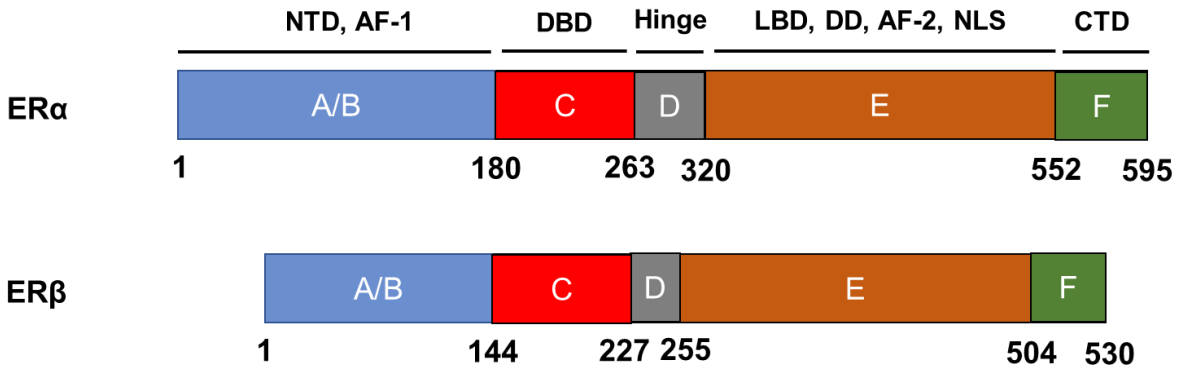

Figure 1. 1: Schematic representation of the structure of human ERα and ERβ.
(A). schematic drawing of the primary structure of human ERα and ERβ. Both proteins have 6 domains. The N-terminal domain (NTD) is made up of domains A and B and contains an activation function 1 (AF-1) which is necessary for transcriptional activity. Domain C contains a DNA-binding domain, which directly contact DNA. Domain D also called hinge region which is important to the linkage of DBD and ligand binding domain (LBD) and contains a nuclear localization sequence which contributes its nuclear localization. Domain E is the ligand binding domain (LBD) for transcriptional coactivators/co-suppressors binding, a ligand-dependent dimerization functions an activation function 2 domain (AF-2) for transcriptional activity and an additional NLS for nuclear localization. The function of domain F is so far unclear.

While ERα is well-known for ER^+ breast cancer progression, the roles of ERβ in breast cancer cells is contradictory. There are reports of a low level of expression of ERβ in breast cancer and overexpression of ERβ is said to reduce proliferation and/or invasion of several breast cancer cells, such as MCF-7 cells, T47Dcells and MDA-MB231 cells (Hou et al., 2004). Other reports demonstrated that invasive breast cancers highly express ERβ and overexpression promotes cell proliferation and/or invasion of MDA-MB231 cell and accelerates tumor growth and/or metastasis in MDA-MB435 xenograft (Hou et al., 2004; Tonetti et al., 2003). While ERα is of

clinical relevance, the clinical significance of ERβ remains obscure (Iwase et al., 2003; Saji et al., 2005; Shaaban et al., 2003). Therefore, in clinical terms, ER positive breast cancer normally refers to ERα positive tumors. For clarification, unless otherwise stated, all ER mentioned in this thesis will refer to ERα.

ER, as a master player in ER^+ breast cancer, is activated mostly by ligands binding to its LBD. Estrogens are the key ligands for ER activation. Over the decades, the molecular mechanism of estrogen-dependent ER activation has been well established. Generally, estrogens are synthesized in tissues such as ovaries, adrenal as well as adipose tissues (Allen and Doisy, 1983). The main substrate for estrogen biosynthesis is the dietary cholesterol, which undergoes multiple conversions to progestogens, androgens and finally estrogens (Guiochon-Mantel et al., 1999). The estrogen then binds to the ER in the cytoplasm resulting in a conformational change of ER, dimerization of the ER and translocation of the estrogen/ER complex into the nucleus (Le Dily and Beato, 2018). The complex then binds estrogen response elements (ERE) in the promoters of target genes and recruits co-activators or corepressors to modulate the expression of target genes (Klinge, 2001); Besides, the ER is also tethered to already bound transcription factors through protein-protein interaction to regulate cooperatively the expression of distinct genes. The known transcription factors that interact with the ER include stimulating protein-1 (SP1), nuclear factor kappa B (NF-κB), and p53. SP1 was considered as a general transcription factor that is required for the activation of large number of "housekeeping genes" as well as genes responsible for metabolism, cell proliferation/growth and cell death (Black et al., 2001). Previous studies indicated that ER enhanced SP-1 binding to the promoter regions at GC-rich site, which increased expression of multiple genes, such as progesterone receptor B (PRB), GATA binding protein 1 (GATA1) and signal transducer and activator of transcription 5 (STAT5) (Björnström and Sjöberg, 2005; O'Lone et al., 2004). The transcription factor NF-κB regulates many genes that are essential primarily for the development, maintenance and function of innate and adaptive immune system (Kumar et al., 2004). ER has been shown to inhibit NF-κB activity in an estrogen-dependent manner in numerous studies. It is commonly known that the inhibition of NF-κB by ER occur through multiple mechanisms: 1), ER inhibits IKK-B (inhibitor of nuclear factor Kappa B kinase subunit beta) activity; 2), ER inhibits the degradation of IκBs (Inhibitors of NF- κB); 3), ER blocks DNA binding activity of NF-κB; 4), ER competitively binds to coactivators of NF-κB (Kalaitzidis and Gilmore, 2005). p53 is a well-known transcription factor with anti-tumor effect. In ER^+ and p53 wild type breast cancer, these two transcription factors are reported to regulate each other´s activity. A direct interaction between p53 and ER was mutually reported by Yu, et

al, 1997 who showed that wild type p53 physically interacted with ER in vivo and repressed ER transcriptional activity but the ability to inhibit ER transcriptional activity is completely or partially lost in mutated p53 (Yu et al., 1997). Another research group demonstrated that LBD of ER directly binds to the C-terminal domain of p53 and the p53-ER complex binds to promoters of p53 downstream targets, such as p21, PCNA to repress p53 transcriptional activity (Liu et al., 2006). Therefore, a negative regulation loop was established between p53 and ER. Further work revealed that estrogen do not only activate ER but also enhanced p53-ER interaction, which facilitated ER-mediated p53 inactivation in a dominant negative regulation mode. Therefore, in ER^+ and p53 wild type breast cancers, p53 is initially inactivated. Giving the fact that ER pathway promotes breast cancer proliferation, and p53 pathway impedes breast cancer cells proliferation, these two pathways are antagonistically co-regulated. The strategy of reactivation of p53 does not only restore the intrinsic function of p53 as tumor suppressor, but also blow up its anti-tumor ability by inhibition of ER transcriptional activity. Indeed, ionizing radiation considerably elevated p53 protein levels but disrupted p53-ER interaction in MCF-7 cells, stabilization of p53 accompanied with several p53 targets activation and repressed ER transcriptional activity. In line with cellular mechanism, MCF-7 xenograft mice mode showed a significant tumor reduction after ionizing radiation treatment (Liu et al., 2009). Notably, clinical trial from VIII and IX with 1092 breast cancer cases indicated that a significant qualitative interaction of p53 and ER was observed. The patients whose tumors did not express ER but express p53 was associated with better disease-free survival (DFS) and overall survival (OS), while the patients whose tumors express both ER and p53 had worse DFS and OS (Coates et al., 2012). These findings suggest that approaches that target p53-ER interaction for p53 reactivation in ER^+ breast cancer may receive a boosting anti-tumor effect.

In addition to the estrogen-dependent activation of ER, ER can also be activated in the absence of estrogen (Bennesch and Picard, 2015; Maggi, 2011). The estrogen-independent activation of ER relies on phosphorylation of serine and/or tyrosine residues by different protein kinases. For examples, protein kinase A phosphorylated ER at Ser236 for activation of ER, while protein kinase C phosphorylated Tyr536 in the ligand binding domain of the receptor. Activation of ER in response to mitogen-activated protein kinase (MAPK) pathway triggered by phosphorylation of Ser118 and Ser167 in the AF-1 region at the N-terminal domain of ER (Lannigan, 2003).

1.1.4 Endocrine therapies for ER$^+$ breast cancer

ER$^+$ breast cancers are initially dependent on activation of ER by estrogen. However, both estrogen-dependent and -independent activation of ER activate pro-survival gene expression and promote proliferation and tumorigenesis of cancerous ER$^+$ breast cells (Torres-Arzayus et al., 2010). To counteract these activities, endocrine therapies, such as aromatase inhibitors (AIs), selective ER modulators (SERMs), selective ER down-regulators (SERDs) and proteolysis targeting chimeras (PROTACs) has been developed and approved for adjutant treatment of patients with breast cancer (Aggelis and Johnston, 2019).

In postmenopausal women, the main sites for the production of estrogen are skin, adipose tissue and breast. Aromatase, localized in the breast tumor produces sufficient estrogen from androgens for tumor growth. Therefore, more estrogen specific targeted therapy is required in postmenopausal women (Nelson and Bulun, 2001). Aromatase inhibitors (AIs) deplete systemic estrogen levels by blocking the conversion of androgens to estrogens. Thus AIs are extremely useful for the treatment of ER+ breast cancer in postmenopausal women (Montemurro et al., 2009). Currently, the clinical use of AIs can be classified into two major groups: steroidal aromatase inhibitors (SAIS) and non-steroidal aromatase inhibitors (NSAIs) (Narashimamurthy et al., 2004). SAIs irreversibly inhibit the convention of androgens to estrogens and are androstenedione scaffolds consisting of cyclopentanoperhydrophenanthrene as core nucleus, such as exemestane (3rd generation), 4-hydroxyandrostenedione (2nd generation) and Testolactone (1st generation). NSAIs, such as anastrozole (3rd generation), Fadrazole (2nd generation) and aminoglutethimide (1st generation), do not contain any steroidal moiety and reversibly inhibit aromatase activity (Kharb et al., 2020; Recanatini and Cavalli, 1998). Though both SAIs and NSAIs have been successfully used in clinical practice against ER$^+$ breast cancer in postmenopausal women, the fact that estrogen has activity in multiple organs cause serious side effects and toxicity. These include impact on the reproductive system, with vaginal and urothelial irritation, osteopenia, osteoporosis, bone fractures, headaches, depression and cognitive dysfunction (Condorelli and Vaz-Luis, 2018). Therefore, a safer and better hormone-targeted therapy for adjuvant treatment in ER$^+$ breast cancer in postmenopausal women was developed.

SERMs are anti-estrogens that are designed to compete with estrogen binding to the ER and they modulate ER activity by changing the cofactors that are involved in ER activation (Nilsson and Koehler, 2005). SERMs can be classified into four different major groups according to their chemical structure: triphenylethylenes (Tamoxifen), benzothiophenes (Raloxifene),

phenylindoles (bazedoxifene), tetrahydronaph-thalenes (lasofoxifene) (Patel and Bihani, 2018). The most well-known SERM is Tamoxifen, which has been extensively studied and approved as the first line endocrine therapy drug for decades. The first preclinical report proved that tamoxifen has antiproliferative activity for ER^+ breast cancer goes back to the 1970s (Lippman and Bolan, 1975). However, it was noted that tamoxifen exhibited a poorer activity in vitro compared its activity in vivo (Allen et al., 1980; Jordan et al., 1977). Thirty years later, it was discovered that the in vivo efficacy of tamoxifen can be attributed to its active form 4-hydroxytamoxifen (OHT), generated by cytochrome p450 enzymes, such as CYP2D6, CYP3A and CYP2C (Brauch et al., 2009; Johnson et al., 2004). Intriguingly, tamoxifen has both antagonistic and agnostic activities. As an antagonist, the binding of tamoxifen to ER resulted in the recruitment of ER corepressors, such as nuclear receptor co-repressor 1 (NCOR1) and silencing mediator for retinoid and thyroid hormone receptor (SMART), and the formation of a silenced transcriptional complex, which repressed ER target gene expression (Klinge et al., 2004). As an agonist, the binding of tamoxifen to ER recruited coactivators such as nuclear receptor co-activator 1(NCOA1) and formed transcriptional complex, which binds to the promoters of tamoxifen-sensitive genes to enhance their expression (Romano et al., 2010). The antagonistic and agonistic effects of tamoxifen have also been confirmed in vivo mouse xenograft experiment. Mice implanted with MCF-7 xenograft showed reduced of tumor growth upon administration of tamoxifen, while mice implanted with EnCa101 (endometrial cancer cells) continued to growth upon tamoxifen treatment (Gottardis et al., 1988). In line with these in vitro and in vivo findings, clinical researches have also noted that tamoxifen usage is associated with high risk of endometrial cancer development (Fisher et al., 1994; Fisher et al., 2005).

The fact that ER signaling is not completely abrogated by SERMs treatment due to the agonistic effect of tamoxifen prompted the development of more effective antagonists termed SERDs. SERDs are anti-estrogens that are designed to destabilize the ER by promoting ER protein degradation, and abolishing ER signaling via blocking ER transcriptional activity (McDonnell and Wardell, 2010). Fulvestrant is the most representative SERD that was identified as a pure anti-estrogen agent in 1980s (Wakeling, 1989). It was proposed that fulvestrant binds to monomeric ER and prevents ER dimerization. This binding did not only lower the accessibility of ER to chromatin but also accelerated ER turnover through the ubiquitin-proteasome pathway (Fawell et al., 1990). Fulvestrant, derived from ICI182780 demonstrated high potency both in vitro and in vivo models of breast cancers (Wakeling and Bowler, 1992; Wakeling et al., 1991), was effective in inhibiting the growth of tamoxifen-resistant tumors due to its pure anti-estrogenic effects (Hu

et al., 1993). The first clinical use of fulvestrant was approved for metastatic ER^+ breast cancer patient and indeed made progress on 250 mg dose. Later, fulvestrant administrated as 500 mg dose was shown to be non-toxic with increased bioavailability and efficacy, which is the current approved dose for the treatment of advance ER^+ breast cancer patients (Di Leo et al., 2010; Robertson et al., 2012).

A new and promising approach to the treatment of ER+ breast cancer is PROTACs (Proteolysis targeting chimeras). PROTACs have recently emerged as an approach for undruggable cancer targets by hijacking the ubiquitin-proteasome system to induce target degradation (Moon and Lee, 2018). Mechanistically, PROTACs is a hetero-bifunctional molecule complex that consist of a ligand for the protein of interest (POI), an E3 Ubiquitin ligase recruiting ligand, and a linker between the two ligands. PROTACs initiate target degradation by forming ternary complex with the POI and E3, which leads to subsequent polyubiquitination of the POI and 26S proteasome mediated degradation (Pettersson and Crews, 2019). ARV-471, a PROTAC molecule that specifically targets ER and induces ER degradation was identified in 2019 and has been approved by the United State Food and Drug Administration (US FDA) for clinical trials. Notably, Y537S and D538G ER mutants are the most frequently induced ER mutants by endocrine therapies and these two mutants are reported to be less effectively inhibited by fulvestrant (Toy et al., 2017). However, ARV-471 has also been proved to be capable of degrading Y537S and D538G ER mutants and inhibiting tumor growth in a patients-derived xenograft harboring $ESR1^{Y537S}$. (Flanagan et al., 2019). Besides, Hu, et al demonstrated that a new PROTAC molecule termed ERD-308 induced ER degradation with more efficacy than fulvestrant in MCF-7 cells as well as in T47D cells (Hu et al., 2019). These findings showed a promising prospect for PROTACs in cancer treatment. However, considering the fact that PROTACs heavily rely on a ternary complex formation for target degradation, the design of POI-ligand affinity and E3-ligand affinity remains the biggest challenge to obtain the effective ternary complex for PROTACs-based therapy.

1.1.5 Resistance of endocrine therapy in ER^+ breast cancer

Approximately 50% patients with advance disease do not response to tamoxifen. Also, up to 20% of patients who received tamoxifen as adjuvant therapy faced with tumor relapse. Even AIs, only reduces 30% of recurrence within 5 years, not thereafter (Early Breast Cancer Trialists' Collaborative, 2015). Increased investigations have demonstrated that endocrine resistance inevitably occurs in ER+ metastatic breast cancer (Arpino et al., 2009). Recently, both laboratory-based and clinical-based approaches have been used to reveal the mechanism of endocrine

therapy resistance and to categorize them as follow: 1), estrogen-independent ER reactivation, such as gain-of-function via ER mutations; 2), alteration of ER interaction with co-factors (co-activator/corepressor); 3), cross-talk with receptor tyrosine kinases and activated proliferation and pro-survival pathways, such as PI3K-AKT-mTOR pathway and MAPK pathway (AlFakeeh and Brezden-Masley, 2018).

Estrogen-independent ER reactivation can be triggered by ER mutations and aromatase activity alteration following SERMs and AIs treatments. Studies have indicated that a long-term treatment with tamoxifen caused point mutation (frequently at Y537 and D538) in the ER LBD, which activated the ER transcriptional activity in an estrogen-independent manner and caused approximately 20% recurrent ER^+ breast cancers (Jeselsohn et al., 2015). Importantly, these point mutations in ER do not only lower the sensitivity to tamoxifen and fulvestrant, but also result in resistance to AIs. Besides, a long-term treatment with AIs caused amplification of *CYP19A1*, a gene which encodes aromatase. *CYP19A1* amplification increase aromatase activity and also leads to estrogen-dependent ER activation, which resulted in decreased sensitivity to AIs and eventually progression to incurable metastatic disease (Magnani et al., 2017).

Alteration of ER interaction with co-factors also frequently contributed to endocrine therapy resistance. For example, although nuclear co-repressor (NCoR) is a vital co-factor recruited by tamoxifen-ER complex to exert its antagonistic function, however, more than 85% tamoxifen-refractory tumors overexpress COP9 signalosome subunit 5 (COPS5), which promotes proteasomal degradation of NCoR and switches tamoxifen from ER antagonist to a potent ER agonist (Lu et al., 2016). Patients who did not receive tamoxifen therapy showed high expression of steroid coactivator-3 (SRC-3) associated with good prognosis and have long disease-free survival (DFS). On the contrary, patients who received tamoxifen therapy showed high expression of SRC-3 associated with poor prognosis and worse DFS. Further investigation suggested that the elevated expression of SRC-3 resulted in the switch of antagonistic activity of tamoxifen-bound ER to an agonistic role (Osborne et al., 2003). Besides, HOXB7 that serves as an ER coactivator and promotes transcription of HER2, MYC and other ER targets in tamoxifen-resistant cells is completely repressed by fulvestrant in MCF-7 xenografts (Jin et al., 2015). A final example of alteration of ER with cofactors is FOXA1, a co-factor recruited by ER complex that opens up densely packed chromatin to make it transcriptional accessible by ER (Carroll et al., 2005). Several studies confirmed that tamoxifen treatment resulted in amplification of FOXA1 leading to an enhanced ER transcriptional activity (Cocce et al., 2019; Fu et al., 2016).

Endocrine therapy resistance is often increased with aberrant expression of growth factors, such as human epidermal growth factor 2 (HER2), epithelial growth factor receptor (EGFR) and insulin-like growth factor 1 receptor (IGF1R) (Nayar et al., 2019; Razavi et al., 2018; Schiff et al., 2004). These growth factors and their receptors are commonly known as receptor tyrosine kinases (RTKs). The cross-talk of these RTKs with ER promotes ER phosphorylation and dimerization which leads to estrogen-independent activation and contributes to cell growth, proliferation and survival through further cross-talk with downstream pathways, such as PI3K-AKT-mTOR pathway and MAPK pathway (AlFakeeh and Brezden-Masley, 2018; Schiff et al., 2004). Indeed, additional PI3K pathway antagonist and MAPK pathway antagonists improved the outcome of DFS when combined with hormone-therapies in ER^+ breast cancer patients. For example, a specific PI3K inhibitor Alpelisib in combination with fulvestrant prolonged progression-free survival of patients with advance breast cancer who only received endocrine therapy (André et al., 2019). Similarly, the mTOR inhibitor Everolimus combined with AIs for treatment of metastasis breast cancer also showed improvement to progression-free survival in patients (Baselga et al., 2012); Besides, the AKT inhibitor capivasertib in combination with fulvestrant has also shown preliminary efficacy in endocrine-resistant ER^+ breast cancer (Ludmir et al., 2020). The cross-talk of MAPK pathway with ER mainly through neurofibromatosis type 1 (NF1), a key component in the MAPK pathway that is frequently mutated in endocrine-resistant ER^+ breast cancer cells. Studies have indicated that loss of NF1 in ER^+ breast cancer cells promoted ER-independent cyclin D1 expression. Therefore, resistance to anti-estrogen caused by NF1 could be therapeutically targeted with CDK4/6 inhibitors (Pearson et al., 2020).

Resistance to endocrine therapy is a complex biological process of cells response to drug stress. Over the last few decades, the explosion of research in the field of endocrine therapy resistance in ER^+ breast cancer has extensively broadened our knowledge in cancer resistance. Therefore, the mechanisms of endocrine therapy resistance are not limited to the summary above. Other mechanisms such as epigenetic modification of ER, Epithelial to mesenchymal transition (EMT), cancer stem cells (CSCs), metabolic reprogramming and tumor microenvironment are some of the factors that also frequently contribute to endocrine therapy resistances [review: (AlFakeeh and Brezden-Masley, 2018; D'Souza et al., 2018; Hanker et al., 2020; Rasha et al., 2021)]. All these acquired knowledges are significantly vital for the future development of novel drug to overcome therapy resistance.

1.2 BAG1 in ER$^+$ breast cancer

To overcome programmed cell death, such as apoptosis and autophagy, tumor cells have adopted and evolved via multiple mechanisms. One of these mechanisms involve the action of members of the BCL-2 associated athanogene (BAG) family (Mariotto et al., 2020). The word athanogene originally from Greek athánatos, which means “against death”, as suggested in its name, describes the ability of BAG family members to protect cells from death stimulus and play a vital role in cancer cells overcoming programmed cell death.

1.2.1 The human BAG Family of proteins

The BAG genes are a family of evolutionarily conserved with a BAG domain and homologues identified in different species ranging from fungi to mammals (Doong et al., 2002; Mariotto et al., 2020). BAG1 protein was the first identified BAG family member by Takayma via using recombinant BCL-2 protein as a probe to screen a mouse embryo cDNA library in a lambda phage expression vector (Takayama et al., 1995). Using BAG1 as a probe in a screen of lambda gt11 expression library as well as a yeast-two-hybrid screen, HSP70 was identified as the interaction factor of BAG1. BAG1 was later found to bind to the ATPase domain of HSP70 (Takayama et al., 1999). Thereafter, more proteins that share similar structure to BAG1 were identified to interact with HSP70, and were named BAG2, BAG3, BAG4 and BAG5 (Takayama et al., 1999). BAG6 was initially found as an apoptosis regulator interacting with Reaper, which later was also confirmed as a binding partner of HSP70 protein (Thress et al., 1998; Thress et al., 2001). Recently, crystal structure and biochemical characterization have demonstrated that the BAG domain in BAG6 is not a canonical BAG domain, which compromised its ability to inhibit HSP70 refolding of substrates (Mock et al., 2015).

As a conserved protein family, all BAG family members contain BAG domain which shares 40% to 60% homology among the sequences. Each BAG family member contains only one BAG domain with the exception of BAG5, which possess 5 BAG domains. The BAG domain is responsible for binding to the ATPase domain of HSP70 (Sondermann et al., 2001). Except for the common shared BAG domain, there are also some specialized domains that may be shared among the BAG family members. For example, a unique ubiquitin-like (UBL) domain in BAG1 that directs HSP70 client proteins to proteasome degradation has also been found in BAG6 protein (Esser et al., 2004). Besides, a proline-riche domain (PxxP) that is responsible for protein-protein interaction in BAG3, has also been identified in BAG6 (Figure 1.2A) (Leznicki et al., 2013; Ni et al., 2019). The Coil-coil region (CC) in BAG2 and WWP repeat motif in BAG3 (WW) haven’t been found in the

other BAG family proteins. Up to now, BAG family members have been reported to play multiple roles that are linked to cell proliferation and pro-survival pathways, such as negatively response of cells to apoptosis and autophagy and positive response to cell cycle, proliferation, migration and invasion (Mariotto et al., 2020).

The human BAG1 gene codes for four BAG1 isoforms due to the use of alternative translation start sites (Takayama et al., 1998; Yang et al., 1998). The largest BAG1 isoform (BAG-1L) is translated from an up-stream relatively weak start code CUG, which produces a 50 KD protein with 345 amino acids. BAG-1L contains the conserved BAG domain, an UBL domain and a unique nuclear localization sequence (NLS), which makes BAG-1L a nuclear protein. Three in-frame down-stream AUG start codes give arise to another three BAG1 isoforms: BAG-1M, BAG-1 and BAG-1S, which possess 274, 230 and 217 amino acids respectively (Figure 1.2B). However, BAG-1S is not consistently detected as its expression is relatively low and inconspicuous in some cell types (Tang, 2002).

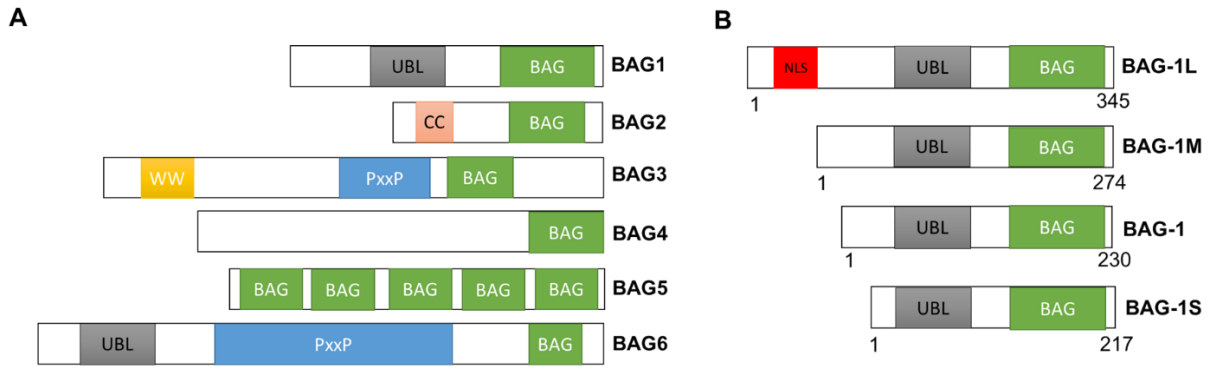

Figure 1. 2: Schematic representation of the structure of human BAG family members.
(A). schematic drawing of the primary structure of human BAG family members. BAG domain (green), Ubiquitin-like domain: UBL (gray), Coil-coil region: CC (pink), WWP repeat motif: WW (yellow), proline-rich domain: PxxP (blue). (B). schematic drawing of the primary structure of human BAG1 proteins isoforms. BAG domain (green), Ubiquitin-like domain: UBL (gray), nuclear localization sequence: NLS (red).

1.2.2 BAG1 in modulation of nuclear hormone receptors

After initial reports of BAG1 as a BCL-2 interaction partner that protects cells against death stimuli, further studies have demonstrated that BAG1 isoforms exhibit unique functions. In particular, they serve as nucleotide exchange factors for the molecular chaperone Hsp70 (Höhfeld and Jentsch, 1997; Sondermann et al., 2001). Meanwhile, the co-interacting partners of BAG1

isoforms have remarkably increased in number. In addition to BCL-2 and the molecular chaperone HSP70, the most frequently binding partners knowns are nuclear hormone receptors (NHR) such as androgen receptor (AR), estrogen receptor (ER), progesterone receptor (PR), vitamin D receptor (VDR), retinoic acid receptor (RAR), glucocorticoid receptor (GR) and mineralocorticoid receptor (MR) (Table 1.1) (Cato and Mink, 2001; Pratt and Toft, 1997; Takayama and Reed, 2001).

The modulation of nuclear receptor action by the BAG1 proteins occur at multiple levels. For example, BAG-1L interacts with both the N-terminal and C-terminal of the AR. The N-terminal interaction requires the BAG domain and it occurs at tau5 region of the AR in the presence of HSP70, which consequently leads to a change in conformation of the receptor and finally enhanced transactivation by the AR (Shatkina et al., 2003). The C-terminal interaction requires the NH_2-terminal domain of BAG-1L and it occurs at COOH termini of the AR. Further study has indicated that deletion of the NH2-terminal domain of BAG-1L or the cytoplasmic BAG-1M that only possess the N-terminal interaction with AR is less effective to enhance the transcriptional activity of the AR due to a defective C-terminal interaction with AR (Shatkina et al., 2003). Similarity, BAG-1L has also been reported to enhance estrogen-dependent ER transcriptional activity as overexpression of BAG-1L leads to approximately 5-fold increase in ER response to estrogen response (Cutress et al., 2003). Though BAG-1M was also reported to interact with ER, it did not result in increased ER transcriptional activity (Cutress et al., 2003). Furthermore, a fused nuclear localization sequence (NLS) to BAG-1S was not sufficient to stimulate ER transcriptional activity, suggesting the N-terminus of BAG-1L, which is not present in the cytoplasmic BAG1 isoforms is important for ER transactivation. In contrast to the transcriptional activation of AR and ER by BAG1 isoforms, negative regulation of NHR has also been reported. For example, the transcriptional activity of PR was reported to be repressed by BAG-1L and BAG-1M through binding to the N-terminus and DNA binding domain of PR (Knapp et al., 2012). Likewise, BAG-1M was found to inhibit the transcriptional activity of the GR through binding to the hinge region of the receptor (Kullmann et al., 1998). Taken together, the modulation of nuclear hormone receptors is BAG1 isoform specific, and may also require the participation of other regulatory proteins.

Table 1. 1: BAG1 isoforms in modulation of nuclear hormone receptors

BAG1 isoforms	Binding hormone receptor	hormone binding	DNA binding	Transcription activity	References
BAG-1L	AR	-	-	Enhanced	(Froesch et al., 1998)
	ER	Increased	-	Enhanced	(Cutress et al., 2003)

	PR	-	Repressed	Repressed	(Knapp et al., 2012)
	VDR	Increased	-	Enhanced	(Guzey et al., 2000)
BAG-1M	ER	-	-	n.d.	(Cutress et al., 2003)
	PR	-	Repressed	Repressed	(Knapp et al., 2012)
	RAR	-	Repressed	Repressed	(Liu et al., 1998)
	GR	-	Repressed	Repressed	(Kullmann et al., 1998)
	MR	-	-	Repressed	(Knapp et al., 2012)

Note: update from review (Cato and Mink, 2001)

1.2.3 BAG1 action in ER$^+$ breast cancer

BAG1 expression is deregulated in multiple cancers, including breast cancer (Tang et al., 1999), prostate cancer (Krajewska et al., 2006), cervical cancer (Yang et al., 1999), endometrial cancer (Moriyama et al., 2004), lung cancer (Rorke et al., 2001), colorectal cancer (Kikuchi et al., 2002) and squamous cell carcinoma (Shindoh et al., 2000). In breast cancer, BAG1 is frequently overexpressed in invasive breast cancers (Tang et al., 1999). A stronger correlation between nuclear BAG-1 (BAG-1L) expression and tumor grade has been identified in two independent studies, indicating that a reactively high level of BAG-1L expression is related to low tumor grade (Tang et al., 1999; Townsend et al., 2002). These data suggest that BAG1 may have a potential clinical utility as a prognostic marker in early stage of breast cancer (Papadakis et al., 2017; Sauerbrei and Haeussler, 2018).

The BAG1 actions in ER+ breast cancer has been reported to occur through a wide range of interaction partners consisting of nuclear hormone receptors, HSP70/HSC70 chaperones, BCL-2 family members along with other binding partners, such as RAF-1(Figure 1.3). ER is the dominant nuclear receptor in ER$^+$ breast cancers and BAG-1L potentiates the transcriptional activity of ER. This leads to altered transcription of downstream targets in estrogen signaling, and facilitates proliferative activity and survival ability in responses to hormone (Cutress et al., 2003). The action of BAG1 on BCL-2 family members promotes cell survival by protecting cells against cytotoxic stimuli induced cell death such as chemotherapeutic drug treatment, suggesting that BAG1-BCL-2 action may potentially be involved in drug resistance (Pusztai et al., 2004; Tang et al., 2004). Down-regulation of BAG1 significantly enhanced the sensitivity of both MCF-7 cells and tamoxifen-resistant MCF-7 to tamoxifen treatment (Liu et al., 2014). The action of BAG1 on HSP70/HSC70 chaperone mainly relies its action on the substrates of the molecular chaperone. For example, BAG1 binds to the ATPase domain of HSP70 and in cooperation with HSP90 alters the conformation of p53, which regulates the activated and inactivated form of p53 (Dahiya et al., 2019; King et al., 2001). BAG1 also functions by binding to other signaling factors. For example,

BAG1 binds to RAF-1 leading to the activation of the signal-related kinase (ERKs) and mitogen-activated protein kinase (MAPK) that promote cell proliferation and metastasis (Kizilboga et al., 2019; Wang et al., 1996).

In summary, the action of BAG1 in ER^+ breast cancer regulates apoptosis, metastasis, transcription as well as proliferation. Therefore, targeting BAG1 maybe a valuable approach for ER^+ breast cancer therapy.

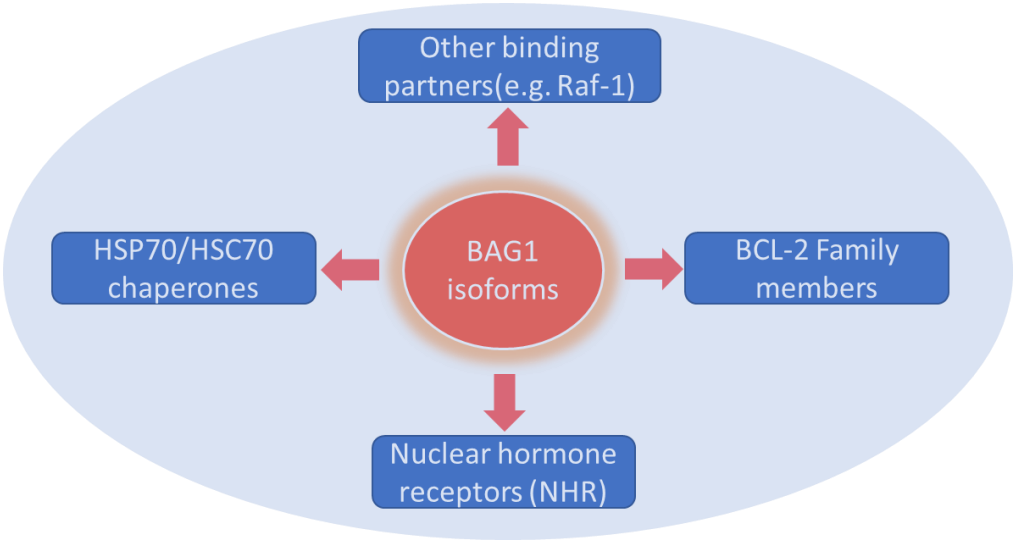

Figure 1. 3: BAG1 actions in ER+ breast cancers.
BAG1 acts through interaction with a wide range of binding partners, such as RAF-1, BCL-2 family members, HSP70/HSC70 chaperones and nuclear receptors. The interaction of BAG1 with RAF1 activates MAPK signaling cascade and leads to breast cancer cell proliferation; the interaction of BAG1 with BCL-2 family members protect breast cancer cells against death stimuli; the interaction of BAG1 with nuclear receptors, in ER^+ breast cancer especially with ER, mediates estrogen-dependent cell growth. Taken together, all these BAG1 actions result in ER^+ breast cancer cell survival.

1.3 Aim of this work

Breast cancer is one of the most frequently diagnosed cancers in women. It is estimated that one in eight women would potentially develop invasive breast cancer over the course of their lifetime (Torre et al., 2016). Since ER^+ breast cancer defines the largest group of beast carcinoma, multiple ER-directed hormone therapies including aromatase inhibitors (AIs), selective estrogen receptor modulators (SERMs) and selective estrogen down-regulators (SERDs), have been developed. Over

the decades, the overall survival rate for ER^+ breast cancer patients have significantly improved based on these hormone therapies along with adjutant cancer treatments. However, these hormone therapies are frequently accompanied with endocrine resistances and multiple side effects. It is therefore, necessary to develop new approaches for ER targeted therapy with novel mechanism that may potentially overcome endocrine therapy resistance. One of the mechanisms is through the co-chaperone BAG1 that is highly expressed in ER^+ breast cancer and plays pivotal role in the activation of ER signaling. BAG1 is an anti-apoptotic protein that protects tumor cells against programmed cell death and causes anti-cancer drug resistance in multiple cancers including breast cancer (Liu et al., 2014; Liu et al., 2017; Lv et al., 2019). While silencing BAG1 enhanced chemotherapeutic drug-induced apoptosis in ER^+ breast cancer cells, overexpression of BAG1 confers cellular resistance to chemotherapy (Kilbas et al., 2019; Pusztai et al., 2004). Thus, targeting BAG1 as a novel indirect strategy for regulating ER signaling with a view to overcoming endocrine therapy resistance in ER^+ breast cancer is the ultimate goal of this work. To achieve this, a small molecule that targets BAG1 is to be developed and its mode of action is to be assessed as an inhibitor of ER action and breast cancer cell proliferation.

Chapter 2: Materials and Methods

2.1 Materials

2.1.1 Chemicals and reagents

Chemicals/Reagents	Source
Acetone	ROTH, Karlsruhe, Germany
Acrylamide/bis-acrylamide	Sigma-Aldrich, Taufkirchen, Germany
Agar	Nordwald, Hamburg, Germany
Agarose	Peqlab, Erlangen, Germany
Ampicillin	ROTH, Karlsruhe, Germany
Ammonium persulfate (APS)	Sigma-Aldrich, Taufkirchen, Germany
Bovine serum albumin (BSA)	PAA Laboratories GmbH, Pasching, Austria
β-mercaptoethanol	ROTH, Karlsruhe, Germany
Calcium chloride	ROTH, Karlsruhe, Germany
Cycloheximide	Sigma-Aldrich, Taufkirchen, Germany
Chloroform	Sigma-Aldrich, Taufkirchen, Germany
DAPI	Invitrogen, Karlsruhe, Germany
Di-Sodium hydrogen phosphate (Na_2HPO_4)	ROTH, Karlsruhe, Germany
Dulbecco's Modified Eagle Medium (DMEM)	Gibico, Invitrogen, Germany
dNTP	Roche, Mannheim, Germany
DNA loading buffer	Peqlab, Erlangen, Germany
Ethanol	ROTH, Karlsruhe, Germany
Ethylenediamine tetra-acetic acid (EDTA)	ROTH, Karlsruhe, Germany
Formaldehyde	ROTH, Karlsruhe, Germany
Fetal Bovine Serum (FBS)	Gibico, Invitrogen, Germany

Fulvestrant	SIGMA, USA
Glycerol	ROTH, Karlsruhe, Germany
Glycine	ROTH, Karlsruhe, Germany
Guanidine hydrochloride	Sigma-Aldrich, Taufkirchen, Germany
HEPES	ROTH, Karlsruhe, Germany
Hydrogen Chloride (HCl)	ROTH, Karlsruhe, Germany
Isopropanol	ROTH, Karlsruhe, Germany
Imidazole	Sigma-Aldrich, Taufkirchen, Germany
InnuPREP RNA kit 2.0	Analytik Jena, Germany
Insulin	Invitrogen, Karlsruhe, Germany
Methanol	ROTH, Karlsruhe, Germany
Milk powder	ROTH, Karlsruhe, Germany
MLRVT (mRNA reverse transcriptase)	Promega, Germany
Non-essential amino acid (NESS)	Invitrogen, Karlsruhe
N, N, N', N'-Tetramethylethylenediamine (TEMED)	Sigma-Aldrich, Taufkirchen, Germany
Nonidet-p40 (NP40)	ROTH, Karlsruhe, Germany
Paraformaldehyde	Fisher, USA
Penicillin/(Streptomycin)	Invitrogen, Karlsruhe, Germany
Phosphate buffered saline (PBS)	Gibico, Invitrogen, Germnay
Phenylmethanesulfonyl fluoride (PMSF)	Sigma-Aldrich, Taufkirchen, Germany
Protein Marker	PeqLab, Erlangen, Germany
QuantiTect SYBR Green PCR kit	Qiagen, Hilden, Germany
RIPM Medium 1640	Gibico, Invitrogen, Germany
Ribonuclease inhibitor	Promega, Germany
Sodium chloride	ROTH, Karlsruhe, Germany

Sodium hydroxide (NaOH)	ROTH, Karlsruhe, Germany
Sodium dodecyl sulfate (SDS)	ROTH, Karlsruhe, Germany
Sodium dihydrogen phosphate ($NaHPO_4$)	ROTH, Karlsruhe, Germany
Sodium pyruvate	Invitrogen, Karlsruhe, Germany
3-(4,5-dimethylthiazol-2-yl)-2,5-diphenyltetrazolium bromide (MTT)	ROTH, Karlsruhe, Germany
Tamoxifen/4HO-Tamoxifen (OHT)	Selleckchem, USA
Tris base	ROTH, Karlsruhe, Germany
Triton x-100	ROTH, Karlsruhe, Germany
Trypsin (0.25%)-EDTA	Gibico, Invitrogen, Germany
Tween-20	ROTH, Karlsruhe, Germany

2.1.2 Instruments and consumables

Items	Source
Balance	Sartorius, Göttingen, Germany
Bio-Rad Electrophoresis equipment	Bio-Rad, München, Germany
Cylinders	Brand, Wertheim, Germany
Cell culture incubator	Heraeus, Fellbach, Germany
Cell culture plastic wares (flask, dishes, plates)	Greiner Bio-One, Frickenhausen
Cleaning bench	W. H. Mahl, Trendelburg, Germany
Confocal Microscope platform STELLARIS6	Leica, Germany
Cooling centrifuge for 15/50 ml falcons	Heraeus, Fellbach, Germany
Cooling centrifuge Eppendorf (1.5ml/2ml)	Eppendorf, Hamburg, Germany
Pipettor (20 µl, 200 µl, 1000 µl)	Thermo Scientific, Langenselbold
ELx 8080IU Ultra Microplate Reader	Bio-Tek Instruments, Rad Friedrichshall
End-over-end rotator	Heidolph Schwabach, Germany

Eppendorf tubes (1.5ml/2ml)	Eppendorf, Hamburg, Germany
Falcons (15ml/50ml)	Greiner Bio-One, Frikenhausen
Filter paper	Whatman, Opfikon (Switzerland)
Freezer (-20 ℃, -80℃)	New Brunswick Scientific, Edison (USA)
Glass pipettes	Brand, Wertheim, Germany
Incubation shaker for bacteria	Infors-HT, Bottmingen (Swizerland)
Inverted microscope	Leica, Wetzlar, Germany
Magnetic stirrer	IKA labortechnike, Stauffen, Germany
Microcentrifuge	Thermo Scientific, Waltham (USA)
Nanodrop ND-1000 Spectrophotometer	Peqlad, Erlenmeyer, Germany
PCR thermocycler	Perkin Elmer, Rodgau, Germany
PCR tubes	Corning, Amsterdam (Netherlands)
96-qPCR plate	Steinbrenner Laborsystem GmbH, Germany
96-qPCR sealing film	Steinbrenner Laborsystem GmbH, Germany
Pipette tips (yellow, blue, white)	Corning, Amsterdam (Netherlands)
PVDF membrane (immobilon-P®)	Millipore, Schwalbach, USA
Real-time PCR system StepOnePlus	Applied Biosystems/life technologies, Darmstadt, Germany
Refrigerator 4 ℃	Liebherr, Ochsenhausen, Germany
Thermo mixter	Eppendorf Hamburg, Germany
Trans-Blot ®Turbo™ Transfer Starter system	Bio-Rad, München, Germany
Vortexer	Julabo, Germany

2.1.3 Oligonucleotides

oligonucleotides	sequences

AGR2 forward primer	5'-GACC AAGCTTTGGATTTCATTTCTG-3'
AGR2 reverse primer	5'-CAGGTTCGTAAGCATAGAGACG -3'
APO-1 forward primer	5'-ACACCAAGTGCAAAGAGGAAGGAT-3'
APO-1 reverse primer	5'-GACC AAGCTTTGGATTTCATTTCTG-3'
AREG forward primer	5′-TGAGATGTCTTCAGGGAGTG-3′
AREG reverse primer	5′-AGCCAGGTATTTGTGGTTCG-3′
BAX forward primer	5’-TTG CTT CAG GGT TTC ATC CA-3’
BAX reverse primer	5’-AGA CAC TCG CTC AGC TTC TTG-3’
CDC6 forward primer	5’-GCTGTGCAGTTTGTTCAG-3’
CDC6 reverse primer	5’-GCTGAGAGGCAGGGCTTT-3’
CDC20 forward primer	5’-CCTCAGAAGCTGTTGGGATG-3’
CDC20 reverse primer	5’-AGAGTTCTGCCTCTGTGTGA-3’
GADD45A forward primer	5'-CTCAACGTCGACCCCGATAA-3'
GADD45A reverse primer	5'-GCCTGGATCAGGGTGAAGTG-3'
GREB1 reverse primer	5’-GAGTGACAATGAGGAAGAG-3’
GREB1 reverse primer	5’-CTCGTTGGAAATGGAGACAA-3’
OSGIN1 forward primer	5’-AGAAGAAGCGAAGAGGTC-3’
OSGIN1 reverse primer	5’-CGGACACAAAGTTATGCC-3’
PDZK1 forward primer	5'-GCAGGCTCAGAACAGAAAGG-3'
PDZK1 reverse primer	5'-TCCAGGGTTTCCACAGACTC-3'
p53 forward primer	5’-TGCGTGTTTGTGCCTGTCCT-3’
p53 reverse primer	5’-GTGCTCGCTTAGTGCTCC CT-3’
P21 forward primer	5’-GACTCTCAGGGTCGAAAACG-3’
P21 reverse primer	5’-GCGGATTAGGGCTTCCTCTT-3’
PUMA forward primer	5’-GACCTCAACGCACAGTACGAG-3’

PUMA reverse primer	5’-AGGAGTCCCATG ATG AGA TTGT-3’
PGR forward primer	5’-CTTAATCAACTAGGCGAGAG-3’
PGR reverse primer	5’-AAGCTCATCCAAGAATACTG-3’
pS2 forward primer	5’-CAATGGCCACCATGGAGAAC-3’
pS2 reverse primer	5’-AACGGTGTCGTCGAAACAGC-3’
Rib36B4 forward primer	5’-CCGGATATGAGGCAGCAG-3’
Rib36B4 reverse primer	5’-GAAGGCTGTGGTGCTGTAGG-3’
SLC7A11 forward primer	5’-ATGCAGTGGCAGTGACCTTT-3’
SLC7A11 reverse primer	5’-CATGGAGCCAAAGCAGGAGA-3’
UBE2C forward primer	5’-GGATTTCTGCCTTCCCTGAA-3’
UBE2C reverse primer	5’-GATAGCAGGGCGTGAGGAAC-3’

2.1.5 Antibodies

Primary Antibodies

Targets	Description	Source
β-actin	Mouse monoclonal	Santa Cruz
Estrogen receptor (ER)	Mouse monoclonal	Santa Cruz
BAG1	Mouse monoclonal	Santa Cruz
p53	Rabbit polyclonal	Invitrogen
MDM2	Rabbit polyclonal	Invitrogen
Mortalin	Mouse monoclonal	Santa Cruz

Secondary antibodies

Secondary antibodies	Source
Goat anti-Mouse HRP	Daka Demark
Goat anti-rabbit HRP	Daka Demark
Alexa Fluor 488 goat anti-mouse	Invitrogen

Alexa Fluor 546 goat anti-rabbit	Invitrogen

2.1.6 cell lines

Names	Description
MCF-7	An estrogen receptor positive breast cancer cell line isolated in 1970 from a 69-year-old white woman, MCF-7(Michigan Cancer Foundation-7) referring to the institute in Detroit where the cell line was established in 1973(Soule et al., 1973).
MDA-MB-231	An estrogen receptor negative breast cancer cell line that was established from pleural effusion of a 51-year-old Caucasian woman with a metastatic mammary adeno-carcinoma in 1978(Cailleau et al., 1978)
T47D	An estrogen receptor positive breast cancer cell line derived from the pleural effusion of a ductal carcinoma found in mammary gland of an elderly woman in 1982(Horwitz et al., 1982)
TRMCF-7	A Tamoxifen resistant human breast cancer cell line that derived from MCF-7 cells by long term treatment with the drug tamoxifen (Briand and Lykkesfeldt, 1984).
ZR-75-1	An estrogen receptor positive breast cancer cell line derived from the ascites of 63 year-old woman with ductal carcinoma in 1990(Darbre and Daly, 1990)

2.1.7 software

Microsoft word 2010, Microsoft Corporation; Microsoft word 2010, Microsoft Corporation, Microsoft excel 2010, Microsoft Corporation; GraphPad Prism6, GraphPad Software, San Diego, California, USA; StepOnePlus sofeware version2.3, Applied Biosystems, Darmstadt, Germany; FlowJo version 10.8.1, BD Bioscience, Germany; R 4.1.1 for windows 10 with all packages involve in transcriptomic data analysis.

2.2 Methods

2.2.1 Solution preparation

10% Ammonium persulfate (APS): 1 g APS dissolved in 10 ml sterilized water.

1 mg/ml Bovine serum albumin (**BSA)**: 10 mg BSA dissolved in 10 ml sterilized water.

10 mg/ml Cycloheximide (CHX): 10 mg Cycloheximide dissolved in 1 ml sterilized water. To be used as 1 to 1000 dilution.

1% NP-40 lysis buffer: 8.76 g NaCl, 50 ml 1 M Tris pH 8.0, 10 ml 500 mM EDTA, 10 ml NP-40, dissolved with sterilized water to 1 liter.

10% Sodium dodecyl sulfate (SDS): 10 g sodium-dodecyl-sulfate dissolved in 100 ml sterilized water.

50×TAE buffer: 242 g Tris base, 57.1 ml glacial acetic acid, 100 ml 0.5 M EDTA pH 8.0, dissolved with sterilized water to 1 liter.

20×TBS buffer: 264.4 g Tris-HCl, 38.8 g Tris base, 350.6 g NaCl and 8 g KCl dissolved in 2 liters sterilized water, pH adjusted to 7.4

TE buffer: 1 ml 1 M Tris pH 8.0, 200 µl 0.5 M EDTA pH 8.0, sterilized water added to 100 ml, autoclaved for sterilization.

1.5 M Tris pH 8.8: 45.43 g Tris base, add sterilized water to 250 ml, adjusted pH value to 8.8, autoclaved for sterilization.

1 M Tris pH 6.8: 45.43 g Tris base, sterilized water added to 250 ml, adjusted pH value to 6.8, autoclaved for sterilization.

10 × Western buffer: 290 g glycin, 58 g tris base dissolved in 2 liters sterilized water.

10 × Annexin V binding buffer: 0.1 M HEPES/NaOH (pH 7.4), 1.4 M NaCl, 25 mM CaCl2. For a 1X working solution, 1 part of the 10X Annexin V Binding Buffer was diluted to 9 parts of distilled water.

2.2.2 Cell culturing

MCF-7, T47D, ZR-75-1 and MAD-MB231 cells were cultured in standard conditions at 37°C, 5% of CO2 and 95% of humidity in an incubator (Steri Cult 200, Forma Scientific Labortech GmbH, Göttingen, Germany). All cell lines were cultured in sterile Cellstar Petri dishes (Greiner Bio-One, Nürtingen, Germany). Cells were confirmed to be mycoplasma-negative using the VenorGeM Classic Mycoplasma Detection Kit for conventional PCR machines (Minerva Biolabs, Berlin, Germany). Cells were cultured until confluency of 80-90% was reached. The cell culture medium was then removed and cells were carefully washed with 1x PBS (-MgCl2/-CaCl2). To detach cells from the culture vessel 0.5-1 ml of 0.25% Trypsin-EDTA were added to the cells and incubated for 5 min at 37°C. Trypsin action was stopped by adding at least tenfold volume of fresh medium to the cells. Cells were then transferred into a falcon tube and Trypsin was removed by centrifugation at 800 rpm for 3 min. Cells were taken up in fresh medium and seeded at the desired dilution. For long-term storage all mammalian cells were cultured on 15 cm2 cell culture plates until 80- 90% confluency was reached. The cells were then washed with 1x PBS (-MgCl2/-CaCl2) and were detached from the plate using 1 ml of 0.25% Trypsin-EDTA for 5 mi at 37°C. trypsin action was stopped by adding at least tenfold volume of fresh medium to the cells. Cells were then transferred into a falcon tube and Trypsin was removed by centrifugation at 800 rpm for 3 min. Cells were resuspended up in 2 ml of 90% (v/v) FCS and 10% (v/v) DMSO and 1 ml each was transferred in cryotube. The cells were slowly frozen at -80°C in freezing containers filled with isopropanol. To take frozen cells into culture cryotubes were thawed quickly (maximum 1 min) at 37°C in a water bath. Cells were then transferred into fresh medium and centrifuged at 800 rpm for 3 min (Biofuge Heraeus pico, rotor # 3328) to remove residual DMSO. Cells were taken up in fresh medium and plated onto new cell culture plate.

For hormone depleted medium cell culturing, MCF-7 and T47D cells were cultured in RPMI1640 minus phenol red (white medium) supplemented with 3% (v/v) charcoal-stripped FBS (CCS) and 1% penicillin/streptomycin) and 1% (v/v) L-Glutamine (Gibco, Invitrogen, Karlsruhe, Germany).

For tamoxifen resistant MCF-7 cell culturing, cells were cultured in RPMI1640 minus phenol red (white medium) supplemented with 3% (v/v) charcoal-stripped FBS (CCS) and 1% penicillin/streptomycin), 1% (v/v) L-Glutamine (Gibco, Invitrogen, Karlsruhe, Germany) and 10^{-7} M tamoxifen (Selleckchem, USA, cat# S1238).

2.2.4 RNA samples preparation

For RNA extraction 5 x 10^4 were cultured in 6-well wells in phenol red free RPMI 1640 medium enriched with 3% (v/v) charcoal-stripped FBS (CCS) for three days. Thereafter, cells were pre-treated with 10^{-8} M E2 for 1 h and then treated with 1 µM X15695 for 16 h. For RNA extraction from eukaryotic cells the innuPREP RNA Mini Kit (Analytic Jena AG, Jena, Germany) was used. The cells were washed with 1x PBS (-$MgCl_2$/-$CaCl_2$) and subsequently 400 µl RL Buffer (Lysis buffer) was added to the cells. Samples were incubated for 3 min at room temperature. Cell lysates were pipetted into a Spin Filter D which was placed into a receiver tube and centrifuged at 11.000 rpm for 2 min (Eppendorf centrifuge 5417R, rotor F45-30-11). Spin Filter D was discarded and the flow-through was transferred to a Spin Filter R column which was placed in a new receiver tube and centrifuged at 11.000 rpm for 2 min (Eppendorf centrifuge 5417R, rotor F45-30-11). The flow-through was discarded. The Spin Filter D was placed in a new receiver tube and was washed with 500 µl of washing solution HS and centrifuged at 11.000 rpm for 1 min (Eppendorf centrifuge 5417R, rotor F45-30-11). The filtrate was discarded and Spin Filter R was placed in a new receiver tube. In second washing step 700 µl of washing solution LS were added to the column and the column was centrifuged at 11.000 rpm for 1 min (Eppendorf centrifuge 5417R, rotor F45-30-11). The flow-through was discarded again and the column was dried from residual ethanol by empty centrifugation with a fresh collection tube for 3 min at 11.000 rpm. The Spin Filter D was then placed in a new 1.5 ml collection tube and 30 µl of RNAse-free water (Promega, Mannheim, Germany) were put directly to the spin column membrane. RNA was eluted by centrifugation at 8.000 rpm for 1 min. RNA concentration was measured using a NanoDrop ND-1000 (Thermo Fisher Scientific, Karlsruhe, Germany).

2.2.5 Synthesis of complementary DNA (cDNA)

For cDNA synthesis 1 µg of the DNase-free, purified RNA was incubated with 200 ng of Random Primer at 70°C. For qualitative and quantitative control of cDNA synthesis the reaction mixtures were split equally. Afterwards, 1 mM dNTPS (VWR, Darmstadt, Germany) and M-MLV reaction buffer (Promega, Mannheim, Germany) was added to both samples. As a negative control one reaction mixture was incubated without reverse transcriptase, while 200 u of M-MLV (Moloney Murine Leukemia Virus) reverse transcriptase (Promega, Mannheim, Germany) were added to the sample. The cDNA synthesis was carried out in a T100 Thermal Cycler (BioRad, Feldkirchen, Germany) with the following protocol:

Table 2. 1: **Protocol for reverse transcription**

Temperatures (°C)	Time (min)
25	10
42	60
70	10
8	infinity

2.2.6 cDNA concentration measurement

The concentration of synthesized cDNA was measured by Nanodrop ND-1000 Spectrophotometer (Thermo Fisher Scientific, Karlsruhe, Germany) with ssDNA (single strand) interface. After measurement, cDNA samples were diluted with nuclease free water to a final concentration of 50 ng/µl, stored at -20°C for further experiments.

2.2.7 Real time quantification PCR

For quantitative Real-Time PCR 4 µl cDNA (200 ng) were incubated with 10 pmol forward and reverse primers, 10 µl of 2x GoTaq qPCR Master Mix (Promega, Mannheim, Germany) and 4 µl of nuclease-free water (Promega, Mannheim, Germany). The reaction was performed with a final volume of 20 µl in a StepOnePlus Real Time PCR Reader with the following protocol:

Table 2. 2: Protocol for quantitative Real Time PCR

Steps	Temperatures (°C)	Time	Cycles
1	95	15 min	
2	95	15 sec	
3	60	30 sec	35 cycles from step2 to 4
4	95	15 sec	
5	60	1 min	

The fluorescence after intercalation of SYBR Green to double stranded DNA was detected. For each experimental set up a fixed threshold was defined in the exponential phase between cycles 15 and 40, when the PCR product exactly duplicates, to obtain comparable threshold cycles (C_t

values) for analysis. The relative mRNA expression of target genes was normalized by the C_t value of housekeeping gene Rib36B4 (human ribosomal subunit 36B4) and calculated by $\Delta\Delta C_t$ method.

2.2.8 RNA Sequencing

5×10^4 MCF-7 and T47D cells were seeded in 6-well plate and cultured with hormone-depleted medium for 3 days. Subsequently, cells were treated with 10 nM 17-β-estradiol (E2), 1 µM X15695 and 1 µM X15695 together with 10 nM E2, 1 h pretreatment of X15695 was performed prior to the E2 treatment. The same volume of DMSO treatment was used as vehicle group. The RNA samples were prepared with InnuPREP RNA mini kit 2.0 (Analytic Jena, Germany) as described in 2.2.4. The mRNA libraries were generated using IlluminaTruSeq standard mRNA sample kit I with 1 µ g of total RNA per sample. The library preparation and sequencing were performed by Novogene in UK. Fastq files were processed with Kallisto and mapped against the human references genome "Homo_sapiens.GRCh38.cdna.all", Differential expression analysis was performed using R package (limma) with Log2 fold changes ≥ 1 and p(FDR)≤0.05). Gene Ontology (GO) analysis and Gene Set Enrichment Analysis (GSEA) were performed by using R packages including GSEABase, Biobase, gprofiler2, clusterprofiler and msigdbr with Molecular Signature Database(GSEA | MSigDB (gsea-msigdb.org))

2.2.9 protein sample preparation

Cells were washed with 1×PBS and centrifuged to get cell pellet, an acquired amount of 0.5% NP-40 lysis buffer that contains 1 mM PMSF was added to the samples. Pellet was re-suspended with lysis buffer by pipetting up and down and then incubating on the ice for 10 min. Cells were furtherly lysed by sonification for 3 min and incubated on ice for 10 min. Samples were then centrifuged at 14000 rpm (Eppendorf centrifuge 5417R, rotor F45-30-11) for 10 min at 4°C to remove cellular debris. The supernatant was transferred to a new tube and stored at -20°C for further use.

2.2.10 Protein concentration Measurement

Two µl of proteins samples were mixed with 500 µl Bradford solution and labeled as test group, 2 µl of NP40 lysis buffer were mixed with 500 µl Bradford solution and served as blank group. Two µl of serial dilution with the indicated concentration of BSA samples were mixed with 500 µl Bradford solution to construct standard curve. A hundred and fifty µl of the mixture were transferred to 96-well plate and triple assays were set for each sample. The absorbance of the

samples was measured with an ELISA reader (ELx808 Ultro Microplate Reader, Bio-Tek) at 550 nm wave length. The data of protein samples were calculated with an Origin 2019b software.

2.2.11 SDS-PAGE

Protein samples were denatured with 2×loading buffer at 95°C for 10 min, and then separated by SDS-PAGE (sodium dodecyl sulfate polyacrylamide gel electrophoresis) using a mini-gel electrophoresis device. Basically, Proteins were separated according to their sizes by SDS-PAGE (sodium dodecylsulfate polyacrylamide gel electrophoresis) (Laemmli, 1970). Therefore, 10% (v/v) polyacrylamide gels (10% (v/v) Rotiphorese Gel 30; 375 mM Tris-HCl, pH 8.8; 0.1% (v/v) SDS; 0.1% (v/v) APS; 0.4% (v/v) TEMED) were cast in SDS-PAGE apparatus (BioRad, Mini-PROTEAN® Tetra Vertical Electrophoresis Cell, Feldkirchen, Germany). To ensure straight edges the separating gel was overlaid with Isopropanol, which was removed after polymerization of the gel. On top of the separating gel a 5% (v/v) stacking gel (5% (v/v) Rotiphorese Gel30; 125 mM Tris-HCl, pH 6.8; 0.1% (v/v) SDS; 0.1% (v/v) APS; 1% (v/v) TEMED) was cast and a comb was placed on top to allow the formation of sample pockets. The electrophoretic separation was performed in 1xSDS-PAGE running buffer (25 mM Tris Base, 200 mM Glycine, 0.1% (w/v) SDS) in the running chamber. The desired amount of cell lysate was diluted in sample buffer, boiled at 95°C for 5 min and was loaded onto the SDS gel. Electrophoresis was performed at 120 V until the bromophenol blue reached to the bottle of the gels.

2.2.12 Western blotting and immunodetection

After the SDS-PAGE, the protein on the gel was transferred onto a PVDF (polyvinylidene difluoride) membrane by using a trans-blot Bio-Rad transferring system. Briefly, three pieces of Whatman filter paper which have similar sizes to the gel were equilibrated with transfer buffer and laid onto the blotting device. The equilibrated PVDF membrane was placed on the top of the paper, the gel was placed on the top of the PVDF membrane and one piece of equilibrated paper was placed onto the gel. The bolting device was closed and placed into a blotting chamber. The chamber was filled with transfer buffer. The blotting was performed at 30 V overnight. The next day. The membrane was stained with ink for 5 to 10 min. The membrane was then placed in 5% (w/v) milk solution and incubated on the shaker at room temperature for 1.5 h for blocking antibody unspecific binding. The membrane was washed three times with 1×TBST buffer and cut into different pieces according to the molecular weight of the target proteins. The primary antibodies (mouse anti-human ER antibody, mouse anti-human mortalin antibody, mouse anti-human BAG1 antibody, mouse ant-human p53 antibody and mouse anti-human β-actin antibody)

were diluted in the required dilution with 5% milk solution. The membrane was incubated with its counterpart antibody solutions at room temperature on the rotator for 1.5 h. The membrane was washed again with 1×TBST buffer five times to remove unbound antibody. The secondary goat anti-mouse antibodies were diluted at 1:2000 dilution (v/v) in 5% milk solution (w/v) and incubated with the membrane at room temperature on the rotator for 1 h. The membrane was washed six times with 1×TBST buffer and developed with mixture of ECL solution I and II in ChemiDoc Imager (Bio-Rad, USA).

2.2.13 Co-immunoprecipitation

Prior to immunoprecipitation, 90% protein A and 10% protein G agarose beads were incubated with the desired antibodies at 4°C overnight. Agarose beads incubated with anti-IgG was used in control group. The next day, the agarose beads were blocked with 10 % BSA solution (w/v) at room temperature for 1 h, and the agarose beads were washed with 1×PBS and centrifuged at 4°C, the supernatant was removed and 500 µl of cell lysates were mixed with agarose beads and incubated at 4℃ for 1.5 to 3 h. Samples were centrifuged at maximal speed for 10 s, the supernatant was removed and the agarose beads were washed three times with lysis buffer. Forty µl of 2xloading buffer was added to the agarose beads and the mixture was heated for 10 min at 95°C. The samples were loaded onto polyacrylamide gel. The SDS-PAGE and immunoblotting were performed according to the procedure describe in section 2.2.11 and section 2.2.12.

2.2.13 MTT assay

10^4 MCF-7 and T47D cells were cultured with hormone-depleted medium in 96 well plate for three days. Cells were then treated with tamoxifen or increasing concentrations of X15695 (10^{-10} to 10^{-6} M) in the absence and presence of E2 for 48 h. The culture medium was carefully aspirated, and 200 µl serum-free medium containing 5 mg/ml MTT (3-(4,5-dimethylthiazol-2-yl)-2,5-diphenyltetrazolium bromide, MTT) was added to each well and incubated in an incubator (Steri Cult 200, Forma Scientific Labortech GmbH, Göttingen, Germany) at 37℃ with 5% of CO2 and 95% of humidity for 4 h for the formation of formazan crystals. After incubation, the medium was carefully removed, 150 µl Isopropanol was added to each well. The plate was wrapped in foil and shaken on an orbital shaker for 15 to 20 minutes. After MTT formazan was fully dissolved, the optical density (OD) was measured with an ELISA reader (ELx808 Ultro Microplate Reader, Bio-Tek) at wave length of 590 nm.

2.2.14 Clonogenic assay

Cells were cultured as described in section 2.2.2.1 and after they reached to 90% confluency, the culture medium was removed and the cells were carefully washed with 1x PBS (-MgCl2/-CaCl2). To detach cells from the culture vessel 0.5-1 ml of 0.25% Trypsin-EDTA were added to the cells and incubated for 5 min at 37°C. Trypsin action was stopped by adding at least tenfold volume of fresh medium to the cells. Cells were then transferred into a falcon tube and Trypsin was removed by centrifugation at 800 rpm for 3 min. Cells were resuspended in fresh medium, counted and diluted to 1000 cells/ml. One ml of cell suspension was added to 6-well plate, extra 2 ml medium was added to each well to keep all wells at a total volume of 3 ml. Three µl of compounds with indicated concentrations (10^{-8} to 10^{-4} M) were added to each well. The same volume of DMSO was used as control and labeled 'vehicle'. Cell medium containing the indicated concentrations of the compounds was changed once a week. When formation of the colonies in the vehicle groups was visualized in 2 or 3 weeks, the cell medium was removed and rinsed carefully with 1× PBS. One ml fixation buffer (v/v, methanol: acetic acid = 1:1) was added to the well and incubated for 15 min at room temperature. The fixation buffer was removed and 1 ml 0.5% crystal violet solution (v/v) was added and incubated at room temperature for 20 minutes. Crystal violet solution was removed and the plates were rinsed with tap water. The plates were scanned and the colony area of each well was quantified with an ImageJ software.

2.2.15 The cellular thermal shift assay (CETSA)

2.2.15.1 Determination of the apparent melting curve by CETSA

CETSA was performed essential as described by Jafari with minor modifications (Jafari et al., 2014). In brief, cells were cultured to a density of 2×10^6 cells/ml. Fifteen ml of 2×10^6 cells/ml cell suspension was placed in two separate T75 flasks and 15 µl 10^{-3} M compound X15695 was added to one flask and labelled as 'X15695'. The same volume of DMSO was added to another flask and labelled 'Vehicle'. The flask was gently shaken to mix the cells and compound and incubated in the CO_2 incubator at 37°C for 1h. The cell suspension was collected with sterilized pipette, transferred to a marked 15 ml Falcon tube and centrifuged at 300 g for 3 min at room temperature. After centrifugation, the medium was discarded and the cells were washed with 10 ml PBS and centrifuged again at 300 g for 3 min at room temperature. Cell pellet was resuspended in 900 µl PBS by pipetting up and down. Cell suspension was evenly distributed into 8 different 0.2 ml PCR tubes with 100 µl in each tube. Each tube was labelled and heated with at the designed temperature in 96-well thermal cycler for 3 min. Afterwards, the tubes were immediately placed

at room temperature for 3 min and the sample tubes were snap-frozen in liquid Nitrogen for 20 s and immediately placed in a 96-well thermal cycler at 25°C for 3 min. The freeze-thaw cycle was repeated two times to ensure a uniform temperature between tubes. The sample tubes were shortly vortexed after each thawing. The sample tubes were placed on ice after the last freeze-thaw step for 3 min. The samples were then centrifuged at 20000 g for 20 min to pellet cell debris and denatured protein precipitate. 90 µl of each supernatant with soluble proteins was carefully transferred into new tubes. The samples were stored in -20°C or applied to SDS-PAGE and Western blotting experiments as described in 2.2.11 and 2.2.12, respectively. After acquiring the data, the results were first normalized by setting the highest value and lowest value in each set to 100% and 0%, respectively. Data were then fitted to obtain T_{agg} values using Boltzmann Sigmoid equation within GraphPad.

2.2.15.2 Determination of the isothermal dose-response fingerprint by CETSA

Cells were cultured to a density of 4×10^7 cells/ml and 15 µl of 4 mM DMSO stock solution of X15695 was placed in 3 separate well of the first column in a 96-well plate. Ten µl DMSO was placed in the rest of the columns (column 2 to column 12). The stock solution was serially diluted by transferring 5 µl from column 1 to column 2, mixing it thoroughly by pipetting up and down, then transferring 5 µl from column 2 to column 3. After through mixing, the process was continued until to the last column. The serial dilution was then split into two by transferring 5 µl of all solution to a second 96-well plate and was frozen at -20°C as backup. All serially diluted solutions were then diluted 50 folds by the addition of cell culture medium. Five µl of all diluted solution transferred into a 96-well qPCR plate and 15 µl cell suspension (4×10^7 cells/ml) was added to each well in the plate. The plate was incubated at 37°C in a CO_2 incubator for 30 min. The plate was carefully shaken for every 10 min to promote access of the cells to the compound. After 30 min incubation, the plate was placed in the thermal cycler and heated for 3 minutes at 58°C. The plate was then placed at room temperature for 3 min to ensure consistent cooling in the wells. A freeze-thaw cycle was performed 3 times as described in section 2.2.15.1. The samples were then centrifuged at 20000 g for 20 min to pellet cell debris and the denatured protein precipitate and stored at -20°C for further use or directly loaded on a SDS-PAGE and Western blotting was performed as described in section 2.2.11 and 2.2.12, respectively. After acquiring the data, the data were first normalized by setting the highest value and lowest value in each set to 100% and 0%, respectively, data were then analyzed by applying saturation binding curve (rectangular hyperbola; binding isotherm) function within GraphPad.

2.2.16 Immunofluorescence assay

Cells were seeded and treated with the desired conditions on a coverslip inside a 24-well plate. On the following day, cells were washed 3 time with 1×PBS for 5 min and fixed with 4% paraformaldehyde solution for 10 min at room temperature. Then cells were washed 3 time with 1×PBS for 5 min and permeabilized with 0.5% Triton-x-100 for 10 min at room temperature. The cells were washed 3 time again with 1×PBS for 5 min and blocked with 5% BSA (w/v) for 1 h at room temperature. The coverslip was taken out from the plate and placed face-up on parafilm with wet Whatman-paper. Thirty µl of primary antibodies (rabbit anti-human p53 antibody, mouse anti-human ER antibody) with 1:50 (v/v) dilutions were added drop-wise to the coverslip and incubated overnight at 4℃. The coverslip was then put back onto the 24-well plate with the cells on the coverslip facing up. The cells were washed 3 times with 1×PBS for 5 min. Two hundred µl of secondary antibodies (Alexa Fluor 488 goat anti-mouse, Alexa Fluor 546 goat anti-Rabbit) with 1:200 (v/v) dilutions were directly added to the cells and incubated at room temperature for at least 1 h. All subsequent steps were performed in the dark. Namely, the cells were washed 3 times with 1×PBS for 5 min and 200 µl of DAPI solution with 1:10000 (v/v) dilution was added on the coverslip and incubated for 15 min at room temperature. The cells were again washed 3 times with 1×PBS for 5 min. One drop of mounting medium was added onto a clean slide and the coverslip was placed face-up onto the mounting medium. The slide was placed in the dark room for 1 to 2 days to allow the mounting medium to dry. Seven percent ethanol was used to remove the extra mounting medium from the edge of the coverslip. The immunofluorescence signal was detected by confocal microscopy (Confocal Microscope platform STELLARIS6-LSM900, Leica, Germany).

2.2.17 Fluorescence activated cell sorting (FACS) measurements assay

2.2.17.1 Single staining for cell cycle analysis

10^6 cells (MCF-7 and T47D) were cultured in two separate dishes and labeled ‘vehicle’ and ‘treated’ groups respectively. Cells in the treated group treated with 1 µM of x15695, while cells in the vehicle group treated with the same volume of DMSO. After 48 h treatments, cells were harvested and suspended in PBS to prepare single cell suspension. The single cells suspension was centrifuged and resuspended cell in 150 µl PBS. Five ml of ice-cold 70% Ethanol was added dropwise to the cells while vortexing and fixed overnight at 4°C. The fixed cells were then centrifuged at 1,500 rpm (Biofuge Heraeus pico, rotor # 3328) for 5 min to remove the ethanol and resuspended in PBS. After counting, the cells suspension was adjusted to a density of 10^6

cells per 100 µl. One hundred µl cell suspension (10^6 cells) was used for 7-AAD (7-Amino-Actinomycin) straining. An extra of 400 µl PBS was added to diluted the stained cells for FACS (Fluorescence activated cell sorting) measurements. The same number of cells without 7-AAD staining were used for normalization.

2.2.17.2 Double staining for cell apoptosis analysis

MCF-7 and T47D cells were cultured and processed essentially as described in section 2.2.17.1 except that after preparation of the single cell suspension, cells suspension was adjusted to a density of 10^6 cells per 100 µl with 1× Annexin V binding buffer. 100 µl cell suspension (10^6 cells) was applied to 7-AAD and Annexin-V PE straining. An extra 400 µl Binding buffer was added to diluted the stained cells for FACS (Fluorescence activated cell sorting) measurements. Cells without Annexin V and 7-AAD were used for normalization. Cells singly stained with either Annexin V or 7-AAD were used to set up compensation.

2.2.18 Synthesis of imidazopyridine derivatives

Synthesis of compounds with imidazopyridine-based scaffolds was generously carried out by Complat, KIT and made available for this study.

2.2.19 Statistical analysis

All experiments were conducted at least three times. Statistical differences between two groups were analyzed by double tailed Student's T test. For comparison of more than two groups, one-way ANOVA or two-way ANOVA multiple comparison test were used and the p values were calculated by post hoc Tukey's or Sidak's Test with Bonferroni's correction. Data was presented as mean ± SEM, and p value ≤ 0.05 was considered as statistically significant. * $p \leq 0.05$; ** $p \leq 0.01$; *** $p \leq 0.001$ and ***** $p \leq 0.05$, ns represents non-significant.

Chapter 3: Results

3.1 Compound screening in human breast cancer cell lines

Benzothiazoles are one of the pharmacologically privileged rings with potent antitumor activity. Over the past decade, numerous benzothiazole scaffold-based protein inhibitors have been developed and evaluated for targeted therapy in cancers (Haider et al., 2021). Previous research work in our laboratory also reported on a benzothiazole-based scaffold compound termed A4B17 which docks into the BAG domain of the cochaperone BAG1 to inhibit some of the known functions of this protein, such as the its ability to regulate androgen receptor (AR) action and prostate cancer cell growth (Kuznik et al., 2021). A4B17 also exerted an inhibitory effect on the proliferation of estrogen receptor positive (ER^+) breast cancer cell lines (Kuznik et al., 2022), in line with the known action of BAG1 as an activator of ER activity (Cutress et al., 2003).

To build up on the later finding and to develop a more effective BAG1 inhibitor that would better inhibit prostate and breast cancer cells. An *in-silico* screening of 10 million compounds was carried out by Dr. Ravi Munuganti, Vancouver Prostate Centre, Canada, based on the pharmacophore features of Thio-2, another benzothiazole-based compound that we have previously described to inhibit the AR activity in prostate cancer cells via BAG1 (Cato et al., 2017). Fifty compounds were shortlisted that contained benzothiazoles, imidazopyridines, benzoxazoles, pyrazolopyrimidines and benzofurans scaffolds. A focused screen of these compounds for their ability to inhibit clonal expansion of breast cancer cells identified compounds with the imidazopyridine scaffolds as the best inhibitors of ER^+ breast cancer cell proliferation. Therefore, this project started with 17 imidazopyridine derivatives of the core structure that was identified to screen for inhibitors of ER positive breast cancer cells.

To identify the most potent inhibitors among the 17 imidazopyridine derivates for the inhibition of ER^+ breast cancer cells, clonogenic assay was carried out to evaluate the IC_{50} of each compound. This was performed by allowing a set number of cells in the presence or absence of different concentrations of compounds to grow and form colonies over two to three weeks. The colonies were then fixed and stained and quantified to determine which compounds augmented the growth of the cells. The first round of clonogenic assay was conducted in MCF-7 breast cell line and four compounds X15695, X15696, X19724 and X19728 were identified as the most potent based on their concentrations required to reach half-maximal inhibition (IC_{50} = 3.5±1.7 nM), 7.9±1.9 nM, 3.3±0.9 nM, and 6.0±2.4 nM) (see Table 1). These four compounds were counter

selected in three other breast cancer cell lines ZR-75-1 (ER^+), T47D cell line (ER^+) and MDA-MB231 cell line (ER^-). These studies identified compound X15695 as the most potent among the 4 selected compounds with the lowest IC_{50} in MCF-7 cells (IC_{50} = 3.5±1.7 nM), ZR-75-1 cells (IC_{50} = 7.3±1.6nM) as well as in T47D cells (IC_{50} = 10.4±2.8 nM). However, all 4 compounds had no effect on the inhibition of ER^- MDA-MB231 cell proliferation (Table 3.1 and Figure 3.1).

Table 3. 1: imidazopyridine derivates screening in human breast cancer cells

Compounds	MCF-7 (ER^+)	ZR-75-1 (ER^+)	T47D (ER^+)	MDA-MB231 (ER^-)
	IC_{50} (nM)	IC_{50} (nM)	IC_{50} (nM)	IC_{50} (nM)
X15695	3.5±1.7	7.3±1.6	10.4±2.8	n.d.
X15696	7.9±1.9	10.2±2.7	44.7±11.4	n.d.
X19151	135.6			
X19167	486			
X19168	12			
x19712	2846			
x19718	720.2			
X19719	12.9			
X19720	14.5			
X19724	3.3±0.9	154.3±37.5	86.1±69.2	n.d.
x19725	66.99			
X19726	84.63			
X19727	19.17			
X19728	6.0±2.4	39.2±24.3	153.3±67.9	n.d.
X19729	20.83			
X19147	18.3			
X19148	228.3			

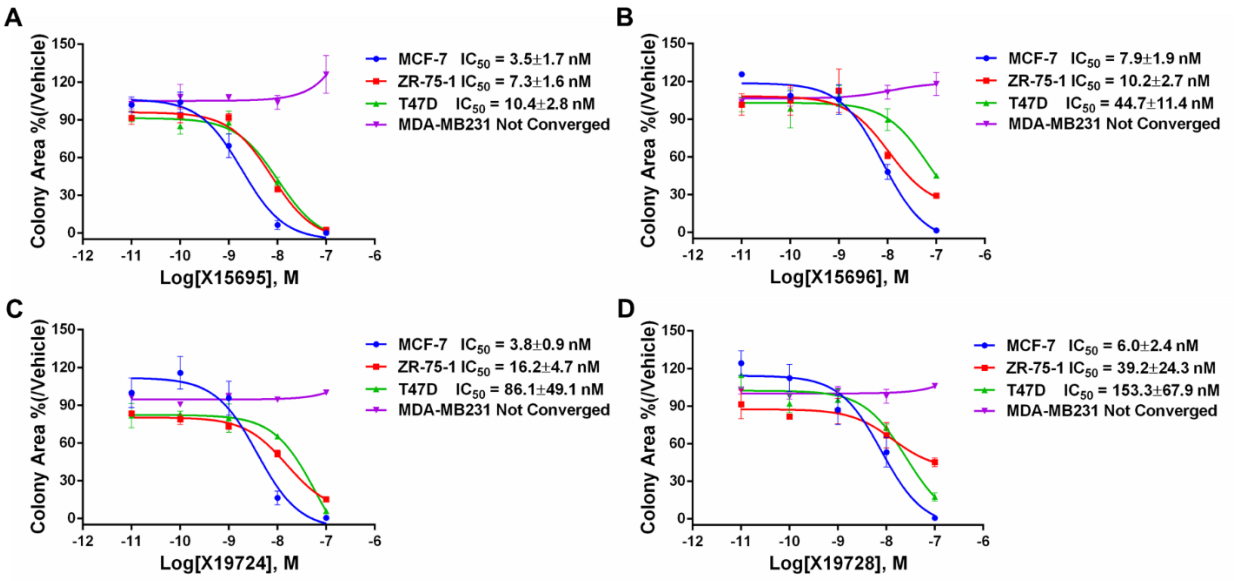

Figure 3. 1: Clonogenic assay of selected compounds in breast cancer cells.
MCF-7 and MDA-MB-231 cells were seeded on 6-well plate at density of 1000 cells/well; ZR-75-1, T47D were seeded on 6-well plate at density of 2000 cells/well. Cells were treated with the indicated serial concentration of X15695, X15696, X19724 and X19728, respectively. Cell medium with indicated concentration of compounds was changed every week. MCF-7 and MDA-MB231 cells were fixed and stained after 2 weeks compounds treatment, ZR-75-1 and T47D cells were fixed and stained after 3 weeks compounds treatment. The colony area of each well was quantified by ImageJ software and the concentrations for half maximal inhibition (IC_{50}) for X15695 (A), X15696 (B), X19724 (C) and X19728 (D) were calculated with a built-in function within GraphPad Prism. Each assay contains 3 biological replicates. The values are the averages ± SEM.

3.2 X15695 is as potent as 4OH-tamoxifen for the inhibition of proliferation in ER^+ breast cancer cells

Imidazopyridine have been expeditiously used for the rationale design and development of novel synthetic analogs in different therapeutic applications (Khatun et al., 2021) and several novel imidazopyridine derivatives have been developed for the targeted therapies in multiple cancers (Damghani et al., 2021; El-Awady et al., 2016). To demonstrate the efficacy of compound X15695 as an inhibitor of breast cancer cell proliferation, its action was compared with two classical ER antagonists (4OH-tamoxifen and fulvestrant) in a clonogenic assay in MCF-7 cells. Figure 3.2A is a representative image of the experiment while Figure 3.2B is the quantification of the results.

Figure 3.2B shows that both X15695 and OHT have IC_{50} values in the nanomolar range, while fulvestrant was over an order of magnitude more potent than the two.

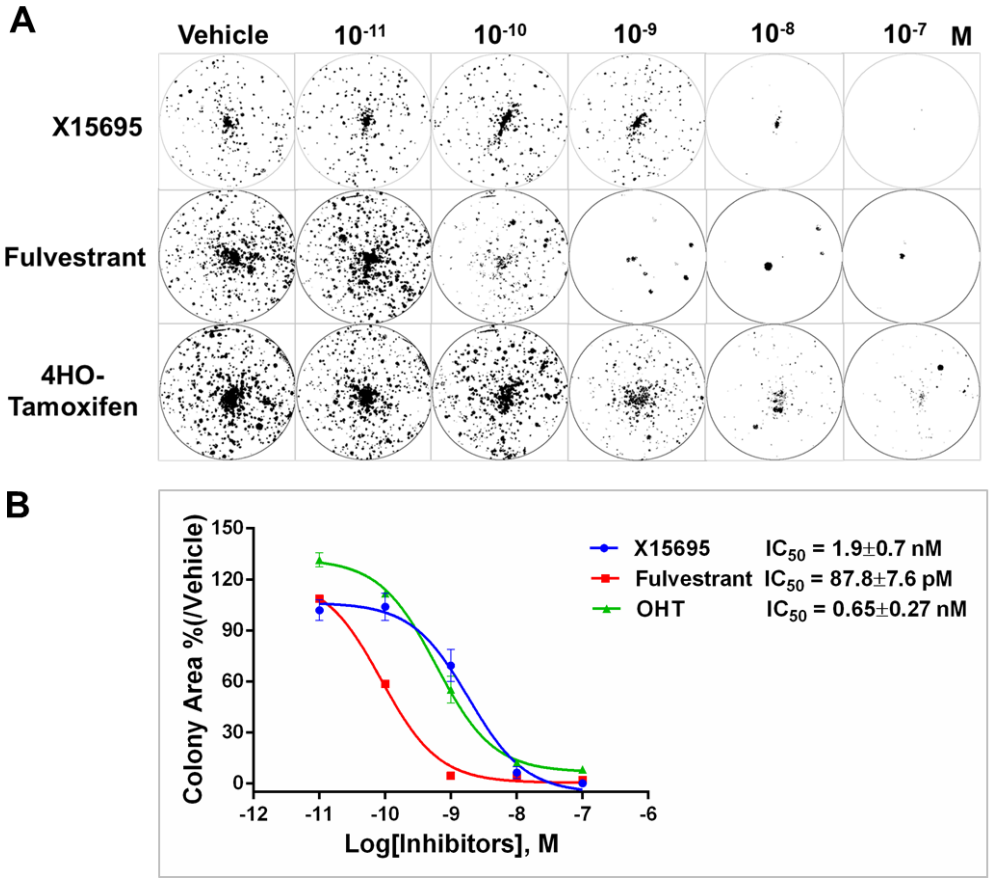

Figure 3. 2: Clonogenic assay of X15695, 4OH-tamoxfen and fulvestrant in MCF-7 cells.
(A). MCF-7 cells were seeded in 6-well plate at 1000 cells/well. Cells were treated with the indicated serial concentrations of X15695, 4OH-tamoxifen and fulvestrant respectively. Cell medium with the indicated concentration of compounds was changed every week. Cells were fixed and stained after 2 weeks of compounds treatment and the colonies area of each well was analyzed by ImageJ software, the IC_{50} of X15695, fulvestrant and 4OH-tamoxifen were calculated with a build-in function within GraphPad Prism. Each assay contains 3 biological replicates. The values are the averages ± SEM.

3.3 Target engagement of X15695

An assessment of the interactions between a drug and its protein target in a physiologically relevant cellular environment constitutes a major challenge in pre-clinical drug discovery. This

challenge can be met by the recently developed cellular thermal shift assay (CETSA) that quantifies the changes in the thermal stability of proteins upon ligand binding in intact cells (Martinez Molina et al., 2013). A protein melting temperature will change upon ligand interaction. Thus, by heating cells (treated with vehicle or compound) to different temperatures, and quantifying proteins in the soluble fraction, one can detect altered protein interactions after for example drug treatment. This can be done for selected proteins of interest by detecting the changes in a Western blot assay.

3.3.1 Apparent melting curve of BAG1 was shifted in response to X15695 treatment

MCF-7 cells were treated with 1 µM X15695 or vehicle (DMSO) for 1 h and subjected to serial temperature treatments ranging from 37℃ to 62℃, then the cells were experienced freeze-thaw cycles to release the soluble proteins and to keep samples under the identical temperature. After centrifugation, the BAG1 proteins remaining in the supernatant was measured by Western blotting after removing the aggregated protein precipitate under the indicated temperature incubation. The results of the Western blot gels show that for all three BAG1 proteins (BAG1L, BAG1M and BAG1), the intensity of the bands in the cells treated with X15695 persisted at higher temperatures compared with the BAG1 proteins from the vehicle treated cells (Figure 3.3A). Quantification of the bands from three different experiments relative to the control β-actin band showed that the BAG1 bands in the X15695 treated samples were indeed more stable than the protein bands from the vehicle treated cells (Figure 3.3B). The apparent melting curves of all three BAG1 isoforms were shifted to the right under X15695 treatment compared to their vehicle with an average T_{agg} of 58℃. The ΔT_{agg} of the BAG1 isoforms vary from 1 to 3℃ under the condition of X15695 treatment (Figure 3.3). The temperature 58℃ was therefore used for the determination of the isothermal dose response fingerprints.

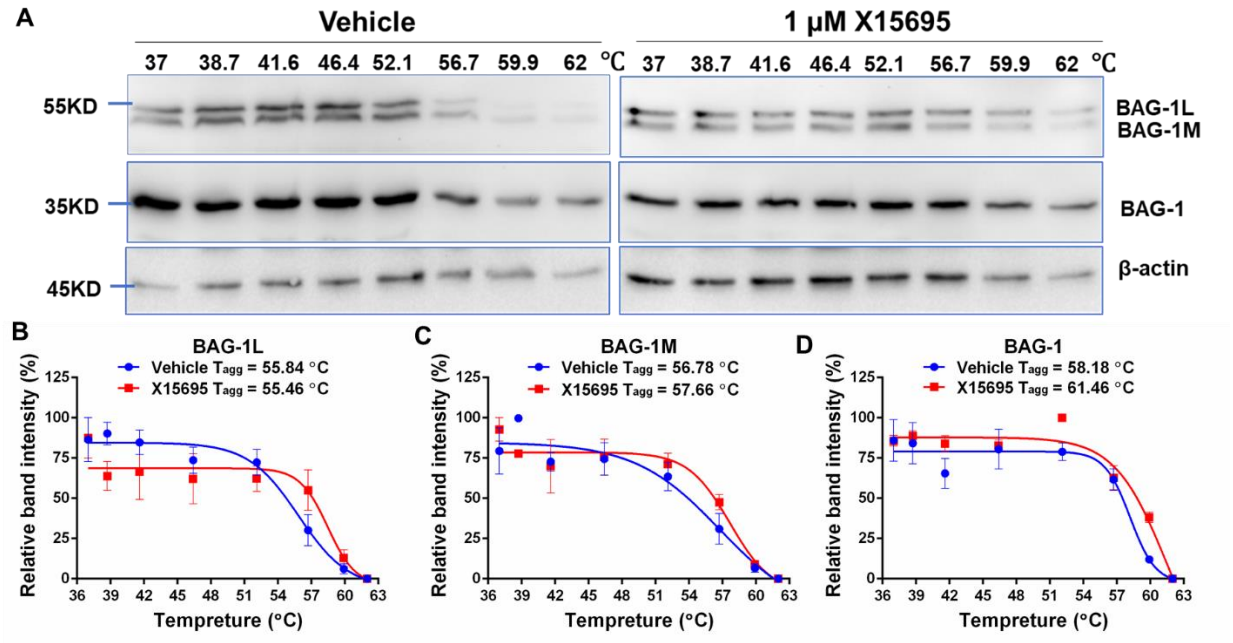

Figure 3. 3: CETSA to determine the engagement of X15695 to BAG1.
(A). MCF-7 cells were incubated with 1 μM X15695 or the same volume of DMSO for 1h, then cells were evenly distributed into 8 PCR tubes and heated in the temperature series (37℃ to 62℃) for 3 minutes, followed by freeze-thaw cycles in liquid nitrogen for 3 times. Cell debris and denatured proteins were removed by centrifugation and the supernatant was used for Western blotting using anti-BAG1 and anti-β actin antibodies. The band intensities were quantified by ImageJ software. The data were fitted to obtained T_{agg} of BAG-1L (B), BAG-1M (C), and BAG-1 (D) using the Boltzmann Sigmoid equation within GraphPad Prism. 3 biological repeats were used for data analysis. The values are the averages ± SEM.

3.3.2 Affinity of interaction of X15695 with BAG1 as determined by isothermal dose response fingerprints experiment of CETSA

To investigate the affinity of X15695 for BAG1, the isothermal dose response fingerprints experiment was performed under serial concentration of X15695 treatment at 58℃. The experiment was conducted essentially as described for the determination of the aggregation temperature T_{agg} except that a fixed temperature 58℃ was used and the incubation of the cells with the compound was carried out over a range of concentrations varying from 0.34 nM to 741 nM. The concentration of X15695 to achieve half-maximal binding to the BAG1 targets was calculated by fitting to a built-in function within GraphPad Prism called" One site—Specific binding". The affinity of X15695 with all the BAG1 proteins was in the nanomolar range (Kd_{BAG1L}

23.4 nM; Kd_{BAG1M} 7.52 nM; Kd_{BAG1} 2.75 nM) which is consistent with the IC_{50} value for the inhibition of breast cancer cell proliferation (Figure 3.4).

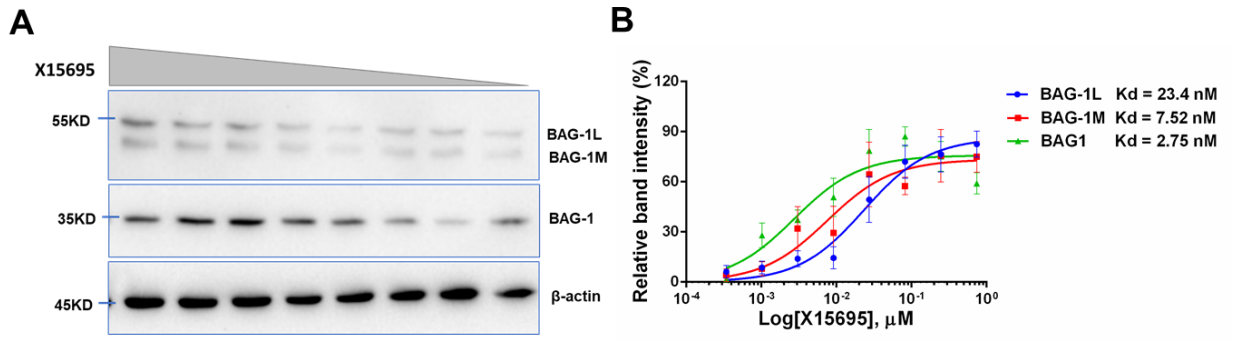

Figure 3. 4: Isothermal dose response fingerprint (ITDRFCETSA) for the engagement of X15695 to BAG1

(A). MCF-7 cells were incubated with increasing concentration of X15695 from 0.341 nM to 741 nM for 30 minutes, then cells were incubated at 58℃ for 3 minutes followed by a three-time freeze-thaw cycles in liquid nitrogen. Cell debris and denatured proteins were removed by centrifugation and the supernatant as used for Western blotting experiment using anti-BAG1 and anti-β actin antibodies. The band intensity was quantified by ImageJ software and the data were analyzed by applying One site—Specific binding function within GraphPad Prism. Three biological repeats were used for data analysis. The values are the averages ± SEM.

3.4 Transcriptomic data analysis of MCF-7 cells in response to X15695 treatment

Having established that X15695 binds to BAG1 in MCF7 cells, the next question was to find out whether it would influence global gene expression more specifically whether it would affect ER response. MCF-7 cells were therefore treated with vehicle, 17-β-estradiol (E2), X15695 and a combination of E2 and X15695. RNA was prepared and submitted to Novogene (Cambridge, UK) for transcriptomics analysis.

After the delivery of the sequencing results, the dataset was firstly analyzed by FastQC for the assessment of quality control of the RNA-sequencing samples. The QC (quality control) report indicated the total raw reads, the raw bases of the reads, the sequencing error and GC content distributions as well as other parameters for quality control were all passed the test (data not shown). Therefore, RNA-sequencing data were valid for data analysis. To analyze the RNA-sequencing data, the raw reads of the sequence was quantified by Kallisto with quant function

to acquire the abundance (Transcript per Million Read, TPM) (Appendix Figure 5.1A), then an edgeR package was used for data wrangling, such as to convert the data from TPM to CPM (Counts per Million Read) (Appendix Figure 5.1B), to filter data from outliers (Appendix Figure 5.1C) and also to normalize the filtered data (Appendix Figure 5.1D). Once all settled, the data were used for sample clustering and principle components analysis (PCA). Both Sample clustering and PCA showed the samples have a clear discrepancy among different conditions and high consistency in the same conditions (Appendix 5.2), suggesting the data were valid for differentially expressed gene analysis and functional enrichment analysis.

To identify differentially expressed genes in response to X15695 in the presence or absence of E2, limma package was used for the comparison of X15695 treatment in the absence of E2 (X15695 vs. Vehicle) and in the presence of E2 (X15695+E2 vs. E2). A Fold change of Log_2(CPM) ≥ 1.0 or ≤ -1.0 was considered as a highly differential expression and an adj. p value ≤ 0.05 used as threshold to cut off non-significantly regulated genes. The results are shown as volcano plots where in the absence of E2 a total of 531 DEGs was acquired - 327 DEGs were down-regulated and 204 DEGs were up-regulated (Figure 3.5A). In the presence of E2, a total of 439 DEGs were obtained - 238 DEGs were down-regulated and 201 DEGs were up-regulated (Figure 3.5B). The upregulated genes were plotted as red dots and the down-regulated genes were plotted as blue dots. Genes that were considered as non-significantly regulated were plotted as grey dots.

To reveal the molecular mechanism of how X15695 affects MCF-7 cells behaviors. Gene set enrichment for hallmark pathway analysis was performed with GSEAbase package, FDR ≤ 0.2 was set as cutoff for non-significantly enriched pathways. The 531 genes differentially expressed genes in response to X15695 were most significantly enriched in p53 pathway, followed by several cell death linked pathways, such as pathway response to UV, hypoxia and apoptosis (Figure 3.5C). In the presence of E2, the 439 DEGs were most significantly enriched in pathways related to estrogen response followed by p53 pathway. Besides, several pathways linked to cell death were also significantly enriched in this condition, such as pathways linked to apoptosis, UV response and inflammatory stress (Figure 3.5D). Some representative DGEs of the p53 and ER signaling pathways are marked in the volcano plots.

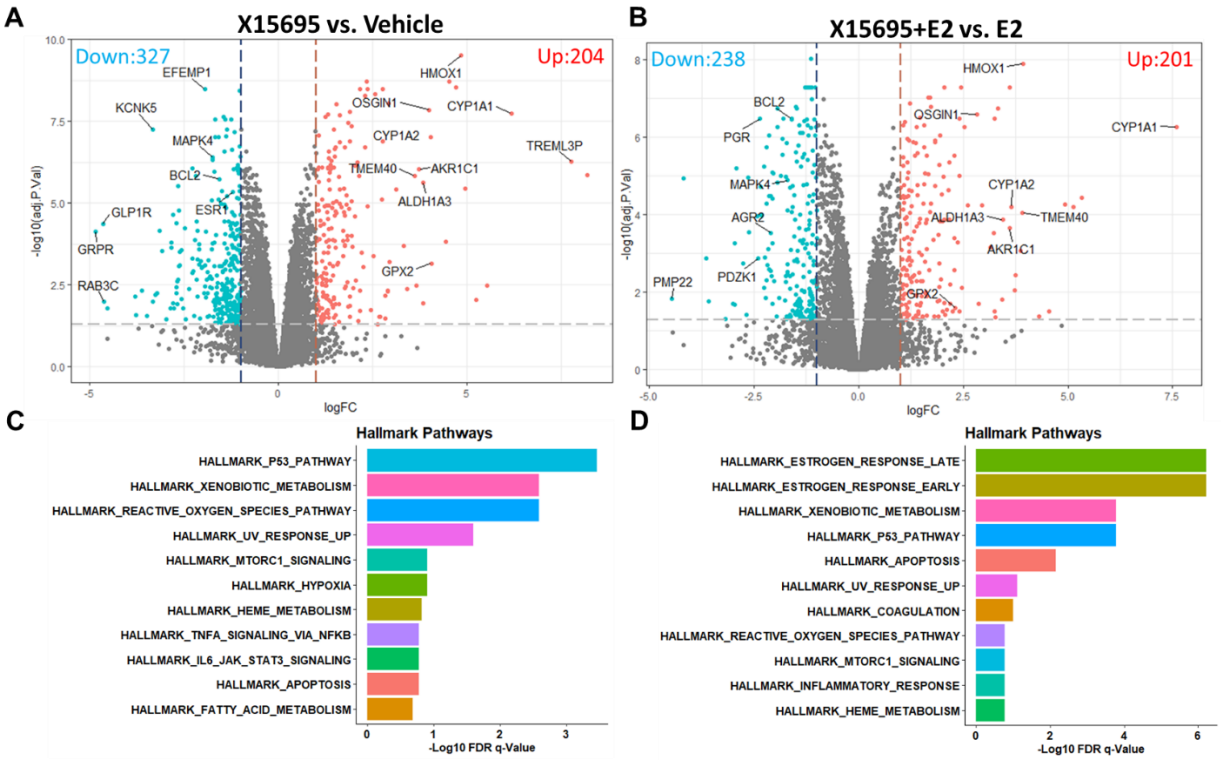

Figure 3.5: Functional enrichment analysis with differentially expressed genes following X15695 treatment in the presence or absence E2 in MCF-7 cells.

(A). Volcano plot of DEGs following X15695 treatment in the absence of E2. 327 DEGs were down-regulated and 204 DEGs were up-regulated at the threshold of |LogFC| ≥ 1.0 and adj. p value ≤ 0.05. (B). Volcano plot of DEGs following X15695 treatment in the presence of E2. 238 DEGs were down-regulated and 201 DEGs were up-regulated at the threshold of |LogFC| ≥1.0 and adj. p value ≤ 0.05. (C). The 531 DEGs that responded to X15695 in the absence of E2 were applied to Gene Set enrichment of hallmark pathway analysis. (D). 439 DEGs that responded to X15695 in the presence of E2 were applied to Gene Set enrichment of hallmark pathway analysis.

3.4.1 X15695 suppressed estrogen signaling in the presence of E2

Estrogen signaling is one of the key pathways which contributes to tumor progression of ER$^+$ breast cancer by promoting cell proliferation, cell cycle progression and inhibiting cell apoptosis (Butt et al., 2005; Gompel et al., 2000). Gene set enrichment analysis (GSEA) indicated both early and late estrogen response were enriched in response to E2 (Figure 3.5C and D), in agreement with previous findings on the role of E2 in breast cancer progression (Samavat and Kurzer, 2015). Almost all the identified genes were enriched in the condition of E2 rather than the condition of E2+X15695, indicating down-regulation by X15695 in presence of E2 (Figure 3.6A and B). For

further information and better visualization of how estrogen signaling is impacted by X15695 treatment, the differentially expressed genes that were enriched both in the early and late stages of estrogen response were presented in a heatmap with their Log2 Fold Change values. All the identified genes were significantly down-regulated under X15695 treatment in the presence of E2. In the absence of E2, although estrogen signaling was not enriched, there was still moderate reduction in the basal level of some of the genes that respond to estrogen signaling (Figure 3.6C). For example, the ER targets GFRA1 and KCNK5 were more strongly reduced by X15695 in the absence of E2 compared to the situation in the presence of E2 while other ER targets such as GREB1 (growth regulating estrogen receptor binding 1), PGR and TFF1 (trefoil factor 1) showed moderated reduction under X15695 treatment in the absence of E2 compared to the presence of E2. ER targets such as BCL-2, IGFBP4 and MYB showed similar reduction levels in both situations, but some other targets including EGR3, AREG, AGR-2, SGK1, and CELSR2 were not affected by X15695 in the absence of E2. Taken together, these findings indicate that X15695 specifically down-regulated ER signaling pathway both in the presence and absence of E2 for the inhibition of ER^+ breast cancer cells growth. However, since only a subset of the downstream targets was inhibited by X15695 in the absence of E2, it is likely that the attenuation of ER signaling in the absence of E2 is mechanistically different the one in the presence of E2.

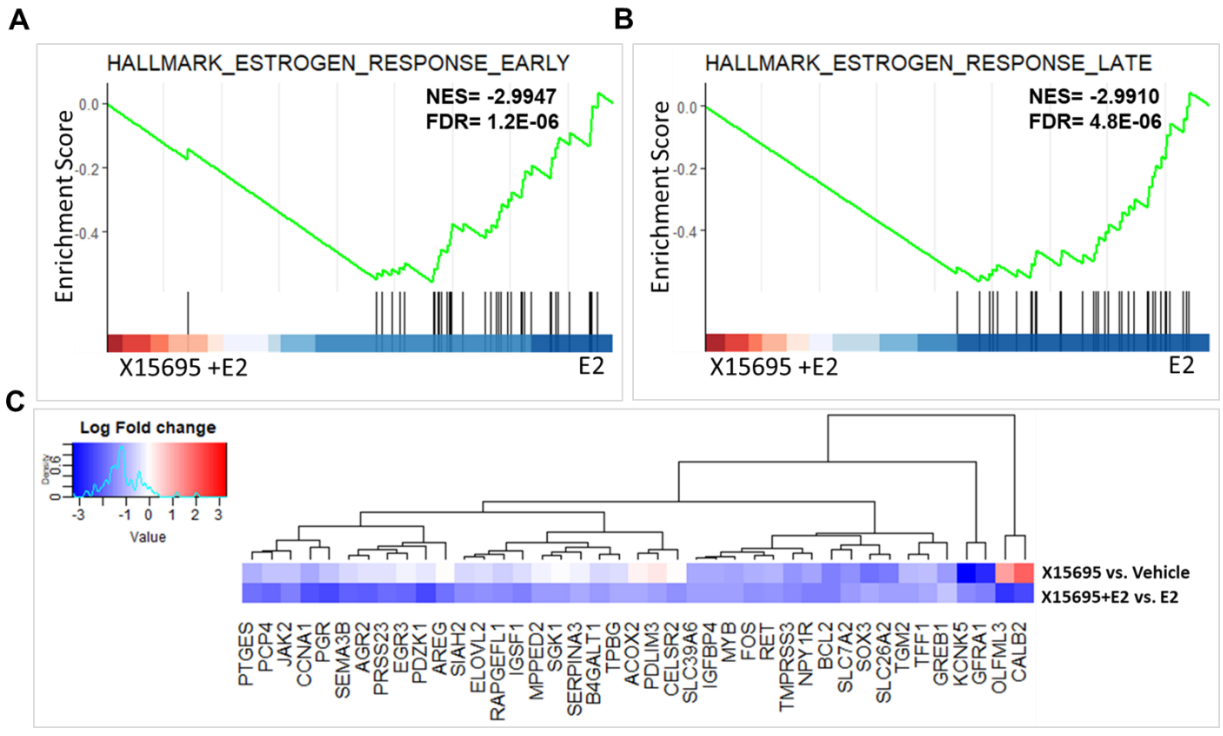

Figure 3. 6: X15695 repressed estrogen signaling in the presence of E2.

(A). Signature of gene set enrichment of early estrogen response in presence of E2. (B). Signature of gene set enrichment of late estrogen response in presence of E2. (C). Heatmap of gene sets involved in estrogen signaling.

3.5 X15695 negatively regulated ER signaling

3.5.1 X15695 down-regulated the downstream targets in ER signaling pathway

To confirm the effect of X15695 on ER transcriptional activity, a select number of ER target genes was analyzed by qRT-PCR in the presence and absence of E2 and X15695. The genes selected are known to contribute differently to breast cancer tumor progression and metastasis. For example, GREB1 is an early estrogen responsive gene for breast cancer growth the function through the PI3K/AKT/mTOR pathway (Haines et al., 2020). AREG (aka Amphiregulin) participates in growth promoting action of breast cancer (Zhao et al., 2019). PGR (Progesterone receptor) is reported to promote invasiveness and metastasis of luminal breast cancer (McFall et al., 2018). AGR-2 (anterior gradient 2) is a member of protein disulphide isomerase family that shows a positive correlation with metastasis in luminal breast cancer (Barraclough et al., 2009; Kereh et al., 2021). TFF1 codes for a secreted protein that can be potentially used as prognostic marker for ER^+ breast cancer (Gillesby and Zacharewski, 1999; Nunez et al., 1987) and PDZK1 (PDZ domain containing 1) reported to contribute to malignancy of ER^+ breast cancer cells (Kim et al., 2014).

Consistent with the transcriptomic data, all these genes were estrogen responsive in the qRT-PCR analysis and X15695 treatment in the presence of E2 significantly downregulated the expression of all of them. Besides, a significant reduction of GREB1, PGR and TFF1 was also observed following X15695 treatment in the absence of E2, as suggested from the heatmap results confirming that indeed compound X15695 attenuates a subset of ER signaling in the absence of E2 (Figure 3.7).

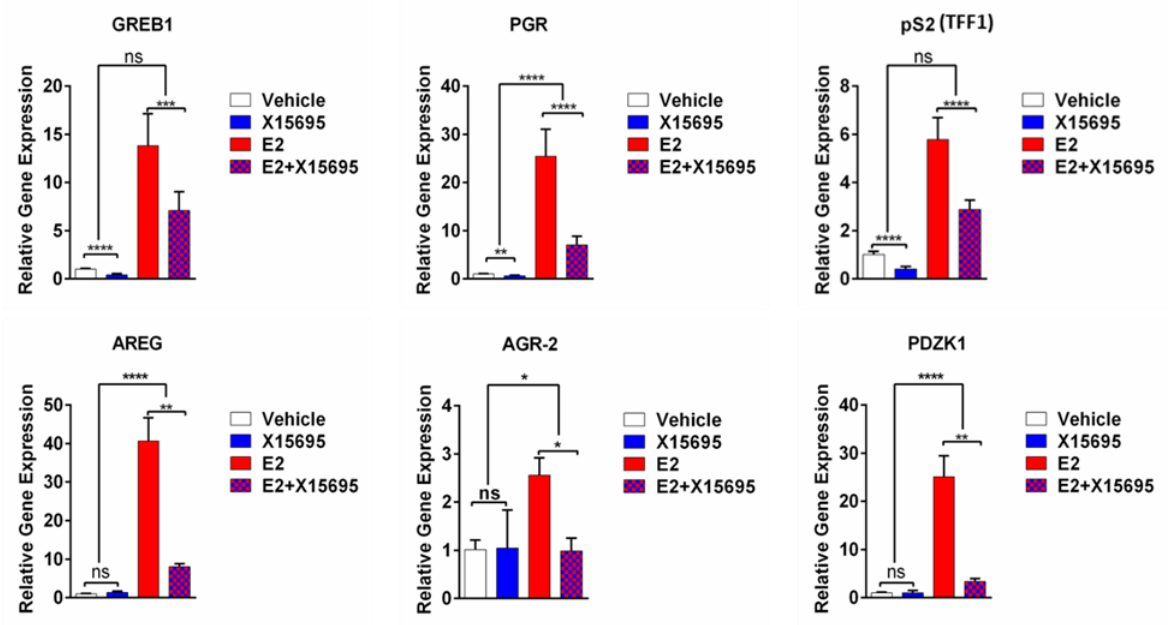

Figure 3. 7: Expression of ER-target genes after X15695 treatment in the presence and absence of E2.

MCF-7 cells were serum starved for 3 days and treated with 1 µM X15695 in the presence and absence of 10 nM E2 for 16 h. Cells were then harvested and lysed for RNA extraction. cDNA was synthesized and q-PCR was carried out to detect the RNA expression of the indicated genes. Four biological replicates were carried out. The data represents the average ± SEM (n =4; * $p \leq 0.05$; ** $p \leq 0.01$; *** $p \leq 0.001$; **** $p \leq 0.0001$). One-way ANOVA and post-hoc Tukey's multiple comparison test were used for statistical analysis. For comparison the fold changes of gene expression with/without hormone, the following formula were used: fold change without hormone = relative gene expression of X15695 treated samples/relative gene expression of vehicle treated samples; fold change with hormone = relative gene expression of (X15695+E2)-treated samples /relative gene expression of E2-treated samples; Double tailed T test was used for statistical analysis of hormone effect.

3.5.2 X15695 promoted ER degradation

The mechanism through which X15695 modulates E2 action was then investigated. Estrogens exert their actions through binding of the hormone to the estrogen receptor (ER) that positively or negatively regulates genes through chromatin binding or through tethering to already bound transcription factors (Fuentes and Silveyra, 2019). To investigate the effect of X15695 on E2 actions, the level of ER protein was first determined after treating. MCF-7 cells treated with increasing dose of X15695 for 48h. The ER protein expression was monitored via Western blotting

and quantified by scanning the intensity of the protein bands. X15695 decreased ER protein level in a dose-dependent manner with the most significant effects observed at 10^{-7} and 10^{-6} M (Figure 3.8A and B), suggesting that X15695 promotes ER degradation.

To confirm this notion, a cycloheximide (CHX) chase assay was performed to determine the half-life of ER protein in the presence and absence of X15695. Cycloheximide is a naturally occurring fungicide which exerts its effects by interfering with the translation step in protein synthesis, thus blocking eukaryotic translational elongation (Ennis and Lubin, 1964). If translation is blocked, the decay of the already synthesized protein could be followed. In the absence of X15695, the ER protein was fairly stable with half-life more than 120 min, which is consistent with the half-life reported in the published literature (Pakdel et al., 1993). However, following treatment with 1 µM X15695, the half-life of ER was shortened to roughly 64 min, demonstrating that X15695 indeed promoted ER protein destabilization (Figure 3.8C and D).

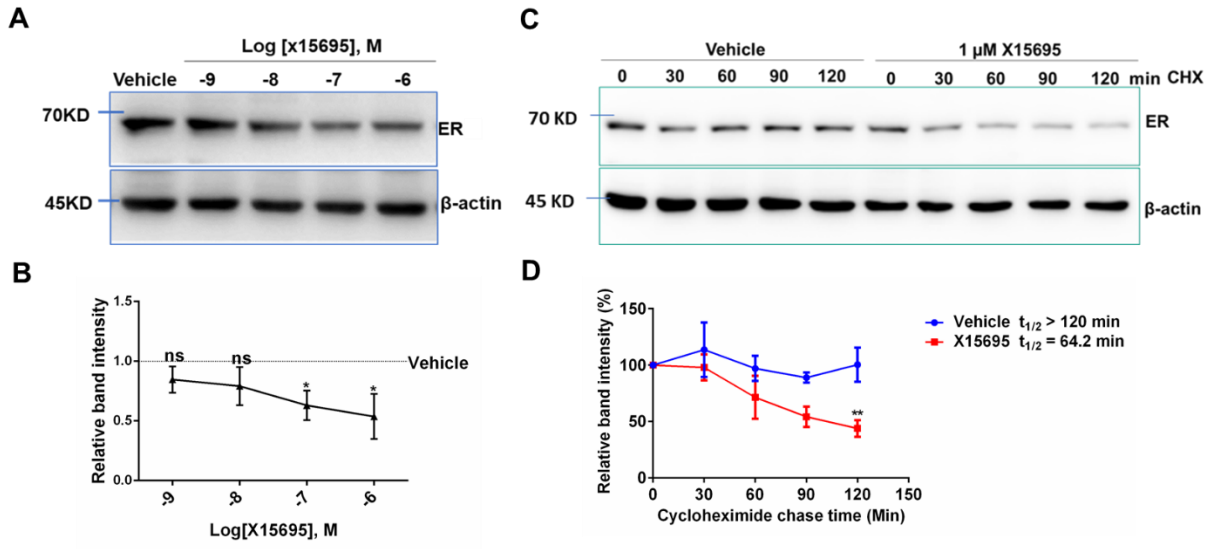

Figure 3. 8: X15695 promoted ER protein degradation.

(A). MCF-7 cells were treated with increasing concentration of X15695 (10^{-9} to 10^{-6} M) or vehicle control (DMSO) for 48 h. Cells were harvested and the ER protein level was monitored by Western blotting using anti-ER antibody, and anti-β-actin antibody was used for protein loading control. (B). Quantification of the level of ER expression after X15695 treatment in MCF-7 cells. The band intensities from 3 biological replicates were scanned and quantified by an ImageJ software. The results are expressed as the intensity of the ER band relative to the β-actin band which was nominally set at 1.0 and the values are presented as the averages ± SEM. * $p \leq 0.05$. One-way ANOVA with post-hoc Tukey's multiple comparison test was used for statistical analysis. (C). MCF-

7 cells were treated with 1 µM of X15695 or the same volume of vehicle (DMSO) for 24 h. Thereafter, the cells were treated with 100 µg/ml cycloheximide and harvested at the indicated time points and Western blot was carried out using an anti-ER antibody. An anti-β-actin antibody was used as loading control. (D). Three biological replicates were quantified and presented as the percentage signal of ER relative to the β-actin signal which was set to 100% at time zero of cycloheximide treatment. The values are presented as the averages ± SEM. Two-way ANOVA with post-hoc Sidak's multiple comparison test was used for p value calculation. ** $p \leq 0.01$.

3.5.3 X15695 inhibited ER nuclei accumulation

In line with ER degradation in full medium, X15695 also destabilizes ER in hormone-depleted medium with and without the supplement of E2 (Figure 3.9A). The degradation of ER by X15695 is one mechanism by which ER activity could be attenuated by X15695. To identify other possible mechanisms for the downregulation of the ER activity by X15695, the nuclear accumulation of the receptor, a key step in ER action, was analyzed. MCF-7 cells were treated with X15695 in the presence and absence of E2 for 16 h. cells were then fixed and coupled with ER primary antibody and Alexa Fluor 488 secondary antibody and the cellular localization of the receptor was monitored by immunofluorescence. In the absence of E2 treatment, ER was mainly localized in the cytosol while, E2 treatment for 16h significantly increased ER accumulation in the nucleus (Figure 3.9A). X15695 treatment, already for 16 h in the absence and presence of E2 resulted in a significant decrease of the fluorescence intensity of ER (Figure 3.9B) which is in line with the previous results in Figure 3.8 that X15695 downregulated ER protein level. As a result, in the presence of both E2 and X15695, the nuclear accumulation of ER was significantly reduced which could impact the transcriptional activity of the receptor. Note that quantification of the fluorescence signal could only be carried out with samples treated with 10^{-7} M X15696 and this showed a drastic reduction of ER signal in the cytoplasm as well as in the nucleus following treatment with X15695 (Figure 3.9B). At a concentration of 10^{-6} M X15695, there was hardly any ER signal detectable and could therefore not be quantified (Figure 3.9B).

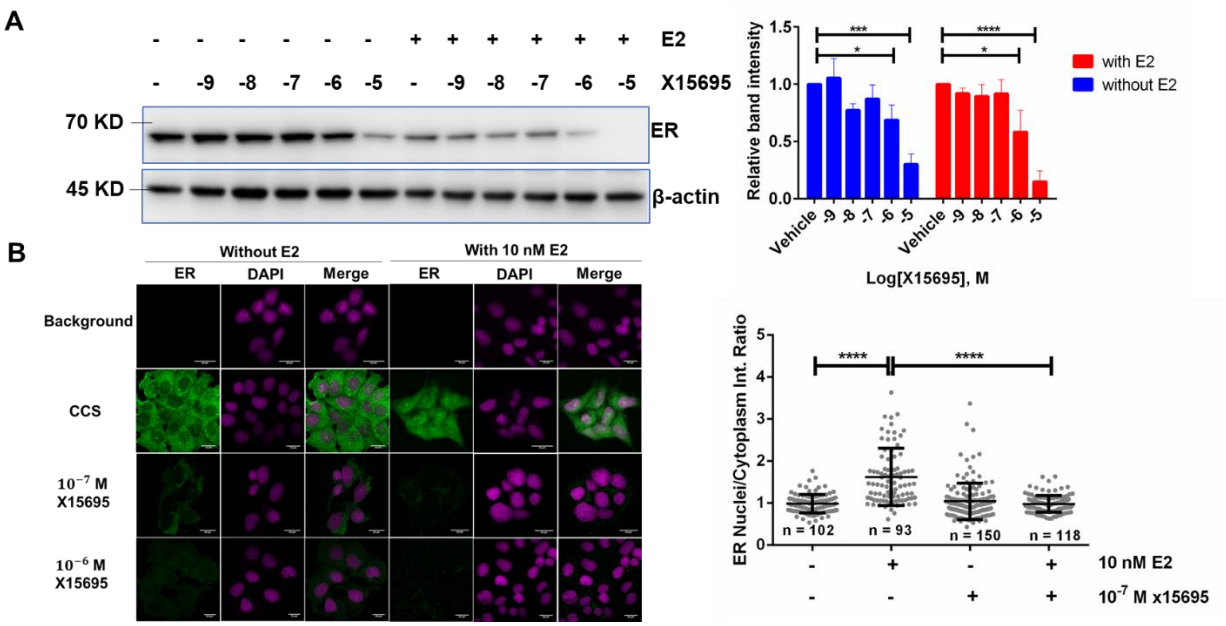

Figure 3. 9: Cellular localization of ER in MCF-7 cells treated with X15695 and E2.
(A). MCF-7 cells were treated with increasing concentrations (10^{-9} to 10^{-5} M) of X15695 in the absence and presence of E2 for 48 h. Cells were harvested and the ER protein level was monitored by Western blotting using anti-ER antibody, and anti-β-actin antibody. β-actin was used for protein loading control. (B). Quantification of the level of ER expression after X15695 treatment of MCF-7 cells. The band intensities from 3 biological replicates were scanned and quantified by an ImageJ software. The results are expressed as the intensity of the ER band relative to the β-actin band which was nominally set at 1.0 and the values are presented as the averages ± SEM. * $p \leq 0.05$; *** $p \leq 0.001$; **** $p \leq 0.0001$. One-way ANOVA with post-hoc Tukey's multiple comparison test was used for statistical analysis. (B). MCF-7 cells were treated with 100 nM and 1 µM X15695 in the presence and absence of 10 nM E2 for 16 h. Cells were then fixed and incubated with an anti-ER primary antibody and Alexa Fluor 488 secondary antibody. Fluorescence images were taken with confocal microscopy (Confocal Microscope platform STELLARIS6-LSM900, Leica, Germany) at 20×3 magnification. The fluorescent intensity was quantified by a CellProfiler software with modification of the example pipeline of human cell Cytoplasm Nuclei translocation analysis. One-way ANOVA and post-hoc Tukey's multiple comparison test were used for statistical analysis. **** $p \leq 0.0001$.

3.6 X15695 activated p53 pathway in MCF-7 cells

3.6.1 X15695 activated p53 pathway in the absence and presence of E2

One of the key signaling pathways regulated by X15695 in the presence and absence of E2 is p53. The GSEA plot shows p53 pathway up-regulated both in the absence and presence of X15695 (Figure 3.10A and B). To gain further insight into the p53 pathway and its targets, the genes identified in this pathway were presented in a heatmap and differences and similarities were compared (Figure 3.10C). The expression of some of the p53 target genes, for example, MDX4 and BTG2 was only activated by X15695 in the presence of E2, while the expression of others, such as, SLC7A11, SLC3A2 and RFPL1 was only upregulated by X15695 in the absence of E2. The expression of the majority of the p53 target genes, such as CDKN1A, HMOX1 and OSGIN1 was strongly upregulated by X15695 both in the presence and absence E2. CDKN1A, also known p21 or WAF1, is a p53 target gene famously known for inducing cell cycle arrest (el-Deiry et al., 1993), while HMOX1 (Heme oxygenase) is a directly p53 target which induces Fe^{2+} overproduction at high levels of oxidative stress tumor cells (Meiller et al., 2007). OSGIN1, on the other hand is a direct p53 target, implicated in p53-induced apoptosis (Yao et al., 2008). In summary, the activation of p53 pathway by X15695 mainly focuses on cell cycle regulation, oxidative stress and apoptosis.

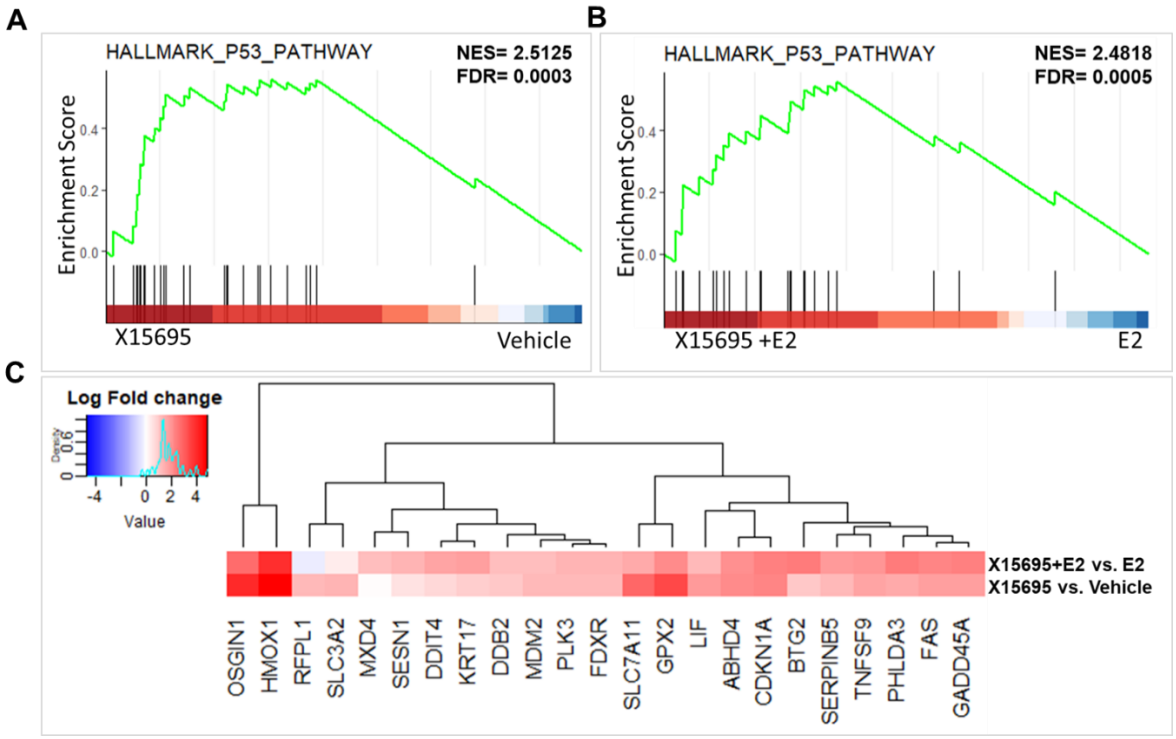

Figure 3. 10: X15695 activated p53 pathway in the presence and absence of E2.
(A). Signature of gene set enrichment of p53 pathway in the absence of E2. (B). Signature of gene set enrichment of p53 pathway in the presence of E2. (C). Heatmap of p53 targets enriched in p53 pathway in the presence and absence of E2.

3.6.2 X15695 up-regulated the downstream targets in p53 signaling pathway

To confirm the results presented in the heatmap (Figure 3.10C), a select number of p53 targeted genes were analyzed by qRT-PCR in presence and absence of X15695 and E2. The genes selected were p53 targeted genes that responsible for G1/S cell cycle arrest (CDKN1A and GADD45A), apoptosis (PUMA and FAS) and oxidative stress (SLC7A11 and OSGIN1) (el-Deiry et al., 1993; Kastan et al., 1992; Nagata, 1996; Nakano and Vousden, 2001; Tang et al., 2021). With the exception of BBC3, X15695 upregulated the expression of all the genes analyzed in the presence and absence of E2 in agreement with the transcriptomics data. The expression of BBC3 on the other hand was upregulated only in the presence of E2 (Figure 3.11).

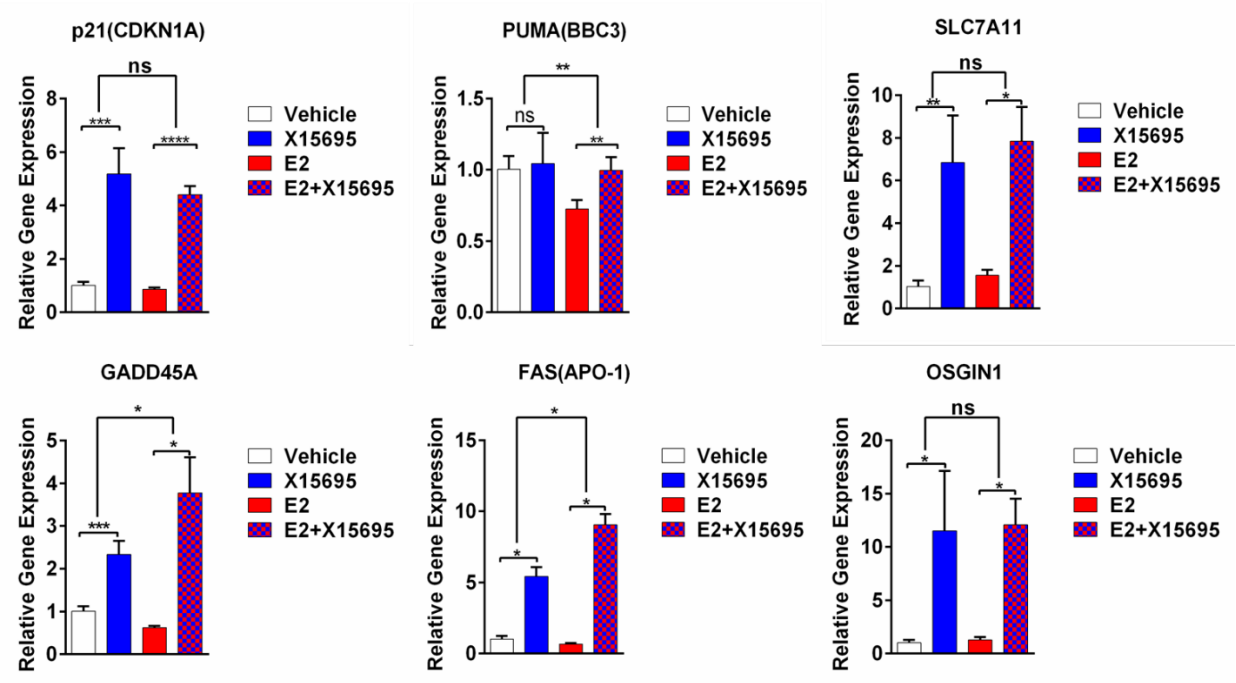

Figure 3. 11: Expression of p53-target genes upon treatment of MCF-7 cells with X15695 in the presence and absence of E2.
MCF-7 cells were serum starved in hormone-depleted medium for 3 days and then treated with 1 µM X15695 in the presence and absence of 10 nM E2 for 16 h. Cells were harvested and lysed for RNA extraction. cDNA was synthesized and qRT-PCR was performed to detect the RNA expression of CDKN1A, GADD45A, BBC3, FAS, SLC7A11 and OSGIN1. The data represents the

averages ± SEM (n =4; * p ≤ 0.05; ** p ≤ 0.01; *** p ≤ 0.001; **** p ≤ 0.0001). One-way ANOVA and post-hoc Tukey's multiple comparison test were used for statistical analysis. For comparison of the fold changes of gene expression with/without E2, the following formula were used: fold change without hormone = relative gene expression of X15695 treated samples/relative gene expression of vehicle treated samples; fold change with hormone = relative gene expression of (X15695+E2)-treated samples /relative gene expression of E2-treated samples; Double tailed T test was used for statistical analysis of hormone effect.

3.6.3 X15695 activated p53 targets in both estrogen-dependent and independent manner

Some of the p53 target genes that are transcriptionally upregulated by X15695 are known to be transcriptionally regulated by the ER. For example, CDKN1A (p21) that is upregulated by X15695 is reported to be negatively regulated by E2 (Liu et al., 2006). To determine the effect of X15695 on the expression of such a gene, p21 and PUMA that is also negatively regulated by E2 (Roberts et al., 2011) were chosen for further analysis. As control, BAX, a p53 target gene that is not regulated by E2 was also analyzed. MCF-7 cells were treated with 10 nM E2 and with different concentrations of X15695 ranging from 10^{-9} to 10^{-6} M for 16 h after which the expression of the three genes was analyzed by qRT-PCR. In the absence of E2, as previously shown X15695 upregulated expression of p21 but not PUMA. Consistent with the published literature, p21 and PUMA were found to be transcriptionally downregulated by E2 (Figures 3.12A and B). The E2-mediated negative regulation of these genes was antagonized by treatment with increasing concentrations of X15695 (Figures 3.12D and E). BAX gene expression was only upregulated by X15695 although it was not affected by E2 treatment (Figures 3.12C and F). These results demonstrate a dual action of X15695. It upregulated the expression of a subset of p53-target genes and it acted as an estrogen antagonist by downregulating estrogen response. As a result, the expression of the p53-target genes that are a transcriptionally regulated by estrogen can additionally be antagonized by X15695.

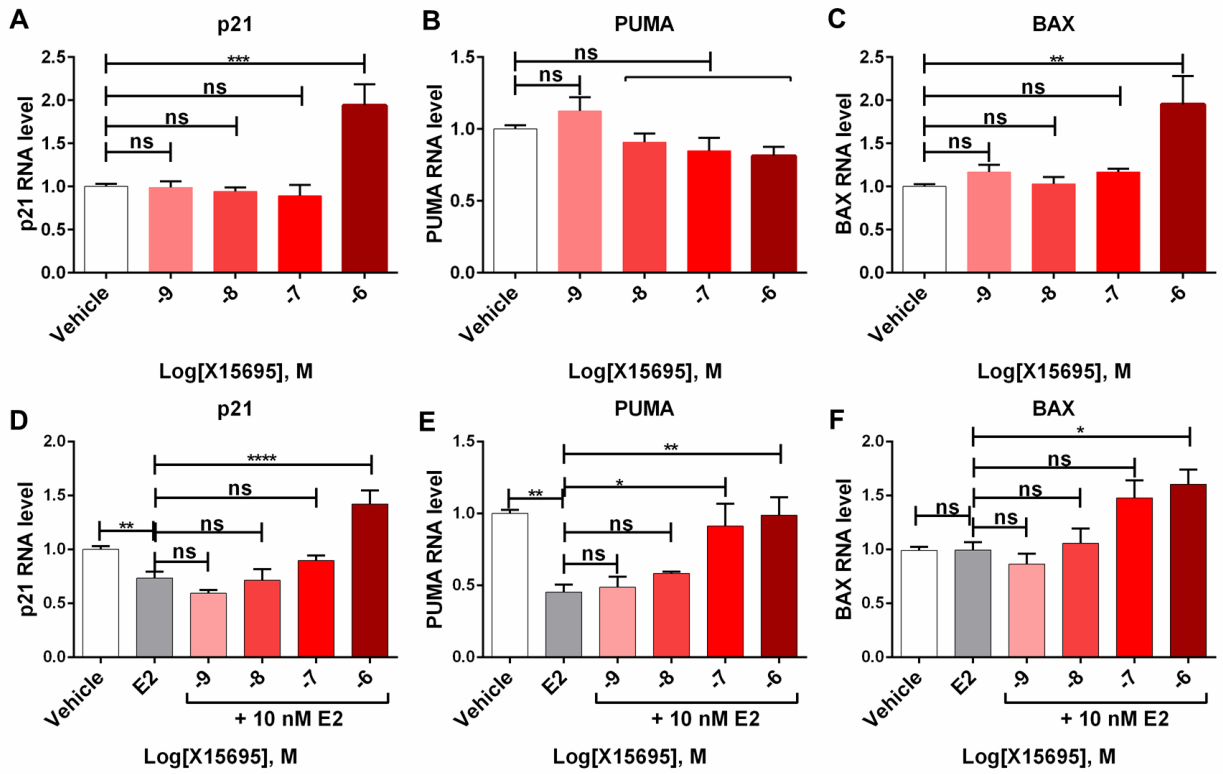

Figure 3.12: Expression of downstream p53 targeted genes upon X15695 treatment in the presence and absence of E2.

MCF-7 cells were starved with hormone-depleted medium for 3 days, then treated with the indicated concentrations of X15695 in the presence and absence of E2 for 16 h. Cells were then harvested and lysed for RNA extraction. cDNA was synthesized and q-PCR was used to detect the RNA expression of p21 (A), PUMA(B) and BAX(C). The expression of p21, PUMA and BAX3 upon X15695 treatment in the presence of E2 was labeled (E-G). The data represents the averages ± SEM (n =3; * $p \leq 0.05$; ** $p \leq 0.01$; *** $p \leq 0.001$; **** $p \leq 0.0001$; ns refers to non-significant). One-way ANOVA and post-hoc Tukey's multiple comparison test was used for the statistical analysis.

3.6.4 X15695 stabilized p53 protein in dose dependent manner

The mechanism by which X15695 alters the expression of p53-target genes in the absence of E2 was analyzed by first determining the effect of X15695 on p53 level of expression. MCF-7 cells were treated with different concentrations of X15695 and the p53 steady mRNA and protein levels were analyzed by qRT-PCR and Western blotting. The steady mRNA levels of p53 after X15695 treatment in qRT-RCT studies did not show a significant difference (Figure 3.13A), but the protein level of p53 was steadily increased with increasing concentration of X15695 treatment,

suggesting a post-transcriptional action of p53 by X15695 on p53 the protein level (Figure 3.13B and C).

Increased p53 protein level is a dynamic process that arises through increased synthesis of p53 protein or through attenuation of p53 degradation. To explore the former process, a cycloheximide chase assay was performed where changes in p53 protein level were followed in time after the termination of protein synthesis by application of cycloheximide. Samples were taken at set intervals and the level of p53 remaining was detected by Western blotting and quantified. After 120 min chase, the level of p53 protein did not change significantly in vehicle treated cells and a half-life with of more than 120 min was observed. In contrast, in X15695 treated cells, the half-life of p53 was reduced to only 90 min (Figure 3.13D and E). These results contrast with the previous finding that the level of p53 protein is increased by X15695 treatment. Therefore, experiments were carried out to determine whether attenuation of p53 degradation contributes to the enhanced p53 level after X15695 treatment. MCF-7 ells were treated with MG132, an inhibitor of proteasomal degradation of proteins in the presence and absence of X15695 and analyzed by Western blotting and quantification. In the absence of MG132, there was a significant accumulation of p53 following X15695 treatment while in presence of MG132, an increased level of p53 was observed in the absence of X15695 which resulted in only a marginal accumulation of p53 following X15695 treatment (Figure 3.13F and G). Collectively, these results show that X15695 stabilize p53 protein level through an inhibition of the proteasomal degradation of p53.

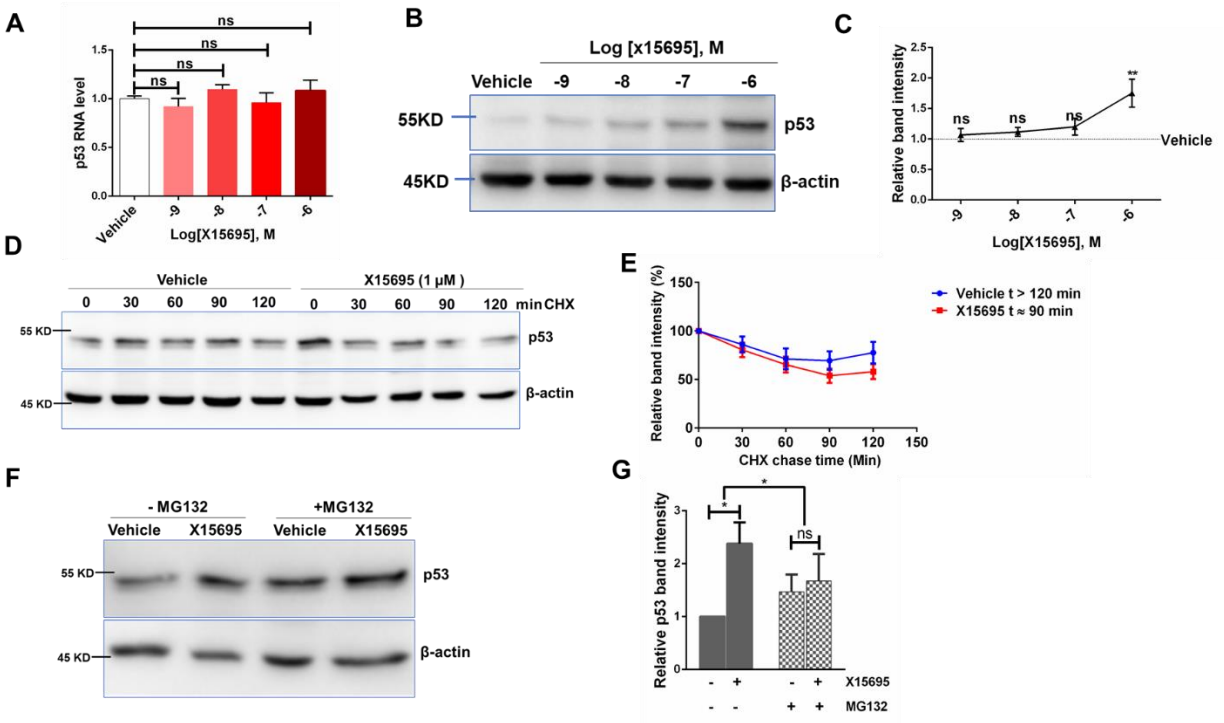

Figure 3. 13: X15695 stabilized p53.

(A). MCF-7 cells were treated with the indicated concentrations of X15695 or with the same volume of vehicle (DMSO) for 48 h and the total RNA was extracted for qRT-PCR analysis to detect p53 mRNA level. The results are the averages ± SEM (n=3; ns represents non-significant). One-way ANOVA with post-hoc Tukey's multiple comparison test was used for statistical analysis. (B). MCF-7 cells treated as in (A). Cells were harvested and p53 protein levels were monitored by Western blot using anti-p53 antibody and anti- β-actin antibody as loading control. (C). Quantification of the protein band intensities using an ImageJ software. The results are the averages ± SEM (n=3; ** $p \leq 0.01$; ns refers to non-significant). One-way ANOVA with post-hoc Tukey's multiple comparison test was used for statistical analysis. (D). MCF-7 cells were treated with indicated concentrations of X15695 or with the same volume of vehicle (DMSO) for 48 h. Cells were then treated with 100 µg/ml cycloheximide and harvested at the indicated time points. The p53 protein level at each time point was monitored by Western blotting using anti-p53 antibody and anti- β-actin antibody as loading control. (E). The protein band intensity in the Western blotting was quantified by an ImageJ software. The results are the averages ± SEM. (F). MCF-7 cells were treated with 0.5 µM MG132 in presence and absence of 1 µM X15695 for 48 h. Cells were harvested and lysed for p53 detection via Western blotting using anti-p53 antibody and anti- β-actin antibody as loading control. (G). The protein band intensity was quantified by an ImageJ software. The results are the averages ± SEM (n=3; * $p \leq 0.05$; ns refers to non-

significant). Two-way ANOVA with post-hoc Sidak's multiple comparison test was used for p value calculation.

3.6.5 X15965 promoted p53 nuclei accumulation

p53 protein stabilization does not necessarily mean p53 activation which is coupled to its transactivation functions (Chernov et al., 1998). As a transcription factor, p53 requires translocation from cytoplasm to nucleus for the regulation of gene expression. As X15695 treatment enhanced the transcriptional activity of some of the p53 target genes (see Figure 3.11), it is very likely that it affected the cellular localization of p53. To investigate whether X15695 altered cellular localization of p53, immunofluorescence experiments were carried out with MCF-7 cells treated with and without X15695 for varying periods of time ranging from 0 h to 48 h. The cells were permeabilized, fixed and stained with p53 primary antibody and Alexa Fluor 488 secondary antibody. The immunofluorescence staining results showed that as early as 8 h of X15695 treatment, the cellular localization of p53 were altered from the cytoplasm to the nucleus. The intensity of nuclear staining intensified with subsequent treatment with X15695 (Figure 3.14A). Quantification of the fluorescence intensity showed that the nuclear translocation of p53 peaked over 24 h with a slight decrease at 48 h (Figure 3.14B).

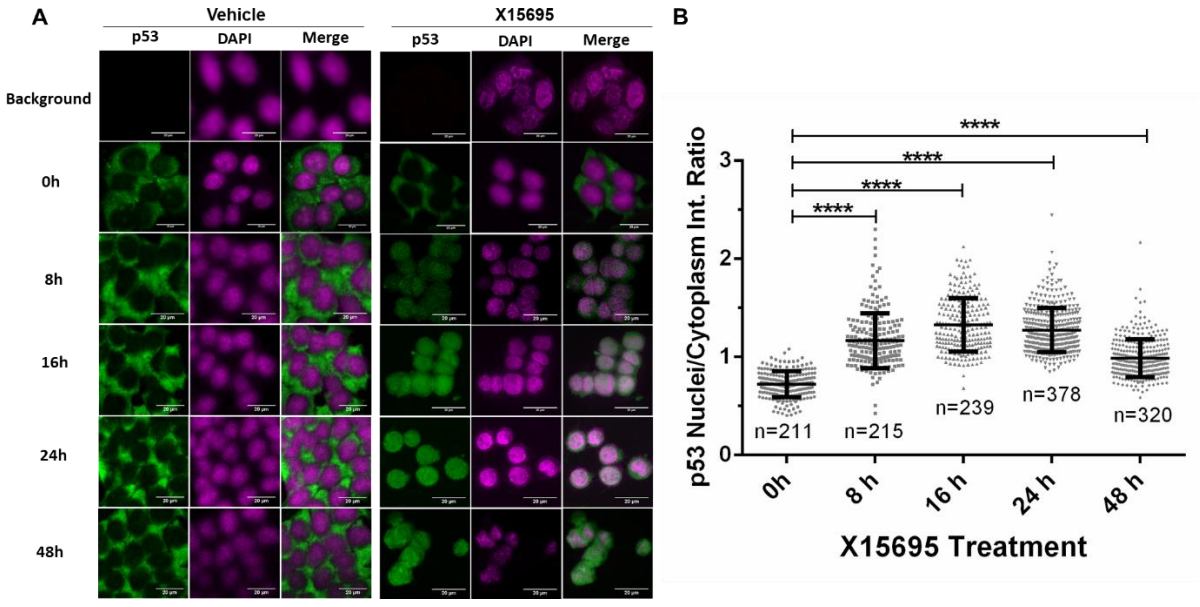

Figure 3. 14: Cellular localization of p53 with and without X15695 treatment in MCF-7 cells. (A). MCF-7 were cells treated with 1 µM X15695 or the volume of vehicle (DMSO) for 0h, 8 h, 16 h, 24 h and 48 h. Cells were permeabilized, fixed and incubated with an anti-p53 primary antibody and Alexa Fluor 488 secondary antibody. Fluorescence images were taken with confocal

microscopy (Confocal Microscope platform STELLARIS6-LSM900, Leica, Germany) at 20×5 magnification. (B). The fluorescent intensity was quantified by a CellProfiler software with modification of the example pipeline of human cell Cytoplasm Nuclear translocation analysis. One-way ANOVA and post-hoc Tukey's multiple comparison test were used for statistical analysis. **** $p \leq 0.0001$.

3.7 Reactivation of p53 by X15695

3.7.1 X15695 reactivated p53 in ER-independent mechanism

Studies have shown that wild-type p53 is sequestered in the cytoplasm in a subset of human tumor cells such as breast cancers (Moll et al., 1992) and that a hsp70 family member, Mot2, could interact with p53 and inhibit its nuclear import (Wadhwa et al., 1998). Mot 2 is also known as heat shock protein family A member 9(HSPA9), Glucose Regulated protein 75 (GRP75), mitochondrial heat shock protein 70 (mtHSP70) or Mortalin. Disruption of the Mortalin-p53 interaction would free the nuclear localization signal of p53 and allow it to be transported into the nucleus (Wadhwa et al., 1998; Walker et al., 2006). A possibility therefore exists that X15695 disrupts p53-Mortalin interaction to account for the nuclear transport of p53 described in Figure 3.6.4 following treatment with X15695.

3.7.1.1 X15695 alters Mortalin-p53 cellular co-localization

MCF-7 cells were treated with X15695 and same volume of vehicle (DMSO) for 16 h then fixed, permeabilized and incubated with primary anti-mortalin and anti-p53 antibodies followed by Alexa Fluor 488/546 secondary antibodies. In agreement with the published literature(Sari et al., 2021), in the absence of X15695, both Mortalin and p53 were mainly localized in the cytoplasm (Figure 3.15A). In the presence of X15695, p53 accumulated in the nucleus, while Mortalin assumed a perinuclear localization (Figure 3.15A). Colocalization analysis showed a low correlation coefficient in the presence of X15695 compared to the situation on its absence (Figure 3.15B), indicating the X15695 treatment reduced Mortalin and p53 co-localization in the cytoplasm. To determine whether the altered cellular localization of p53 is caused by changes in level of Mortalin and p53, Western blot experiments were carried out to determine the effect of X15695 on the two proteins over different times of treatment ranging from 0 to 48 h (Figure 3.15C). Quantification of the Western blot signals of both proteins showed that while X15695

treatment increased p53 abundance as early as 16 h, Mortalin abundance was unaltered over the 48 h (Figure 3.15D and E).

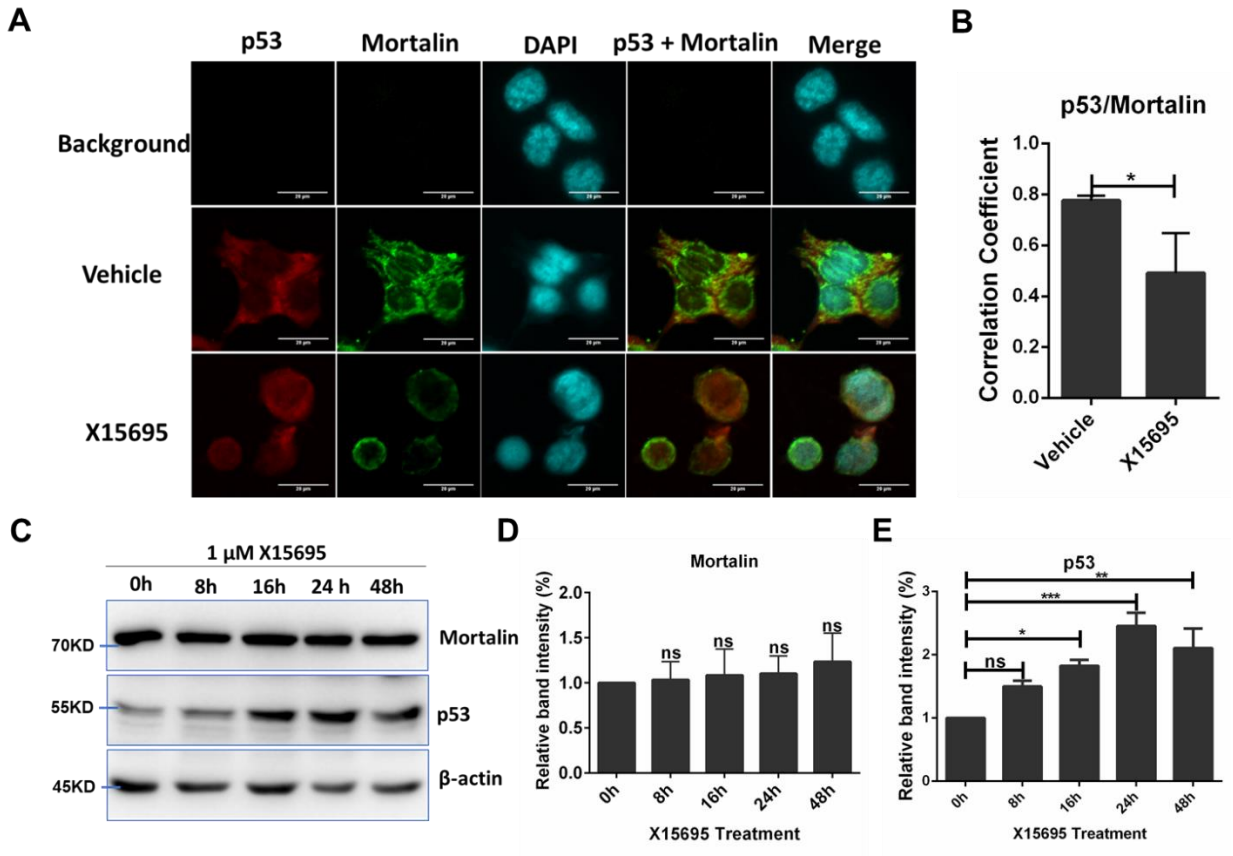

Figure 3. 15: The effect of X15695 on cellular localization of p53-Mortalin complex.
(A). MCF-7 cells were treated with 1 µM X15695 or same volume of vehicle (DMSO) for 16 h. Cells were then fixed, permeabilized and incubated with primary anti-mortalin and anti-p53 antibodies followed by Alexa Fluor 488/546 secondary antibodies. Fluorescence images were taken with confocal microscopy (Confocal Microscope platform STELLARIS6-LSM900, Leica, Germany). (B). The fluorescence intensity was quantified by CellProfiler software with the example pipeline of human cell colocalization analysis. Double tailed T test were used for statistical analysis. (C). MCF-7 cells were treated with 1 µM X15695 and harvested every 8 h over 48 h. Cells were lysed after X15695 treatment and p53 and Mortalin protein levels were monitored by Western blotting using anti-p53 antibody, anti-Mortalin antibody and anti- β-actin antibody as loading control. (D). Quantification of the protein band intensities of Mortalin (D) and p53 (E) by using an ImageJ software. The results are the averages ± SEM (n=3; * $p \leq 0.05$; ** $p \leq 0.01$; *** $p \leq 0.01$; ns refers to non-significant). One-way ANOVA with post-hoc Tukey's multiple comparison test was used for statistical analysis.

3.7.1.2 X15695 disrupted BAG1-Mortalin and Mortalin-p53 complex.

The finding that p53 level was increased upon X15695 treatment while Mortalin level remained unchanged could imply that increased p53 protein complexes with mortalin in the cytoplasm leaving the excess to be translocated into the nucleus. This is unlikely since the cytoplasmic p53-mortalin complex was decreased in the presence of X15695 in the immunofluorescence experiments (Figures 3.15 and B). However, to clearly demonstrate that X15695 affects the p53-mortalin complex, co-immunoprecipitation experiments were performed for the interaction of Mortalin and p53. MCF-7 were cells treated with X15695 for 48 h and the cells were lysed and immunoprecipitated with a rabbit anti-p53 antibody coated agarose beads. The coimmunoprecipitated protein samples were then used for immunoblotting of mortalin. The results clearly showed that X15695 treatment disrupted the mortalin-p53 complex (Figure 3.16A).

X15695 is not known to interact with p53 or mortalin but with BAG1 (see section 3.3). BAG1 is known to bind to and function as a nucleotide exchange factor of HSP70/HSC70 (Sondermann et al., 2001). BAG1 has also been reported to bind other HSP70 family members such as GRP78 (BiP) and GRP75 (mortalin) (Maddalo, 2009). A possibility exists that X15695 disrupts the interaction of BAG1 with mortalin which in turn inhibits the interaction of mortalin with p53. MCF-7 cells were treated with X15695 for 48 h and the cells were lysed and immunoprecipitated with a rabbit anti-BAG1 antibody coated agarose beads. The coimmunoprecipitated protein samples were then used for immunoblotting with anti-mortalin antibody. The results showed that BAG1 indeed interacted with Mortalin and that this interaction was disrupted by prior treatment of the cells with X15695 (Figure 3.16B). The disruption of BAG-1/mortalin interaction by X15695 may explain the X15695-mediated abrogation of mortalin-p53 interaction.

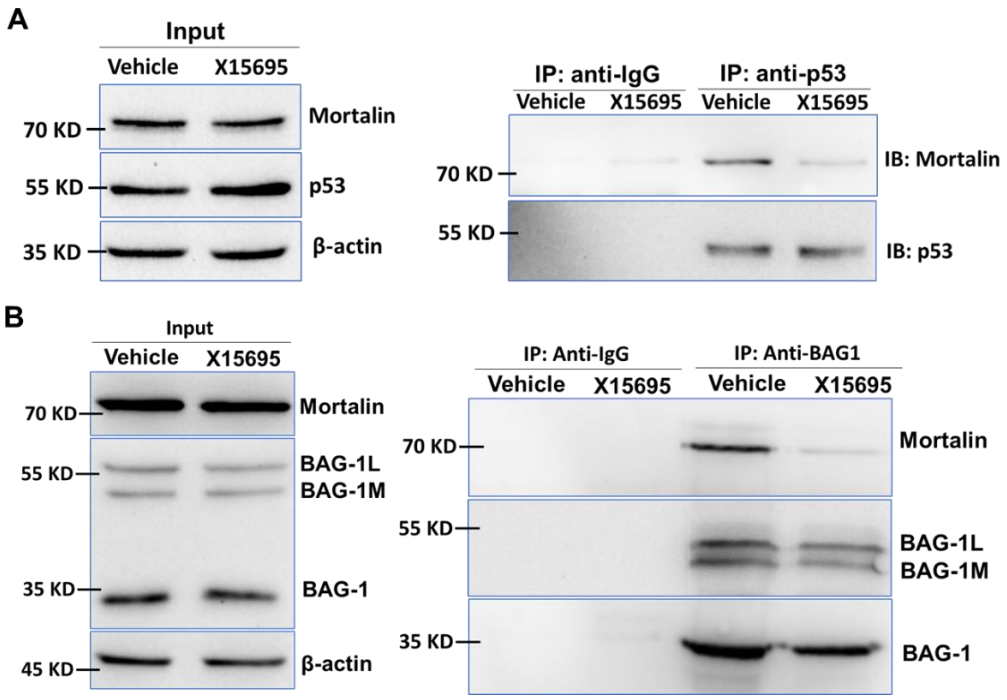

Figure 3. 16: Co-immunoprecipitation of p53, Mortalin and BAG1.
(A). MCF-7 cells were treated with 1 µM X15695 for 48 h and harvested. Ten percent of the cell suspension was lysed and used as input while 90% was lysed and immunoprecipitated with a rabbit anti-p53 antibody coated agarose beads, or an IgG antibody as control. The input and co-immunoprecipitated protein samples were used for immunoblotting using anti-p53 and anti-Mortalin antibodies. (B). MCF-7 cells were treated and processed as in (A) with the exception that the immunoprecipitation was carried out with a mouse anti-BAG1 antibody. The input and co-immunoprecipitated protein samples were used for immunoblotting using anti-mortalin and anti-BAG1 antibodies.

3.7.2 X15695 reactivated p53 in ER-dependent mechanism

In the nucleus, p53 acts as a transcription factor by binding to discrete nucleotide sequences in chromatin and its action can be modulated by other transcription factors that interact with it. For example, in breast cancer cells, the transcriptional activity of wild-type p53 ($p53^{wt}$) can be inhibited by ER (Liu et al., 2006). As X15695 stabilizes p53 and its translocation into the nucleus where the liganded ER resides, a possibility exists that X15695 may also interfere with ER-p53 interaction. To investigate this, co-immunoprecipitation experiment was performed for the interaction of p53 and ER. Consistent with the published literature, E2 treated decreased ER abundance but enhanced ER-p53 interaction (Fuentes and Silveyra, 2019; Molinari et al., 2000),

X15695 treatment decreased p53 protein in ER-P53 complex both in presence and absence of E2 (Figure 3.17). This reveals another mechanism of action of X15695 in the attenuation of p53-ER complex.

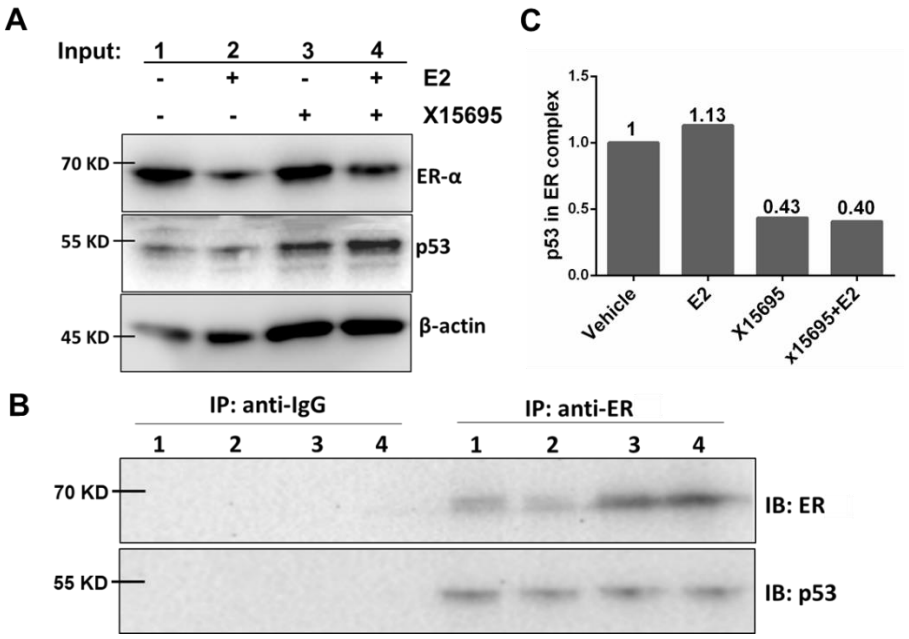

Figure 3. 17: Co-immunoprecipitation experiment for p53 and ER.
(A). MCF-7 cells cultured in hormone depleted medium for 3 days, then treated with 10 nM 17-β-estradiol (E2), 100 nM X15695 and 100 nM X15695 together with 10 nM E2 for 48 h and harvested. 10% cell suspensions were lysed and used as input, 90% of cells suspensions were lysed and immunoprecipitated with an anti-ER antibody coated agarose beads and IgG antibody were used as control. The input and co-IP protein samples were then used for immunoblotting p53 and ER; (B). Quantification of ER and p53 protein expression. The protein band intensity input p53, input ER, coprecipitated p53 and ER were quantified by ImageJ software. The data was first normalized relative to the input p53 and ER respectively (normalized ER = coprecipitated ER/input ER; normalized p53= coprecipitated p53/input p53) and then the ratio of p53 in the ER protein complex was calculated with the formula: p53 in ER protein complex = normalized p53/normalized ER.

3.8 X15695 induced G1/S cell cycle arrest and apoptosis

X15695 treatment strongly impacted the p53 signaling pathway in the studies presented here in the absence and presence of E2. p53 is a tumor suppressor that inhibits tumor cell proliferation

via diverse cellular action such as the induction of cell cycle arrest and apoptosis (Chen, 2016). Giving the fact that p53 downstream targets such as p21 and APO-1 were significantly activated by X15695 treatment (Figure 3.11), one would expect X15695 to have an effect on cell cycle arrest and apoptosis. Therefore, MCF-7 cells were treatment with or without X15695 and with 7-AAD or 7-AAD and Annexin. 7-Aminoactinomycin D is a fluorescent chemical compound with a strong affinity for DNA. It is used as a fluorescent marker for DNA in flow cytometry. Single cells stained with 7-AAD were used for cell cycle analysis. The results showed both X15695 treated and untreated cells have the same cell percentage in G2 phase, while in G1 phase, the percentage is 10% more in X15695 treated cells than in untreated cells, indicating the induction of arrest in the G1/S phase of the cell cycle (Figure 3.18A). Double staining with 7-AAD and Annexin V were used for apoptosis evaluation. Cells that are in early apoptosis are Annexin V positive and 7-AAD negative while cells that are in the late apoptosis or already dead are both Annexin V positive and 7-AAD positive (Zimmermann and Meyer, 2011). Annexin V binding alone cannot differentiate between apoptotic and necrotic cells. To help distinguish between the necrotic and apoptotic cells 7-AAD is used. Early apoptotic cells will exclude 7-AAD, while late stage apoptotic cells will stain positively, due to the passage of these dyes into the nucleus where they bind to DNA. The FACS measurement indicated 1 µM x15695 treated MCF-7 for 48h significantly increased the cell populations in the late stage of apoptosis. (Figure 3.18B).

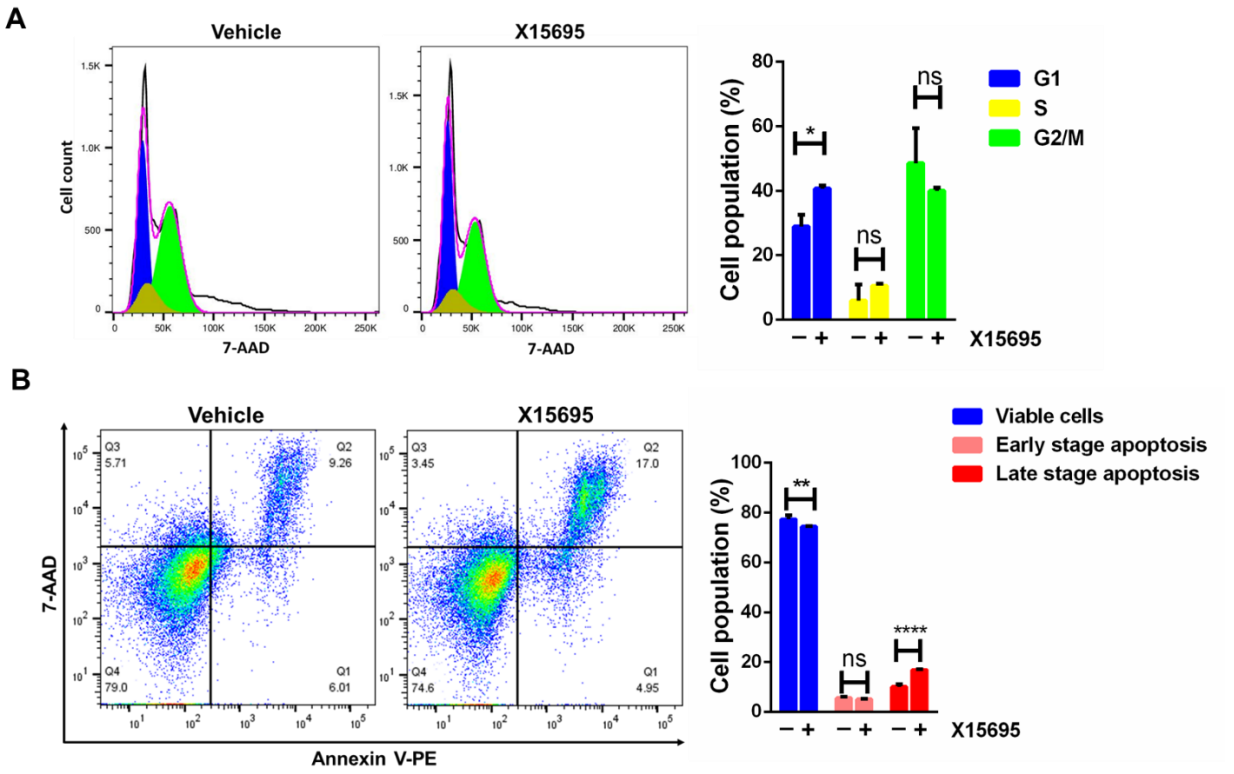

Figure 3. 18: X15695 induces G1/S cell cycle arrest and apoptosis in MCF-7 cells.
(A). MCF-7 cells treated with 1 µM X15695 for 48 h, cells were fixed and stained with 7-AAD only for 5 min. 10^6 cells were used for FACS (Fluorescence activated cell sorting) measurement. All data was analysis by FlowJo software. (B). MCF-7 cells treated with 1 µM X15695 for 48 h were double stained with 7-AAD and Annexin V for 15 minutes. Cells stained with 7-AAD or Annexin V alone were used for compensation of Double staining. 10^6 cells were used for FACS measurement.

3.9 X15695 inhibited MCF-7 cell viability both in the presence and absence of estrogen

As X15695 showed diverse effects on p53 and estrogen signaling pathways both in the absence and presence of E2, all of which are linked to cell proliferation and growth, MTT experiments were carried out to determine how X15659 affected cell viability in the absence and presence of E2. The effect of X15695 was compared to the classical ER antagonists: tamoxifen and fulvestrant.

In MTT assay, the yellow tetrazolium salt (3-(4,5-dimethylthiazol-2-yl)-2,5-diphenyltetrazolium bromide is reduced by the redox potential of mammalian cells to a strongly pigmented formazan product. After solubilization, the absorbance of the formazan can be measured to provide information on the viability of the cells. In the absence of E2, X15695 significantly dose-

dependently inhibited MCF-7 cell viability better than tamoxifen but with about the same efficacy as 1 µM fulvestrant (Figure 3.19A). In the presence of E2, the inhibitory effect of X15695 was less pronounced but still equivalent to that of fulvestrant at 1µM concentration. Tamoxifen did not show any significant inhibitory effect at the concentration used in this experiment (Figure 3.19B). Taken together, X15695 exerts an estrogen-dependent and independent inhibitory effect on MCF-7 cell viability, which is superior to tamoxifen but similar to fulvestrant.

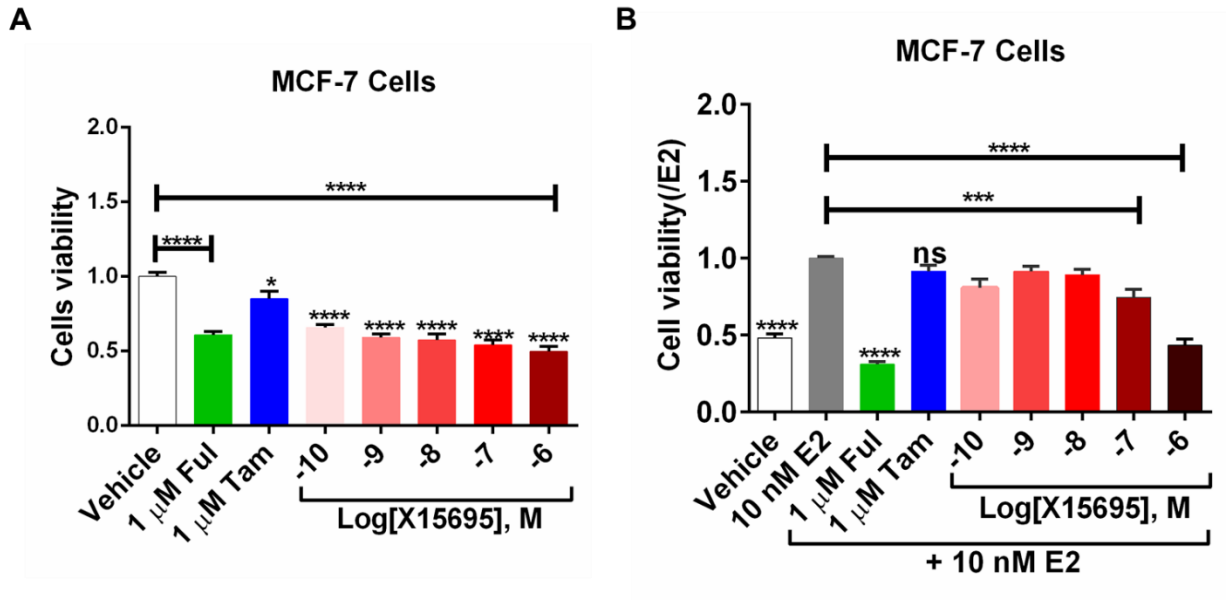

Figure 3.19: Inhibitory effect of X15695 on MCF-7 cell viability in the presence and absence of E2.

MCF-7 cells cultured in hormone-depleted medium for 3 days and then treated with the indicated concentrations of X15695 in the presence (B) and absence (A) of E2 for 48 h. Two classical estrogen antagonists (Fulvestrant and Tamoxifen) were used as positive control for comparison. Cell viability was measured by MTT assay. 5 replicates were used for each experiment, and the experiment was repeated 3 times (N=3, R=5; * $p \leq 0.05$; *** $p \leq 0.001$, **** $p \leq 0.0001$; ns represents non-significant). One-way ANOVA and post-hoc Tukey's multiple comparison test were used for statistical analysis.

3.10 X15695 actions in ER$^+$ breast cancer that harbors mutant p53

About 70-80% of breast cancers are ER$^+$ and the majority of which express wild-type p53, although functionally debilitated while most ER$^-$ breast tumors express mutant p53 (Bertheau et al., 2013). The p53 signaling pathway therefore has to be reactivated in ER$^+$ and ER$^-$ tumors to

enable the inhibition of breast cancer cell growth. The presence of wild-type p53 is reported to have a positive impact on the therapeutic response and prognosis of breast cancer patients (Bergh et al., 1995). However, the therapeutic response of the breast cancer cells that are ER^+ but express mutant p53 remain to be elucidated.

The results presented in this work showed that the p53 pathway significantly contributed to X15695 actions in MCF-7 cells that are ER^+ and express wild type p53 ($p53^{wt}$). The reaction of ER^+ breast cancer cells that express mutant p53 to X15695 remains to be clarified and T47D cells were selected for this study. T47D is a human breast cancer cell line that is ER^+ and expresses mutant p53 ($p53^{L194F}$) (Horwitz et al., 1982; Huovinen et al., 2011). Clonogenic assay in T47D cells demonstrated that X15695 also significantly inhibited their clonal expansion of these cells (Figure 3.1 A). To explore the molecular mechanism of X15695 actions in T47D cells, genome-wide transcriptomic analysis was performed in the T47D cells after treatment with X15695 in the presence and absence of E2.

RNA was extracted and sent for sequencing at Novogene, Cambridge UK as previously described for the MCF-7 cells (chapter 3.4). The sequencing results were analyzed in the same way as the MCF-7 cell results, the raw reads of the sequence was quantified by Kallisto with quant function to acquire the abundance (Transcript per Million Read, TPM) (Appendix Figure 5.3A), then an edgeR package was used for data wrangling, such as to convert the data from TPM to CPM (Counts per Million Read) (Appendix Figure 5.3B), to filter data from outliers (Appendix Figure 5.3C) and also to normalize the filtered data (Appendix Figure 5.3D). Once all settled, the data were used for sample clustering and principle components analysis (PCA). Both Sample clustering and PCA showed the samples have a clear discrepancy among different conditions and high consistency in the same conditions (Appendix 5.4), suggesting the sequencing data in T47D cells were also valid for differentially expressed gene analysis and functional enrichment analysis.

For the RNA-sequencing data analysis in the T47D cells, the same comparisons ("X15695" versus "Vehicle" and "X15695+E2" versus "E2") and thresholds ($|\text{Log2 Fold Change}| \geq 1$; adj. p value ≤ 0.055) were used as described in MCF-7 cell RNA sequencing data analysis. In the absence of E2, a total of 458 DEGs were identified in response to X15695 treatment (280 genes were down-regulated and 178 genes were up-regulated) (Figure 3.20 A). In the presence of E2, 708 DEGs were observed (458 genes were down-regulated and 250 genes were up-regulated) (Figure 3.20 B). Differentially expressed genes and hallmark pathways were analyzed as described in chapter 3.4. The hallmark pathway analysis revealed that in the absence of E2, the

HALLMARK_ESTROGEN_RESPONSE_EARLY was the most significant pathway identified followed by the HALLMARK_ XENOBIOTIC_METABOLISM, suggesting X15695 may play a pivotal role in the xenobiotic metabolism. Besides, the ROS pathway and hypoxia as well as p53 pathway were also enriched though they were not in a dominant position (Figure 3.20 C). In the presence of E2, both early and late stages of estrogen response were significantly enriched in the dominant positions followed by HALLMARK_XENBIOTIC_METABOLISM and the HALLMARK_G2M_ CHECKPOINT. Besides, p53 pathway, ROS pathway, hypoxia and apoptosis were also enriched (Figure 3.20 D). Some of the genes in these pathways are marked in the volcano plot. Based on gene set enrichment of hallmark pathways analysis, the estrogen signaling, p53 signaling and G2/M checkpoint signaling dominantly contributed to X15695 actions in T47D cells.

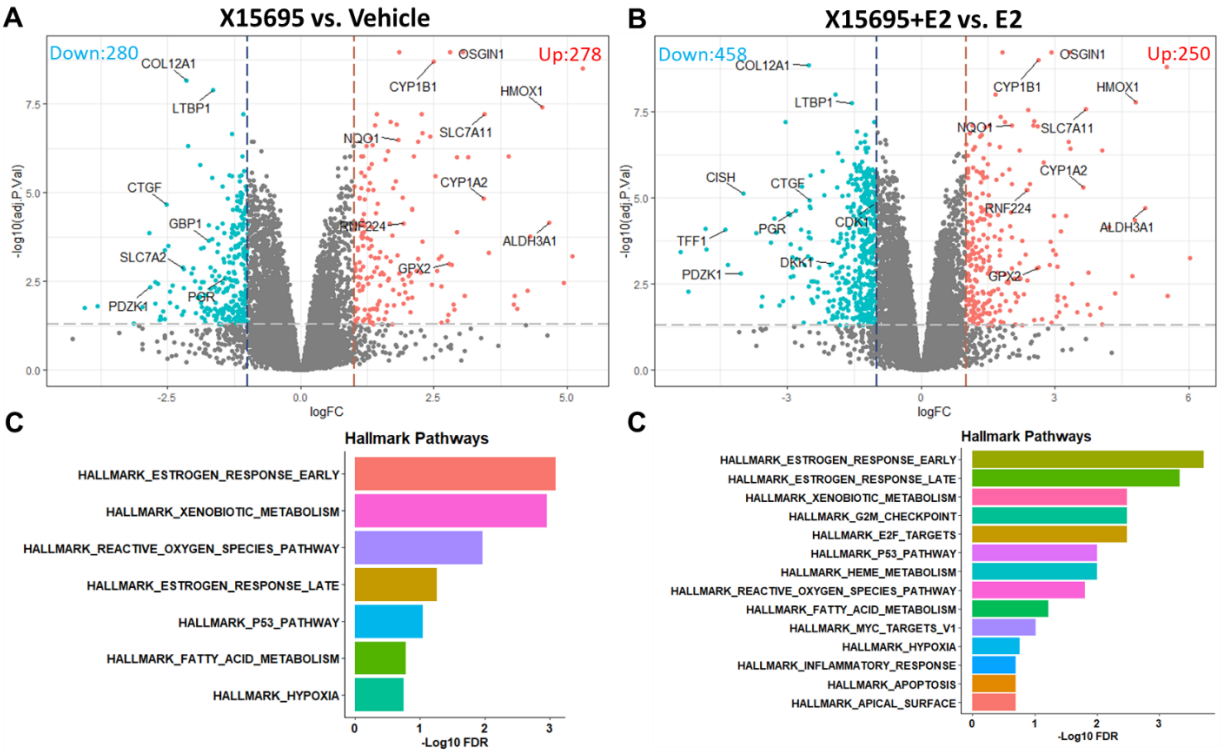

Figure 3.20: Functional enrichment analysis with differentially expressed genes of X15695 treated T47D cells in the absence and presence of E2.

(A). Volcano plot of DEGs of X15695 treated T47D cells in the absence of E2: 280 DEGs were down-regulated and 178 DEGs were up-regulated at the threshold of |LogFC| ≥ 1.0 and adj. p value ≤ 0.05; (B). Volcano plot of DEGs of X15695 treated T47D cells in the presence of E2: 458 DEGs were down-regulated and 250 DEGs were up-regulated at the threshold of |LogFC| ≥1.0 and adj. p value ≤ 0.05. (C). Gene set enrichment of hallmark pathway analysis of 458 DEGs from

X15695treated samples in the absence of E2. (D). Gene set enrichment of hallmark pathway analysis of 708 DEGs from X15695treated samples in the presence of E2.

3.11 X15695 also negatively regulated ER signaling in T47D cells

3.11.1 X15695 differently repressed ER downstream targets in T47D cells compared to MCF-7

To explore whether the same downstream genes in estrogen signaling are targeted by X15695 treatment in T47D cells and MCF-7 cells, the Log2 Fold changes of genes enriched in estrogen signaling in both cell lines are presented in the heatmap (Figure 3.21A). In general, genes that were repressed in T47D cells were also all repressed in MCF-7 cells with the exception of GJA1 and CISH (Figure 3.21A). Besides, there were roughly 19 genes that were significantly down-regulated by X15695 in MCF-7 but only showed a minor down-regulation or an even up-regulation in T47D cells (Figure 3.21A). These results indicated that although the estrogen signaling pathway is repressed by X15695 in T47D cells, the degree of repression was less prominent compared to that in MCF-7 cells, a finding that is consistent with the fact that T47D cells express a relative lower level of ER compared to MCF-7 cells (Yu et al., 2017).

To confirm the X15695-mediated transcriptional regulation of ER targets in T47D cells, several ER targets that were analyzed in T47D cells that were also verified in MCF-7 cells. Identical to the MCF-7 cells, T47D cells were also treated with 1 μM X15695 in the presence and absence of E2 for 16h and the RNA expression level of PGR, PDZK1, GREB1, AGR-2 and AREG was monitored by qRT-PCR. Consistent with the RNA-sequencing data, the expression of PGR and PDZK1 was significantly downregulated by X15695 both in the presence and absence of E2, while the expression of GREB1 was only down-regulated by X15695 in the presence of E2, and the expression of AGR-2 and AREG was not affected by X15695 regardless of the presence of E2 (3.21B). These results demonstrate slight differences in the regulation of ER target genes by X15695 in MCF-7 and T47D cells.

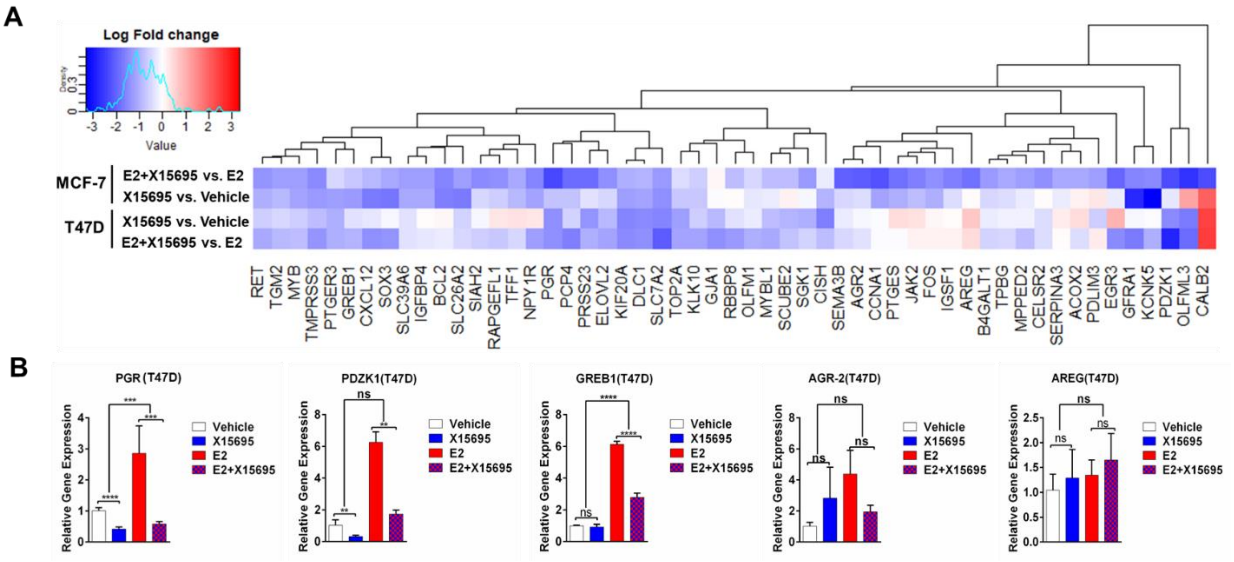

Figure 3.21: X15695 repressed estrogen signaling in T47D cells.
(A). Heatmap of genes enriched in estrogen signaling in T47D and MCF-7 cells treated with X15695 in the presence and absence of E2. (B). T47D cells were serum starved in hormone-depleted medium for 3 days and then treated with 1 µM X15695 in the presence and absence of E2 for 16 h. Cells were harvested and lysed for RNA extraction. cDNA was synthesized and qRT-PCR was performed to detect the RNA expression of PGR, PDZK1, GREB1, AGR-2 and AREG. The data represents the averages ± SEM (n =3; * $p \leq 0.05$; ** $p \leq 0.01$; *** $p \leq 0.001$; **** $p \leq 0.0001$). One-way ANOVA and post-hoc Tukey's multiple comparison test were used for statistical analysis. For comparison of the fold changes of gene expression with/without E2, the following formula was used: fold change without E2 = relative gene expression of X15695 group/relative gene expression of vehicle group; fold change with E2 = relative gene expression of (X15695+E2)/relative gene expression of E2 treated group; Double tailed t test was used for statistical analysis of E2 effect.

3.11.2 X15695 similarly destabilized ER in T47D cells compared to MCF-7 cells

To find out whether the effect of X15695 on ER target gene expression is also caused by destabilization of ER level in the T47D cells as shown in MCF-7 cells, T47D cells were treated with increasing concentration (10^{-9} to 10^{-6} M) of X15695 for 48 h and the protein level of ER was monitored by Western blotting. Consistent with the results in MCF-7 cells, 10^{-6} M X15695 significantly reduced ER protein levels (Figure 3.22A). In line with this result, immunofluorescence staining assay also showed a significant reduction of ER after X15695 treatment of T47D cells

(Figure 3.22B). Taken together, these results indicate that X15695 also promotes ER degradation in T47D cells.

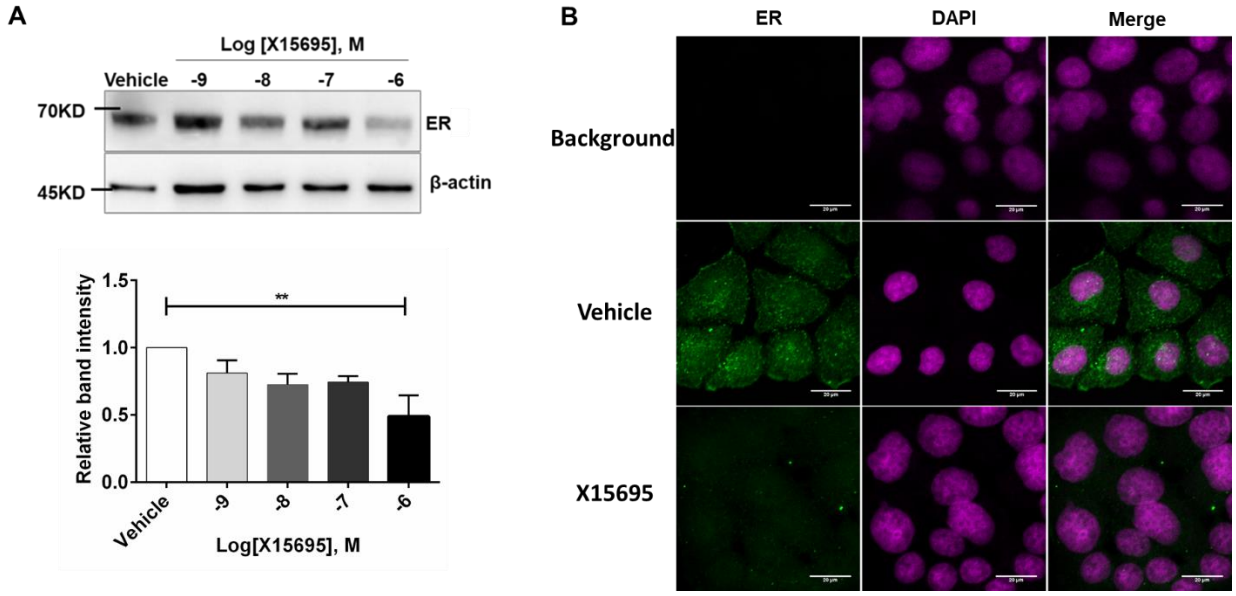

Figure 3. 22: X15695 destabilized ER protein in T47D cells.
(A). T47D cells were treated with increasing concentration of X15695 (10^{-9} to 10^{-6} M) or vehicle (DMSO) for 48h. Cells were harvested and the protein levels of ER were monitored by Western blotting using anti-ER antibody. Anti-β-actin antibody was used for equal protein loading control. The protein band intensities from 3 biological replicates were scanned and quantified by an ImageJ software. The results are expressed as the intensity of the ER band relative to the β-actin band which was nominally set at 1.0 and the values are presented as the averages ± SEM. ** $p \leq 0.01$. One-way ANOVA with post-hoc Tukey's multiple comparison test was used for statistical analysis. (B). T47D were cells treated with 1 µM X15695 or an equivalent volume of vehicle (DMSO) for 48 h. Cells were permeabilized, fixed and coupled with ER primary antibody and Alexa Fluor 488 secondary antibody. Fluorescence images were taken with confocal microscopy (Confocal Microscope platform STELLARIS6-LSM900, Leica, Germany) at 20×5 magnification.

3.12 X15695 also activated p53 signaling in T47D cells

Although p53 in T47D cells is mutated, the GSEA of the RNA-seq results showed activation of the p53 pathway. p53 mutants frequently have oncogenic gain-of-function activities and are known to exacerbate malignant properties to cancer cells (Stein et al., 2019). It is therefore intriguing to find out whether the action of X15695 activated the canonical p53 targets for anti-tumor effect

or activated the gain-of-function targets for exacerbating tumorigenesis in T47D. Thus, the genes enriched in p53 signaling in T47D cells were compared with those from MCF-7 cells. The heatmap showed that 14 genes were activated in T47D cells in response to X15695 treatment, 10 of them overlapped with the genes activated in MCF-7 cells. Of these, HMOX1, SLC7A11, OSGIN1 and GPX2 are mainly related to oxidative stress (Meiller et al., 2007; Yan and Chen, 2006; Yao et al., 2008) and four genes, IFI30, IER3, KLF4 and SLC3A2 were activated in only T47D cells (Figure 3.23A). The function of IER3 in breast cancer is unclear, but others have contradictory roles. While IFI30 was reported as related to poor prognosis (Fan et al., 2021), KLF4 is considered as a favorable prognosis marker and its high expression overcomes tamoxifen resistance by suppressing MAPK signaling pathway (Jia et al., 2018). As opposed to KLF4, SLC3A2 is reported to promote ER^+ breast cancer cell proliferation and tamoxifen resistance (Saito et al., 2022). To verify the X15695-mediated transcriptional regulation of p53 targets in T47D cells, several p53 targets that were analyzed in T47D cells that were also verified in MCF-7 cells. Identical to the MCF-7 cells, T47D cells were also treated with 1 µM X15695 in the presence and absence of E2 for 16h and the RNA expression level of CDKN1A, GADD45A, FAS, BBC3, OSGIN1 and SCL7A11 was monitored by qRT-PCR. Consistent with the RNA-sequencing data, the expression of CDKN1A, SLC7A11 and OSGIN1 was significantly downregulated by X15695 both in the presence and absence of E2, while the expression of GADD45A, FAS and BBC3 was not affected by X15695 regardless of the presence of E2 (3.23B). These results indicated that X15695 contributes to a different cell behavior in T47D cells compared to MCF-7 cells.

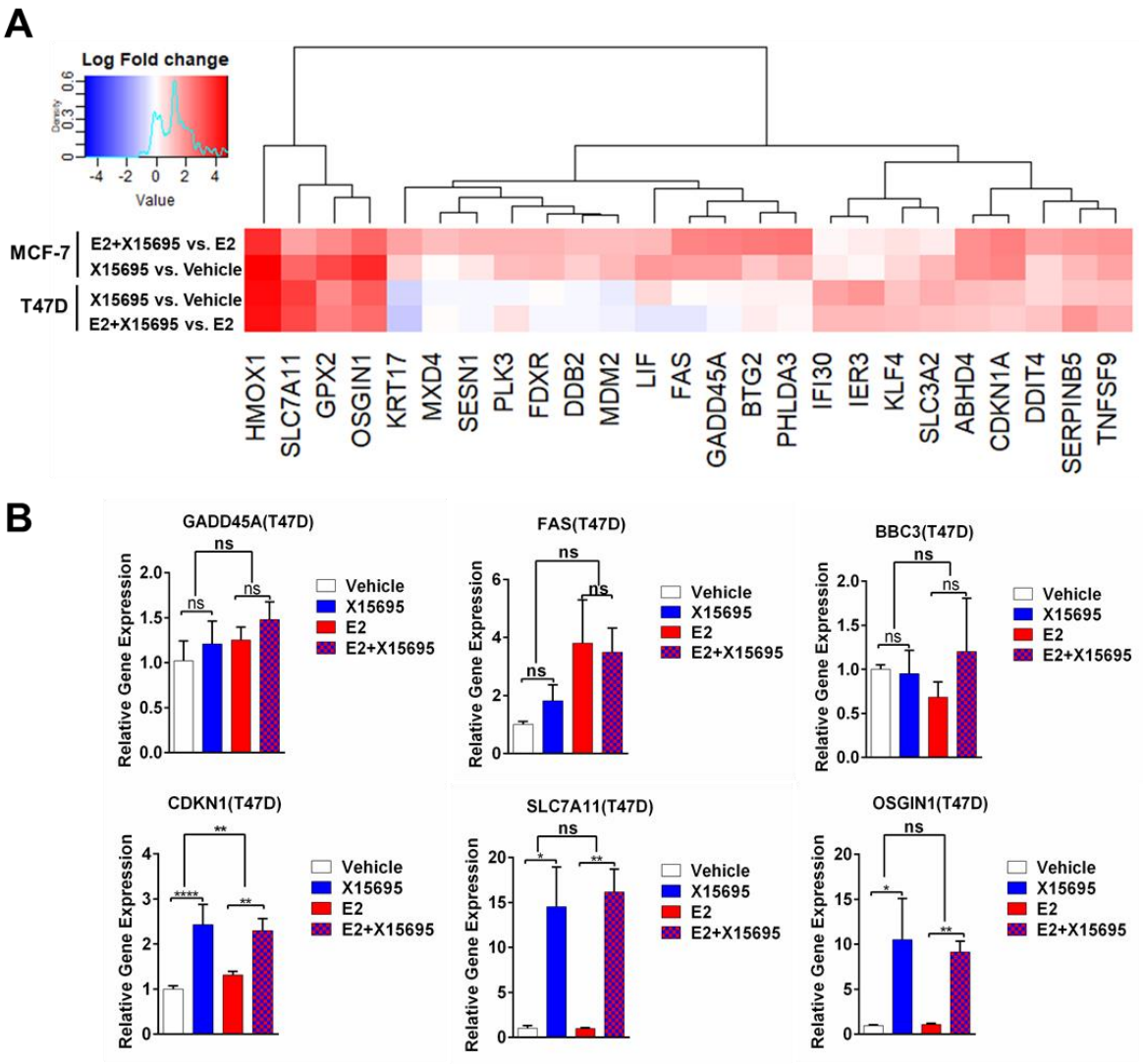

Figure 3.23: X15695 activated p53 signaling in T47D cells.

(A). Heatmap of genes enriched in p53 signaling in T47D and MCF-7 cells treated with X15695 in the presence and absence of E2. (B). T47D cells were serum starved in hormone-depleted medium for 3 days and then treated with 1 µM X15695 in the presence and absence of E2 for 16 h. Cells were harvested and lysed for RNA extraction. cDNA was synthesized and qRT-PCR was performed to detect the RNA expression of GADD45A, CDKN1A, FAS, BBC3, SLC7A11 and OSGIN1. The data represents the averages ± SEM (n =3; * $p \leq 0.05$; ** $p \leq 0.01$; *** $p \leq 0.001$; **** $p \leq 0.0001$). One-way ANOVA and post-hoc Tukey's multiple comparison test were used for statistical analysis. For comparison of the fold changes of gene expression with/without E2, the following formula was used: fold change without E2 = relative gene expression of X15695 treated group/relative gene expression of vehicle treated group; fold change with E2 = relative gene

expression of (X15695+E2)-treated /relative gene expression of E2 treated group; Double tailed t test was used for statistical analysis of E2 effect.

3.13 X15695 blocked G2/M transition in T47D cells

Most studies investigating p53 function have focused attention on genes transactivated by p53. However, it is recognized that repression of target genes may be important for p53-induced cell cycle arrest and cell death. As G2/M checkpoint showed up in response to X15695 action, the gene sets that involved in the G2/M cell cycle arrest were presented in the heatmap with their expression at log2 fold change and compared the results with MCF-7 cells. The heatmap showed that the genes in the G2/M checkpoint were mainly significantly repressed in the X15695 treated T47D cells but not much in the absence of E2 and only marginal in MCF-7 cells (Figure 3.24A). Three genes (UBE2C, CDD6 and CDC20) were analyzed in qRT-PCR studies to confirm the X15695-mediated regulation of genes in the G2/M checkpoint. UBE2C, CDD6 and CDC20 that play critical role in G2/M transition were selected for validation. UBE2C is ubiquitin-conjugating enzyme that participates in cell cycle progression and checkpoint control (Hao et al., 2012). Cells overexpressed UBE2C ignored the mitotic spindle checkpoint signal and forced the cells entering the mitosis phase, which consequently caused cells to lose their genomic stability and acquire malignant properties (Xie et al., 2014). CDC6 (cell division cycle 6) is an essential regulator of DNA replication. It is well known as a key protein that participates in assembly pre-replicative complex at the beginning of DNA replication during G1 phase to S phase transition (Yan et al., 1998). Accumulated evidences demonstrate that CDC6 also plays important role in the activation and maintenance G2 phase to mitosis transition (Borlado and Méndez, 2008). CDC20 (cell division cycle) is reported to meditate G2/M transition via interacting with several cellular components, such as FZR1 (fizzy and cell division cycle 20 related 1) (Chang et al., 2004). Consistent with the heatmap, the qRT-PCR results showed both 3 genes were significantly downregulated in X15695 treated T47D cells in the presence of E2 (Figure 3.24B).

To further confirm the effect on G2/M cells cycle transition, FACS measurement was performed with single staining of 7-AAD to analyze cell cycle distribution of T47D cells with or without X15695 treatment. Indeed, X15695 treatment increased more than 10% of cell population arrested in the G2 phase, indicating X15695 treatment blocked T47D cells G2/M cell cycle transition (Figure 3.24C).

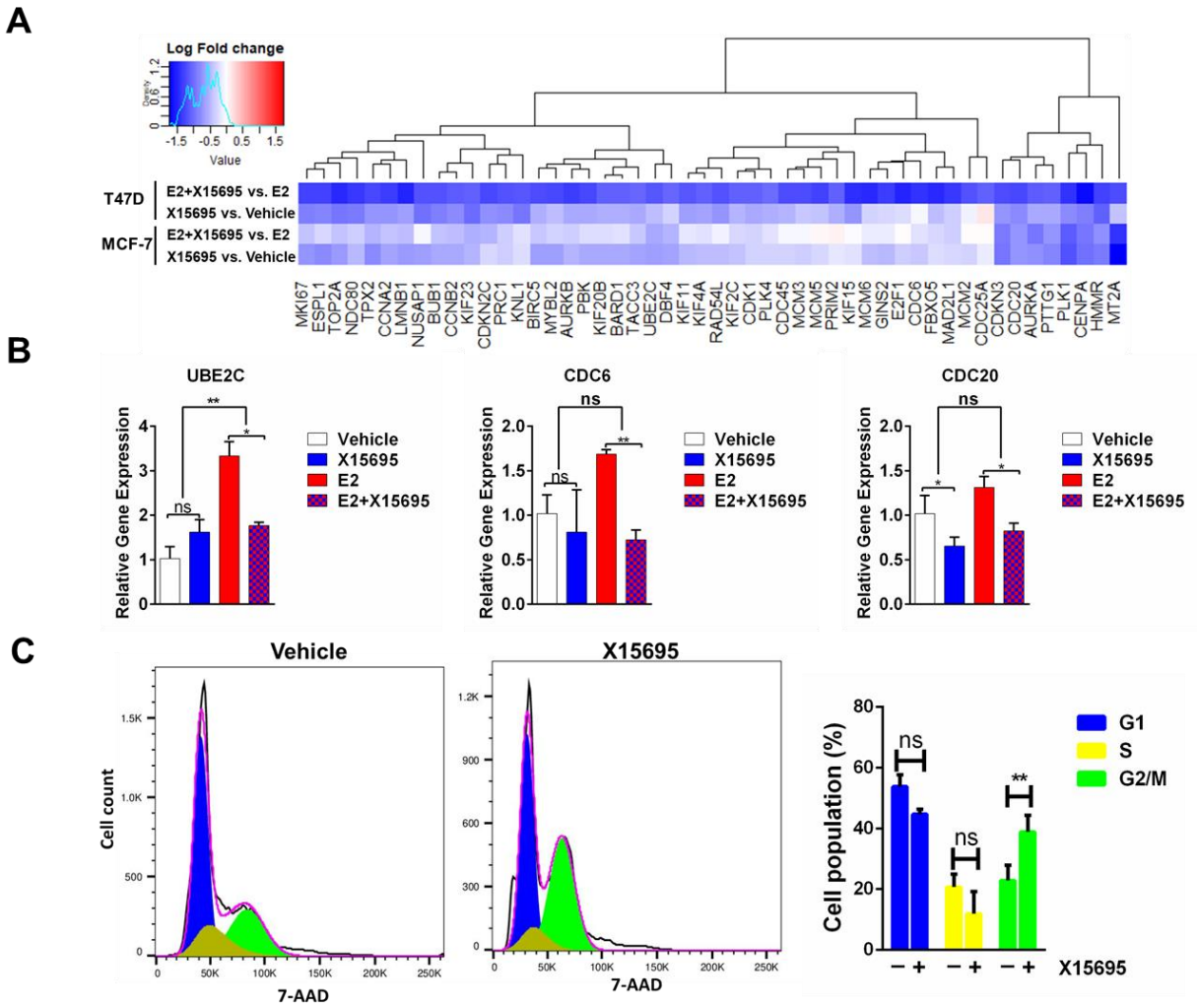

Figure 3.24: X15695 blocked G2/M cell cycle transition in T47D cells

(A). Heatmap of genes enriched in G2/M checkpoint in T47D and MCF-7 cells treated with X15695 in the presence and absence of E2. (B). T47D cells were serum starved in hormone-depleted medium for 3 days and then treated with 1 µM X15695 in the presence and absence of E2 for 16 h. Cells were harvested and lysed for RNA extraction. cDNA was synthesized and qRT-PCR was performed to detect the RNA expression of UBE2C, CDC6 and CDC20. The data represents the averages ± SEM (n =3; * $p \leq 0.05$; ** $p \leq 0.01$; *** $p \leq 0.001$; **** $p \leq 0.0001$; ns refers to non-significant). One-way ANOVA and post-hoc Tukey's multiple comparison test were used for statistical analysis. For comparison of the fold changes of gene expression with/without E2, the following formula was used: fold change without E2 = relative gene expression of X15695 treated samples/relative gene expression of vehicle treated samples; fold change with E2 = relative gene expression of (X15695+E2)/relative gene expression of E2 treated group; Double tailed t test was

used for statistical analysis of E2 effect. (C). FACS measurement for cell cycle. T47D cells were treated with 1 µM X15695 for 48 h. Cells were then fixed and stained with 7-AAD only for 5 min. 10^6 cells were used for FACS measurement. All data was analysis by FlowJo software.

3.14 X15695 did not affect protein stabilization and cellular localization of $\mathbf{p53^{L194F}}$ in T47D cells

As the effect of X15695 on p53 induced cell cycle arrest differs from that observed in MCF-7 cells, it is important to investigate how this difference is brought about. Therefore, the expression level of the mutant p53 following X15695 treatment in T47D cells was monitored by Western blotting and its cellular localization was determined by immunofluorescence. T47D cells treated with increasing concentration of X15695 from 10^{-9} to 10^{-6} for 48 h were used for the Western blotting study and treatment with 1 µM X15695 at different time points was used for the immunofluorescence staining assay. The Western blotting results showed that unlike the situation in MCF-7 where X15695 treatment increased p53 level and its transport into the nucleus, in T47D cells the protein levels of $p53^{L194F}$ was not significantly altered by X15695 treatment (Figure 3.25A) and $p53^{L194F}$ was already nuclear in the absence and presence of X15695 (Figure 3.25B). These results deviate from the results of the effect of X15695 on p53 in MCF-7 cells and point to a different action of the mutant p53 in T47D cells in the presence of X15695.

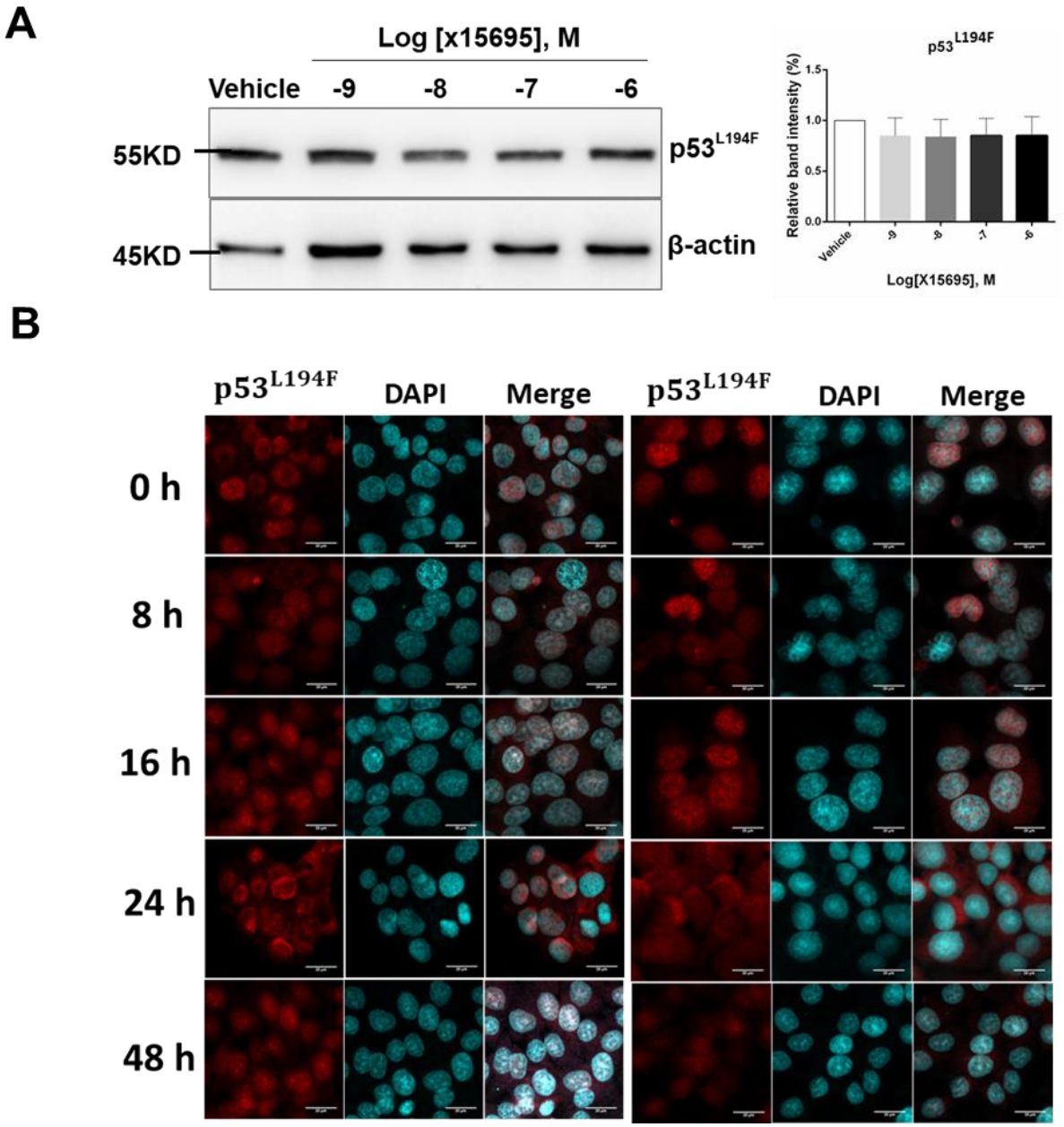

Figure 3. 25: X15695 has no effect on p53 protein in T47D cells

(A). T47D cells were treated with increasing concentration of X15695 (10-9 to 10-6 M) or vehicle (DMSO) for 48 h. Cells were harvested and the protein levels of $p53^{L194F}$ were monitored by Western blotting using anti-p53 antibody. Anti-β-actin antibody was used for equaling protein loading control. Right panel: The intensities of the protein bands from 3 biological replicates were scanned and quantified by an ImageJ software. The results are expressed as the intensity of the ER band relative to the β-actin band which was nominally set at 1.0 and the values are presented as the averages ± SEM, ns stands for non-significant. One-way ANOVA with post-hoc Tukey's

multiple comparison test was used for statistical analysis. (B). T47D cells were cells treated with 1 µM X15695 and an equivalent volume of vehicle (DMSO) for 48 h. Cells were permeabilized, fixed and coupled with Rabbit anti-p53 primary antibody and Alexa Fluor 546 secondary antibody. Fluorescence images were taken with confocal microscopy (Confocal Microscope platform STELLARIS6-LSM900, Leica, Germany) at 20×3 magnification.

3.15 X15695 triggers cell death in T47D cells

To investigate whether X15695 treatment also triggers cell death in T47D cells, T47D cells were treated with 1 µM X15695 and used for apoptosis assay by FACS measurement with double staining of 7-AAD and Annexin V-PE to analyze the apoptotic cell populations in T47D cells. Cells were stained with annexin V-PE positive and 7-AAD negative (Annexin V^+, 7-AAD^-) refer to the early apoptotic cells; Cells stained with annexin V-PE positive and 7-AAD positive (Annexin V^+, 7-AAD^+) refer to the cells in the late stage of apoptosis or cells were already died. The FACS measurement results indicated X1569 treatment increased both the early stage and late stage of apoptotic cell populations, suggesting X15695 also induced apoptosis in T47D cells Figure 3.26A). T47D cells were also treated with a serial concentration (10^{-10} to 10^{-6} M) of X15695 and used in MTT cell viability measurements. The result indicated that 1 µM X15695 treatment for 48 h significantly inhibited viability of T47D cells (Figure 3.26B).

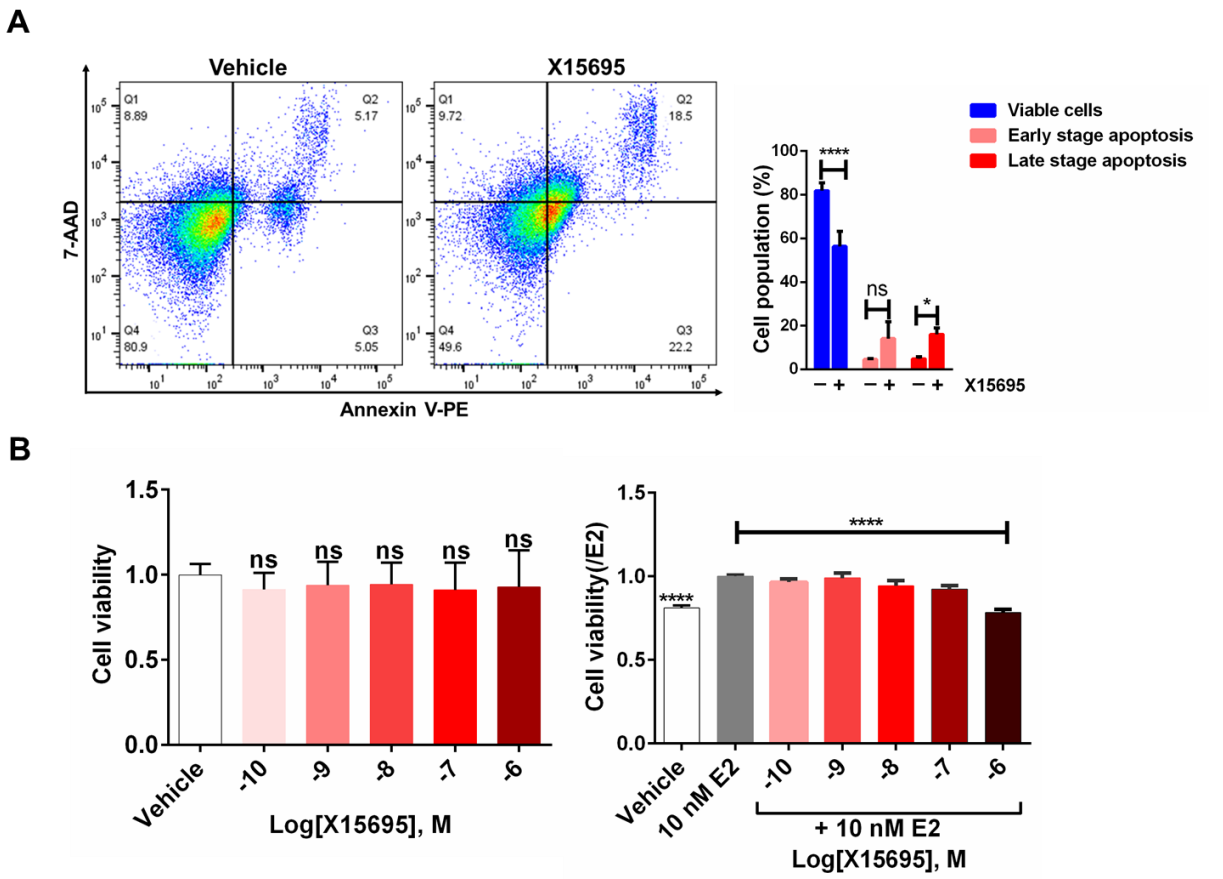

Figure 3. 26: X15695 treatment induced cell death in T47D cells.
(A). FACS measurement for apoptosis. T47D cells treated with 1 µM X15695 for 48 h were double stained with 7-AAD and Annexin V-PE for 15 minutes. Cells stained with 7-AAD or Annexin V-PE only were used for compensation of Double staining. 10^6 cells were used for FACS measurement. (B). T47D cells cultured in hormone-depleted medium for 3 days were treated with the indicated concentrations of X15695 in the absence or presence of E2 for 48 h. Cell viability was measured by MTT assay. Data was presented as averages ± SME, One-way ANOVA and post-hoc Tukey's multiple comparison test were used for statistical analysis (N=3, R=5, **** $p \leq 0.0001$).

3.16 X15695 inhibits the survival and clonal expansion of tamoxifen-resistant MCF-7 cells

The studies so far show X15695 as an antagonist of growth of ER^+ breast cancer cells. Among drugs that are approved for the treatment of ER^+ breast cancers are tamoxifen and fulvestrant. Although treatment of women with ER^+ metastatic breast cancer with tamoxifen is useful in controlling their disease, resistance almost invariably develops, leading to recurrence (Dorssers

et al., 2001). Fulvestrant has been shown to be have activity in some women with tamoxifen resistant but resistance to fulvestrant limits its utility (Nathan and Schmid, 2017). To investigate whether X15695 could be further developed for therapy in such resistant situations, its action was compared with that of tamoxifen and fulvestrant in viability and clonal expansions studies in TRMCF-7 cells (MCF-7 cells treated with 100 nM Tamoxifen over 12 months) (Nawata et al., 1981).

Treatment of the cells with varying range of the three compounds (10^{-11} to 10^{-6} M) for 48 h, showed that while tamoxifen did not alter the viability of the cells, X15695 was as good as fulvestrant in decreasing viability of the cells (Figure 3.27A)

In clonogenic experiments, while tamoxifen failed to inhibit the clonal expansion of the TMCF-7 cells, X15695 and fulvestrant were both efficient in inhibiting the growth of the cells (Figures 3. 27B and C), although in this assay fulvestrant was slightly more efficacious than X15695. Collectively, X15695 is a promising compound for further development for the treatment of endocrine-resistant ER^+ breast cancer cells.

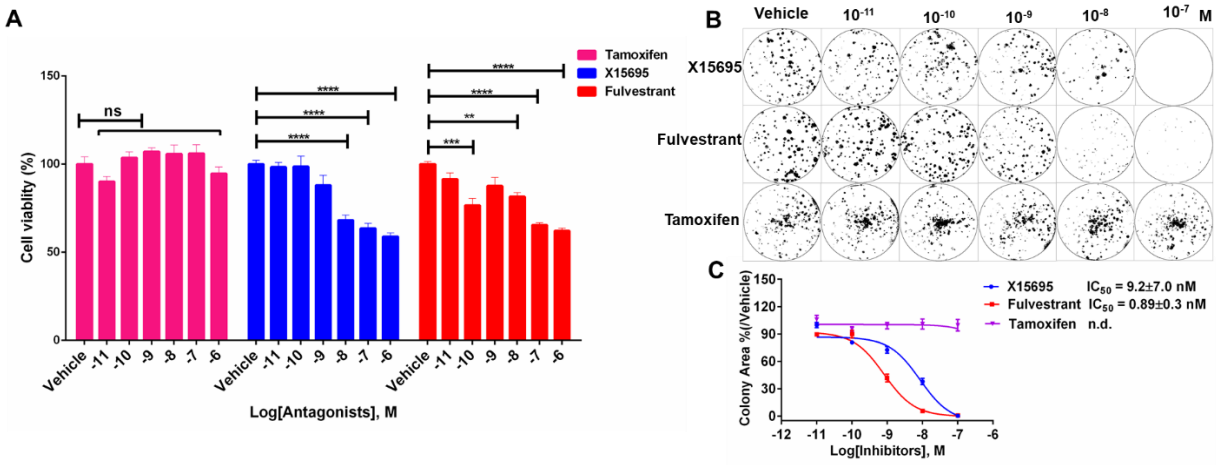

Figure 3. 27: Comparison of the inhibitory effect of X15695, tamoxifen and fulvestrant on Tamoxifen resistant MCF-7 cells.

(A). Tamoxifen resistant cells were treated with the indicated concentrations of X15695, fulvestrant and tamoxifen for 48 h. Cell viability was measured by MTT assay. 5 replicates were used for each experiment, and the experiment was repeated 3 times (N=3, R=5, ** $p \leq 0.01$, *** $p \leq 0.001$, **** $p \leq 0.0001$, ns stands for non-significant). One-way ANOVA and post-hoc Tukey's multiple comparison test were used for statistical analysis. (B). Tamoxifen resistant MCF-7 cells were seeded in 6-well plate at a density of 1000 cells/well. Cells were treated with the indicated serial concentrations of X15695, fulvestrant and tamoxifen for 3 weeks. Cell medium with the indicated concentrations of compounds was changed every week. Cells were fixed and stained

after 3 weeks and the colonies in each well were analyzed by ImageJ software. (C). Quantification of colonies was carried out by ImageJ software and the IC_{50} values of X15695 were calculated with a build in function within primer GraphPad Prism. The points on the curve represent the averages ± SEM.

Chapter 4: Discussion

ER^+ breast cancer is the largest group of breast cancer and frequently diagnosed in women with an estimated 1.7 million new cases in year 2012 (Donepudi et al., 2014). Over the decades, hormone therapies including AIs, SERMs and SERDs have been developed that either target the production of estrogens or the action of the ER for ER^+ breast cancer patients. Although these therapies are successful, clinical outcomes such as DFS (disease free survival) and OS (overall survival) within 5 years are not extremely optimistic due to hormone therapy-induced resistance (Drăgănescu and Carmocan, 2017). A different approach is therefore required for inhibiting the action of the ER that does not directly target the ER. In this work, the cochaperone BAG1 has been chosen to be targeted. BAG1 is highly expressed in ER^+ breast cancer cells and enhances the action of the estrogen receptor (Cutress et al., 2003). It is also an anti-apoptotic protein and protects cells against programed cell death. In a focused screen of compounds that may interact with BAG1, an imidazopyridine-based scaffold compound identified as a small molecule that interacts with BAG1 through an in vivo ligand engagement assay. Studies on the mechanism of action of this compound using transcriptomics analysis showed that the ER and p53 signaling pathways are crucial of its mode of action. Both pathways impact on cell cycle progression and apoptosis, and thereby contribute to growth inhibitory properties to the compound.

4.1 Targeting BAG1 with a novel imidazopyridine-based scaffold compound X15695 in ER^+ breast cancer cells

BAG1 expression is frequently increased in breast cancer and pre-invasive breast cancer compared to normal breast tissues (Brimmell et al., 1999). Clinical studies showed a relative high level of nuclear BAG-1 expression is correlated with a low tumor grade and shorter DFS and OS (Tang et al., 1999; Townsend et al., 2002). A meta-analysis also indicated that the intensity and localization of BAG1 proteins are related to tumor grade and clinical outcome, which makes BAG1 a prognostic biomarker for breast cancer (Papadakis et al., 2017). Hence, BAG1 directed therapy has emerged as a possible novel approach to target breast cancer (Enthammer et al., 2013). As a cochaperone, BAG 1´s main action is to serve as a nucleotide exchange factor of Hsp70. It uses its BAG domain situated at its C-terminus for this function. Hsp70 is also in a complex with Hsp90 for the correct folding of nuclear receptors bringing them into the appropriate conformation for hormone binding. However, because BAG1 has nuclear and cytoplasmic isoforms both of which

carry the BAG domain, it is likely that BAG 1 plays a chaperone role in the action of the ER in the cytoplasm as well as in the nucleus via the action of its BAG domain. The BAG domain has long been postulated to form a pocket for binding of small molecules. Initially the molecule Thio-2 (a benzothiazole-based compound) was reported to dock into this pocket (Enthammer et al., 2013). However, since Thio-2 is very unselective (Enthammer et al., 2013), it was derivatized to A4B17 which was shown to dock quite well into the BAG1 pocket (Cato et al., 2017). As benzothiazoles in general have a large range of other activities, an attempt was made to look out for more selective compounds other than A4B17.

In the work reported here a compound with an imidazopyridine scaffold has been proposed to mediate the action of BAG1. The assay that led to this claim was the CETSA that identifies cellular engagements of ligands by changing the thermal degradation properties of the target proteins when bound to the compound. In the studies presented in this thesis, the denaturation temperatures for all the BAG1 isoforms (both the nuclear and cytoplasmic isoforms) were shown to increase by 2-3^{o}C following treatment of the cells with the compound. This was taken to indicate binding of the compound to the BAG1 proteins. Although the increase in denaturation temperature was not much, in the isothermal dose response footprint analysis that calculates the concentration of compound for the half maximal binding to the BAG domain, a concentration in the nanomolar range was measured. The BAG domain is very resilient to changes and mutations in this domain that are known to alter the function of the protein hardly change or only minimally change the melting temperature of the protein. In one situation only 1^{0}C of change was registered (Nguyen et al., 2020). Against this background, a change of 2-3^{0}C could represent a significant change in the BAG domain that could have great consequences on its function.

The small molecule that was identified to bind to BAG1 has an imidazopyridine scaffold. Imidazopyridines have drawn conspicuous attention in the pharmaceutical researches due to their frequently occurrence in numerous drugs that showed a board range of biological and pharmacological activities, such as anti-tumor (Iqbal et al., 2020), anti-inflammatory (Chen et al., 2013), anti-diabetic (Jiang et al., 2020), anti-viral (Gudmundsson et al., 2009; Paeshuyse et al., 2007), and anti-mycobacterial activities (O'Malley et al., 2018). Imidazopyridine ring system can be classified into four classes based on the position of individual nitrogen atoms, including imidazo[1,2-a] pyridine, imidazo[1,5-a] pyridine, imidazo[4,5-b] pyridine and imidazo[4,5-c] pyridine. The imidazo[1,2-a] pyridine scaffold-based derivatives have been further explored and evaluated for anti-tumor activity in multiple human cancer cell lines. For example, Endoori, et al

(Endoori et al., 2021) reported imidazo[1,2-a] pyridine based 1H-1,2,3-triazole derivatives showed inhibitory effect on HeLa and MCF-7 cells growth with IC_{50} values ranging from 2.35 µM to 120.46 µM. On the other hand, Damghani et al designed and synthesized a series of imidazo[1,2-a] pyridine derivatives containing 1,2,3-traozole moiety, which worked as c-Met kinase inhibitor and showed a significant anti-proliferative effect on c-Met-positive lung cancer cells (EBC-1) and pancreatic cancer cells (AsPc-1, Suit-2 and Mia-Paca-2) (Damghani et al., 2021). The compound X15695 identified in this work also contains a typical imidazo[1,2-a] pyridine but as oppose to the other published compounds it inhibited the clonal expansion of ER^+ breast cancer cells in the nanomolar range. Unlike the studies that showed that the imidazopyridine derivative affected c-Met action, the results presented here do not only show the signaling pathways that are affected by X15695 action but identify BAG1 as the target of X15695 through engagement of the compound in CETSA.

Although no docking experiments were conducted in the present study, the finding of the engagement of X15695 to BAG1 protein in the in vivo thermal shift assay suggests that like A4B17, X15695 possibly docks into the BAG domain. In addition to BAG1, there are other BAG-domain protein members such as BAG2, BAG3, BAG4 and BAG5 that share a highly conserved canonical BAG domain. It is worth nothing that roughly 35% of 310 breast cancer patients examined were classified as either BAG2 high or BAG2(+). Kaplan-Meier plots showed that distant metastasis-free survival was reduced in patients with either BAG2-high or BAG2(+) cancer-associated fibroblasts than in patients of other groups (Yoon et al., 2021). Meta-analysis of gene expression data in 1809 breast cancer patients identified upregulated expression of BAG3 and WBP2NL (WBP2 N-terminal like) to be associated with a significant poor relapse-free survival (RFS) (Nourashrafeddin et al., 2015). Another BAG protein, BAG5 is also overexpressed in many type of human cancers including breast cancer and high expression of BAG5 is associated with poor prognosis (Yue et al., 2016). Collectively, these findings demonstrated that the BAG family proteins are positively expressed in breast cancers and exhibit unfavorable oncogenic activities for tumor progression. This raises questions whether a compound such as X15695 that targets the BAG domain of BAG1 will also be effective in targeting the BAG domains of the other BAG proteins. If this is the case, X15695 will serve as an anti-cancer drug for the treatment of other cancers including breast cancer where these BAG proteins are overexpressed

4.2 X15695 actions promote ER degradation in ER$^+$ breast cancer cells

Studies presented in this thesis show that it is not only an increased expression of BAG1 that is needed for the manifestation of the anti-proliferative action of X15695. For example, in MDA-MB231 cells that expresses significantly high BAG1 levels but lacks ER expression, no inhibitory action of X15695 is noticeable. One explanation for this apparent conundrum is that BAG1-meidtaed X15695 actions majorly through deregulation of ER and p53 signaling pathways. However, these two main actions of X15695 are both compromised in MDA-MB231 cells due to the lack of ER expression and the mutation of p53. The studies presented in this thesis show that the antagonistic action of X15695 on ER is mediated through degradation of the ER. Thus, X15695 can be classified in the group of ER antagonists that are termed SERD (selective estrogen receptor degraders) to which the classical inhibitor fulvestrant belongs because they exert their action through degradation of the receptor. The fulvestrant mediated ER degradation is induced by the formation of unique ER-Fulvestrant conformation, which consequently leads to proteasome-dependent ER turn-over (Reid et al., 2003; Wijayaratne and McDonnell, 2001). The bewildering question is how the engagement of X15695 to BAG1 leads to the degradation of ER. Although this question has not been directly answered in this thesis, there are several published data that could help provide explanation to this phenomenon.

BAG1 gene expresses four BAG1 proteins that are localized in the nucleus and cytoplasm. The nuclear BAG1 (BAG-1L) acts as binding partner for multiple nuclear hormone receptors including ER, AR and VDR for transactivation by the receptors. For example, the BAG domain of BAG-1L is reported to interact with the AF-1 domain in the AR N-terminus in the nucleus, which is responsible for transactivation by the AR. The previously published chemical BAG1 probe, A4B17 disrupts the interaction of BAG-1L with AR leading to the inhibition of AR signaling pathway and consequently inhibits prostate cancer cell growth (Kuznik et al., 2021). Similarly, only the BAG-1L is capable of transactivating ER in ER$^+$ breast cancer (Cutress et al., 2003), suggesting a similar mechanism of enhancement of the transactivation potential of the ER as described for the AR. X15695 that shares a similar pharmacophore feature as A4B17, represses ER singling pathway and inhibits ER$^+$ breast cancer cell growth, suggesting X15695 controls ER transcriptional activity possibly through nuclear BAG1. The cytoplasmic BAG1 isoforms also interact with ER without affecting ER transcriptional activity (Cutress et al., 2003). However, accumulated evidences have demonstrated BAG1 in cooperation with chaperone complex (HSP70-HSC70-HSP40-HSP90) and CHIP (carboxyl terminus of HSC-70-interacting protein), which is responsible for the degradation of unliganded and misfolded ER via 26 S proteasome (Berry et al., 2008; Fan et al., 2005; Lonard

et al., 2000). Furthermore, CHIP-BAG1-HSPs complex preferentially recognizes and degrades misfolded ER compared to unliganded ER (Fan et al., 2005; Tateishi et al., 2004). This process mainly happens in the cytoplasm, suggesting cytoplasmic BAG1 isoforms dominantly contribute to ER degradation. However, upon ligand-binding (estrogen, ER-agonists and antagonists), the chaperone complex (HSP70-HSC70-HSP40-HSP90) dissociates, and the degradation of freed liganded-ER occurs in a CHIP-independent since it happens in CHIP-/- cells to the same extent as in CHIP+/+ cells (Marsaud et al., 2003; Tateishi et al., 2004). This suggests that the liganded-ER degradation is distinct from that of the unliganded ER degradation, but whether BAG1 plays a role in liganded-ER degradation remains unknown. The work presented in this thesis indicates that X15695 induces ER degradation both in the absence and presence of E2. In the absence of E2, two possibilities could be triggered to bring about the X15695-induced ER degradation: 1), the engagement of X15695 with cytoplasmic BAG1 isoforms hijackers ER-CHIP-BAG1-HSPs complex, which promotes the poly-ubiquitination of unliganded ER; 2), the engagement of X15695 with cytoplasmic BAG1 isoforms interferes the appropriate folding of ER, which promotes the misfolded poly-ubiquitination. By these two possibilities, the elevated poly-ubiquitylated ER leads to proteasome mediated ER degradation. In the presence of E2, a possible explanation is that X15695 treatment stabilizes ER-CHIP-BAG1-HSPs complex and prevent the dissociation of CHIP-HSPs complex from ER, which also induces misfolding of ER and mediates its proteasome degradation. Collectively, these findings suggest that the actions of X15695 in ER inhibition may not be a single event brought about BAG1. Therefore, a better understanding of mechanism of X15695 on ER degradation awaits further experimentation.

4.3 X15695 actions activate p53 signaling in ER^+ breast cancer cells

Another main action of X15695 is in the regulation of ER action identified in this work is p53. p53 is one of the most well-known tumor repressor genes that is commonly mutated in various cancers including breast cancer(Olivier et al., 2010). It is well-acknowledged that approximately 50% human cancers harbor one or multiple mutations in p53 gene. However, the observed p53 mutations is less than 30% in total breast carcinomas. Accumulated evidences have demonstrated that the p53 mutations are highly linked to subgroups of breast carcinoma. Specifically, p53 mutation have been reported in 26% luminal-A breast cancer, 41% in luminal-B breast cancer, 50% in HER2(human epidermal growth factor)-enriched breast cancer and 88% in triple negative (ER negative, PR negative and HER2 negative) basal-like breast cancer (Bertheau

et al., 2013). Although more than 70% ER^+ breast cancers express wild type p53, p53 signaling is primarily inactivated and tightly control in multiple ways. The activation of p53 signaling requires two basic actions of p53: 1), translocation of p53 into the nucleus; 2), binding of p53 to chromatin to initiate target gene expression.

The shuttling of p53 from cytoplasm to nucleus relies on association of its the nuclear localization signal (NLS) with microtubule and dynein. Dynein is a microtubule-based and minus-end directed motor protein that travels on microtubules (Giannakakou et al., 2000). Once p53 is delivery to the peri-nuclear region by the dynein cargo, importin proteins α and β recognize the NLS of p53 and transports p53 to the nucleus (Liang and Clarke, 1999). The translocation of p53 into the nucleus could be abrogated by several proteins, such as by the protein mortalin, MDM2 and BCL2 (Liang and Clarke, 2001). Mortalin, a member of HSP70 family binds to the C-terminal amino acid residues 312 to 352 of p53 that is known as the cytoplasmic sequestration domain (CSD, also known as oligomerization domain) (Wadhwa et al., 2002). The binding of mortalin to the CBD domain induces a conformational change in p53 that masks its NLS. Therefore, mortalin sequesters p53 in the cytoplasm and inhibits its transcriptional activity (Kaula et al., 2000; Wadhwa et al., 1998; Wadhwa et al., 2002). In the work presented in this thesis, X15695 treatment has been shown to induce p53 nuclear accumulation in MCF-7 cells, which is most likely linked to mortalin protein. Giving the fact that X15695 is bound to BAG1, a co-chaperone protein that interacts with chaperone protein mortalin (Maddalo, 2009), the disruption of the mortalin-p53 complex by X15695 presented in this work could be brought about indirectly by a disruption of the mortalin-BAG1 interaction. Unlike the situation in HSP70, the BAG1 binding sites locate to the substrate binding domain (SBD) of mortalin instead of its ATPase domain (Maddalo, 2009), while the binding of p53 to mortalin is mapped at the ATPase domain of mortalin (Kaul et al., 2001). Therefore, one could speculate that the sequestration of p53 by mortalin may require the participation of BAG1. The finding that X15695 targets BAG1 reported in this work could disrupt BAG1-mortalin interaction, and thereby disrupting the mortalin-p53 complex. Indeed, the studies presented in this work point to this action of X15695. This compound did not only disrupt the BAG1-mortalin interaction but also the p53-mortalin binding and promoted nuclear transport of p53. However, whether these actions of X15695 occur independently or through the disruption of a ternary complex of BAG1-mortalin-p53 complex remains to be established. Besides, the BAG1 interacting protein BCL2 is also reported to sequester p53 in the cytoplasm by altering its subcellular trafficking and therefore inhibiting its transcriptional activity (Ryan et al., 1994). Anti-BCL2 oligonucleotides leads to a significant p53

nuclear accumulation in γ-irradiated RKO cells compared to control oligonucleotides (Beham et al., 1997). A possibility therefore exists that the nuclear translocation of p53 could also be brought about by a disruption of BAG1-BCL2 complex.

Binding of nuclear p53 to its response-element in chromatin is critical for the initiation of downstream target gene expression. However, this action is also limited in ER^+ breast cancer cells. In ER^+ breast cancer cells, the activation function-2 (AF-2) domain (amino acid residues 283 to 395) of ER directly binds to the C-terminal domain (amino acid residues 319 to 393), which is the region that is extensively modified with ubiquitination and acetylation for the stability and transcriptional activity of p53, respectively (Feng et al., 2005; Liu et al., 2006). The acetylation of 6 lysine residues within the C-terminal domain of p53 (p53-6KR) is pivotal for p53 sequence-specific DNA binding, and mutation of these lysine residues significantly impaired p53 transcriptional activity (Feng et al., 2005; Gu and Roeder, 1997). Indeed, published evidence indicates that the binding of ER to p53 significantly represses p53 transcriptional activity and inhibits p53-targeted gene expression, such as p21 and PCNA (Liu et al., 2006). Therefore, the ER-mediated repression of p53 transcriptional activity described in this work could be caused by the interaction of ER with p53. Under this context, the actions of X15695 destabilized ER and disassociated p53-ER complex offer the explanation for the activation of p53 signaling pathway.

The actions of p53 significantly affect the outcome of ER^+ breast cancer treatments. A clinical research in 1,794 breast cancer patients indicated that p53 mutations in exon 5 to exon 8 had higher risk of breast cancer-specific death as compared to patients with wild type p53 (Olivier et al., 2006). Consistent with this finding, patients with node-positive tumors containing mutant p53 had a significantly lower overall survival rate upon tamoxifen and loco-regional radiotherapy compared to patients with node-positive that express wild type p53 (Bergh et al., 1995). Similar findings were also published in different researches that breast tumors with ER^+ and p53 mutated genotype had a worse tamoxifen response that tumors with ER^+ and wild type p53 genotype, while ER negative and p53 mutant genotype tumors had even worse tamoxifen response than tumors with ER^+ and p53 mutated genotype (Berns et al., 2000; Elledge et al., 1997). In summary, the actions of wild type p53 is initially repressed by ER, while the actions of mutant p53 negatively contribute to the survival of patients with ER+ breast cancer. Therefore, the approaches that reactivate wild type p53 action in ER^+ breast cancer serves as a valuable strategy in ER-directed hormone therapy. Recently, the abrogation of mortalin-p53 interaction as a therapeutic strategy to reactive the wild type p53 actions has drawn public's attention for cancer treatments (Elwakeel, 2022; Yun et al., 2017). Numerous protein-protein interaction (PPI) abrogators have

been developed for different cancers including breast cancer (Nigam et al., 2015; Pham et al., 2019; Sane et al., 2014; Wang et al., 2014). However, none of these compounds have successfully entered clinical practice. One of the biggest challenges for the abrogation of mortain-p53 interaction is the appropriate protein-protein interface to target. The major acknowledged binding sites involved in the interaction are amino acid residues 312 to 352 within the oligomerization domain (or cytoplasmic sequestration domain) of p53 and amino acid residues 253 to 282 within the ATPase domain of mortalin (Kaul et al., 2001; Wadhwa et al., 2002). However, other independent researchers have demonstrated interactions involving amino acid residues 361 to 393 within the C-terminal domain of p53 and amino acid residues 434 to 679 within the substrate binding domain of mortalin (Gabizon et al., 2012; Iosefson and Azem, 2010). These discrepancies in the interaction sites make it difficult to decide on which interaction interface to target with small molecules. The current mortalin-p53 interaction abrogators are either directly targeting the ATPase domain of mortalin or the oligomerization domain of p53 (Elwakeel, 2022). Targeting the oligomerization domain is critical as this domain is essential for the tetramerization of p53 to form a transcriptionally activate tetramer. Engagement of the compounds with this domain may run the risk of inactivating p53 functions. Unlike the so far reported mortalin-p53 interaction abrogators, the work performed in this thesis shows that X15695 targets the mortalin-p53 interaction indirectly through the cochaperone BAG1. This is therefore a novel approach that may obviate the current difficulties to abolish the interaction of the two proteins.

4.4 Pharmacological profile of X15695 in comparison to clinical ER antagonist fulvestrant

A further action of X15695 identified in this work is the inhibition of growth and survival of tamoxifen-resistant MCF-7 cells. Tamoxifen is widely used in endocrine therapy in postmenopausal women with ER^+ breast cancer (Jordan, 1988). Although tamoxifen treatment reduces the mortality rate of ER^+ breast cancer patients, the long-term treatment of tamoxifen results in acquired resistance and leads to recurring of tumorigenesis (Goetz et al., 2005). Approximately 40% of breast cancer patients develop to tamoxifen resistance with poor prognosis (Early Breast Cancer Trialists' Collaborative, 2005). Fulvestrant, with a binding affinity over 100-fold more than the binding of tamoxifen to ER and with the ability to induce ER turnover is considered a pure ER antagonist and a better choice to overcome tamoxifen and/or AIs induced resistance (Boér, 2017; Dowsett et al., 2005). Indeed, clinical trials have demonstrated that

fulvestrant alone or in combination with other anticancer drugs significantly improves the progression-free survival (PFS) of postmenopausal patients with primary and advanced breast cancer acquired endocrine therapy resistance (Baselga et al., 2012; Perey et al., 2007). The current anticancer drugs used in combination with fluvestrant, CD4/CD6 inhibitors (e.g. palbociclib and ribociclib) and inhibitors targeting PI3K/AKT/mTOR pathway (e.g. pictilisib and buparlisib) have shown positive improvement for PFS in breast cancer patients. However, additional anticancer agents inevitably increase the drug toxicity and burden the drug tolerance of patients, which eventually limits the drug dosages to an extent and compromises their effectiveness. So far, CD4/CD6 inhibitors are the only approved anticancer agents by FDA that are applied in combination with fulvestrant for pre-/peri- and postmenopausal women with breast cancer progressing after endocrine therapy (Boér, 2017). At the molecular level, studies in this thesis show that X15695 compares quite well to fulvestrant. It promotes ER degradation; it inhibits growth and viability of tamoxifen resistant MCF-7 cells, suggesting that it has the potential to overcome tamoxifen resistance in patients when further developed. Of note, the action of X15695 that activates p53 signaling pathway and triggers cell cycle arrest and apoptosis identified in this work could possibly mimic the function of CD4/CD6 inhibitors and inhibitors targeting PI3K/AKT/mTOR pathway, respectively. Collectively, this work sheds light on basic knowledge of the actions of X15695 on ER^+ breast cancer cell growth and offers cellular evidence that the compound has the potential to overcome endocrine therapy resistance. For better development of X15695 as clinical anticancer agents, extensive efforts are still required.

Chapter 5: Appendix

5.1 Distribution and normalization of RNA-sequencing data in MCF-7 cells

Before get insight into the RNA -Sequencing data, the raw data (Transcript per Million Read, TPM) was assessed and presented as Median ±SD (standard deviation) (Figure 5.1A), the majority of the data distributed within Median as 5000 TPM with SD less than 1000 TPM. To remove the outliers, an edgeR package was used to present the data from TPM to CPM (Counts per Million Read) (Figure 5.1B), to filter data from outliers (Figure 5.1C) and to normalize the filtered data (Figure 5.1D).

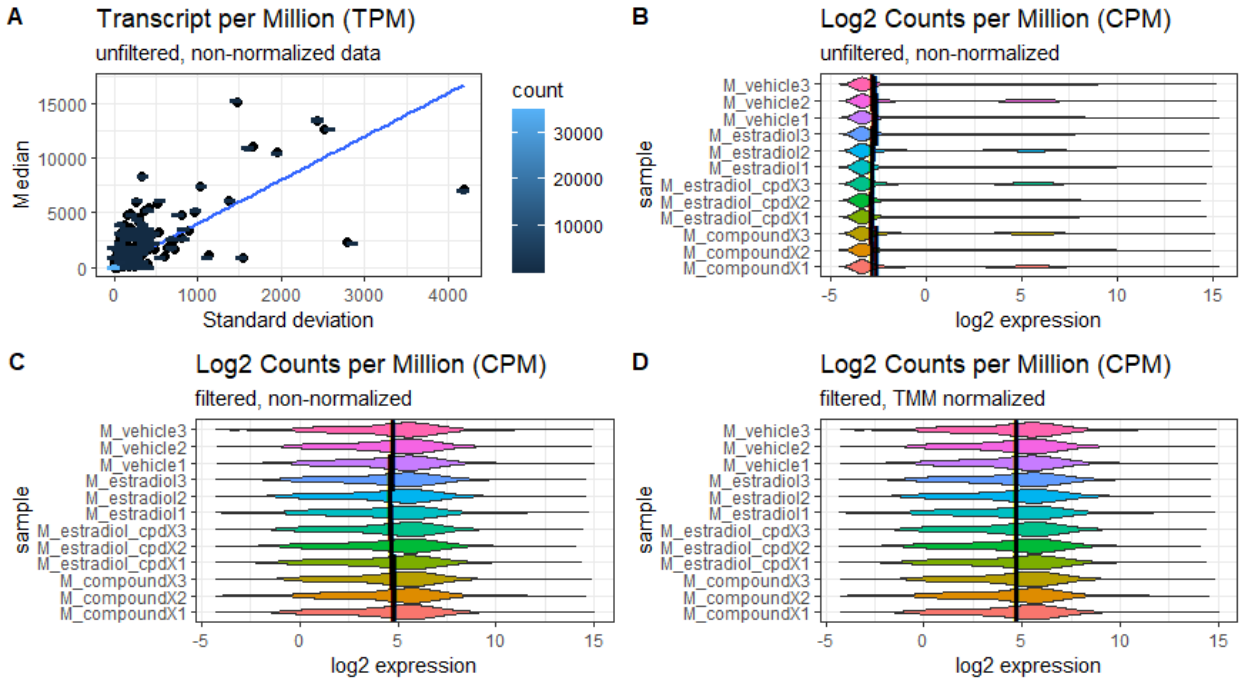

Figure 5.1: RNA-sequencing data Wrangling of MCF-7 cells.
(A). a matrixStats package was used to calculate the counts, median and standard deviation of each transcript, data was then presented with (Median±SD) by ggplot package. An edgeR package was used to present the data with CPM (Counts per Million Read) without filtering and normalization (B) with filtering but without normalization (C) and with filtering and normalization (D).

5.2 Principal Component Analysis (PCA) of RNA-sequencing data in MCF-7 cells

Principal component analysis (PCA) is a mathematical algorithm that make it possible to visually assess similarities and difference between samples and determine whether samples can be categorized (Ringnér, 2008). In these RNA-sequencing samples, four conditions ("Vehicle", "E2", "X15695", "E2+X15695") and three biological replicates for each condition were used. To evaluate similarities and difference among the samples, samples were first clustered with hclust functions in R (Figure 5.2A), the clustering tree showed all 12 samples can be categorized into four subgroups, and each subgroup contains the samples treated with the same condition, indicating samples behaviors generally similar within each condition.

To further assess the similarities and differences between samples, the ratio of variances in each principal component (PC) were calculated (Figure 5.2B). Plotting of PC1 and PC2 clearly showed all samples can be categorized to 4 groups, though PC1 and PC2 only covers 60% of total variances (Figure 5.2C). Besides, a detailed plotting including PC1 to PC6 which covers more than 80% of total variances still showed all samples can be grouped into 4 conditions under each principal component, though there is a small difference between samples at the same condition (Figure 5.2D). Taken together, all samples are highly consistent within the same treated condition, indicating data are valid for Differentially Expressed Gene (DGE) analysis in the next step.

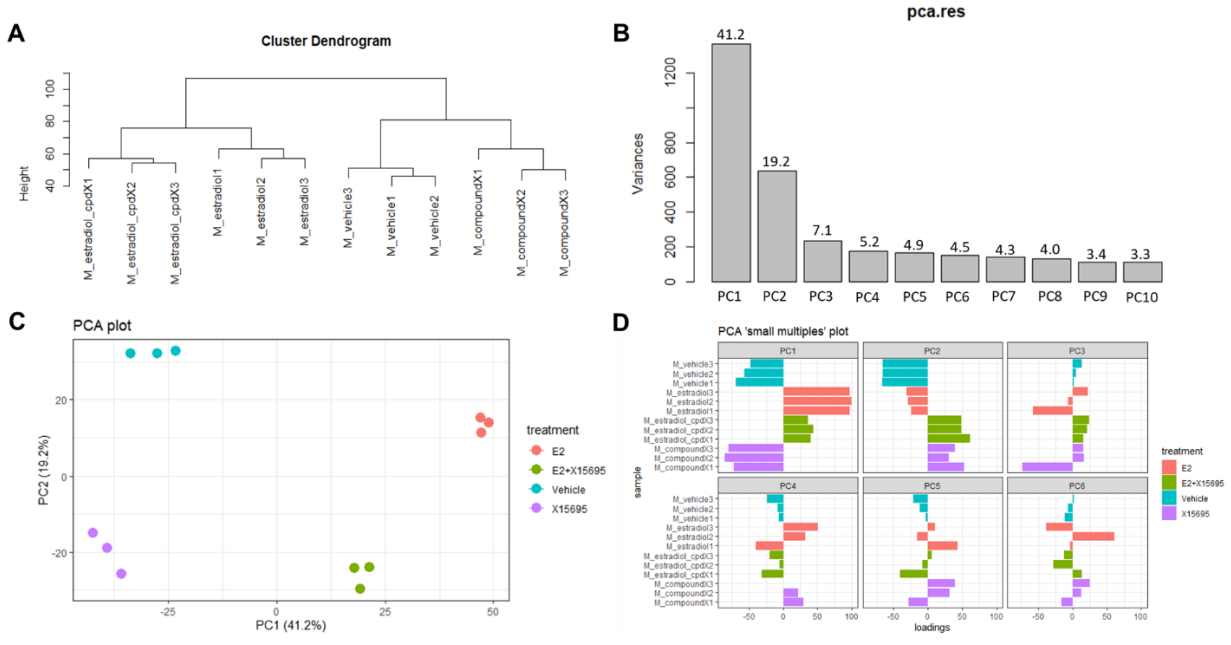

Figure 5. 2: Sample clustering and PCA analysis in MCF-7 cells.

(A). the clustering tree of 12 samples. (B). screen plot for the ratio of variances in each principal component. (C). ggplot for principal component 1 and principal component 2. (D). multiple plots for principal component 1 to 6.

5.3 Distribution and normalization of RNA-sequencing data in T47D cells

To analyze the RNA-sequencing data of T47D cells, the same algorithm used for MCF-7 cells RNA-sequencing data processing were applied to T47D cells RNA-sequencing date. the raw data (Transcript per Million Read, TPM) was assessed and presented as Median ±SD (standard deviation) (Figure 5.3A), the majority of the data distributed within Median as 10000 TPM with SD less than 1000 TPM. To remove the outliers, an edgeR package was used to present the data from TPM to CPM (Counts per Million Read) (Figure 5.1B), to filter data from outliers (Figure 5.1C) and to normalize the filtered data (Figure 5.1D).

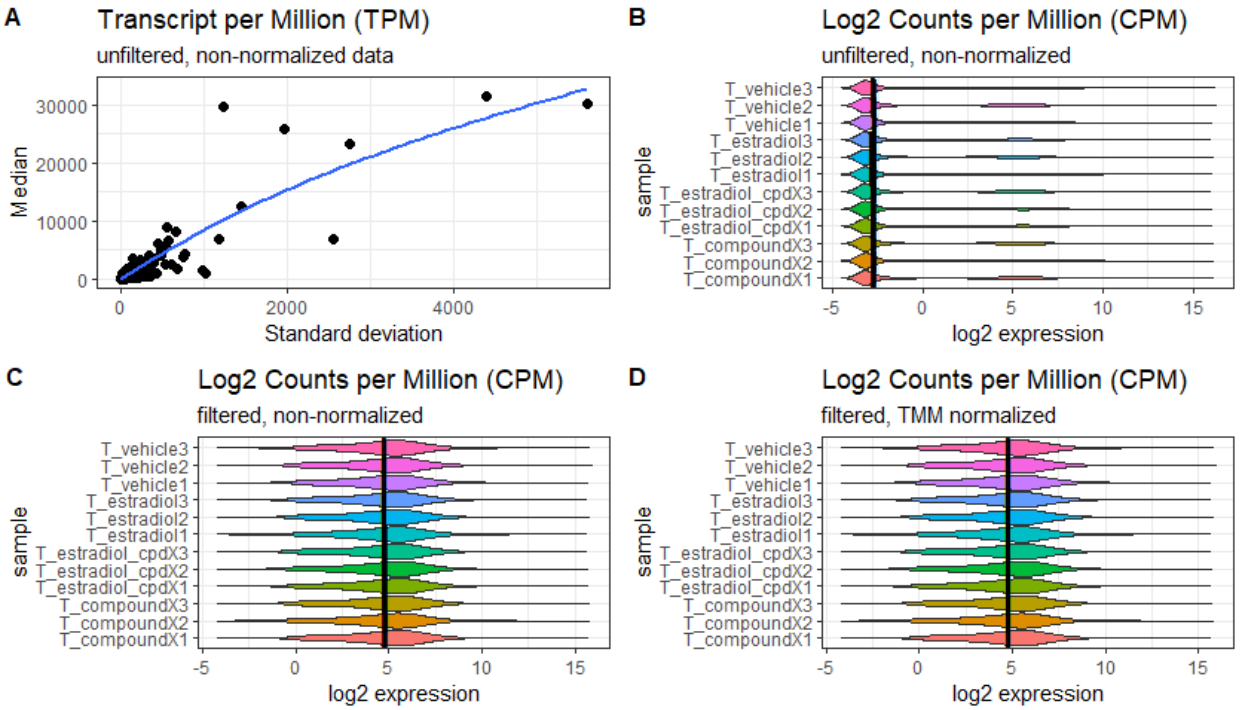

Figure 5. 3: RNA-sequencing data Wrangling of T47D cells.
(A). a matrixStats package was used to calculate the counts, median and standard deviation of each transcript, data was then presented with (Median±SD) by ggplot package. An edgeR package was used to present the data with CPM (Counts per Million Read) without filtering and

normalization (B), with filtering but without normalization (C) and with filtering and normalization (D).

5.4 Principal Component Analysis (PCA) of RNA-sequencing data of MCF-7 cells in combinations with T47D cells

Since MCF-7 cells expressed ER and wild type p53, while T47D cells expressed ER and mutant p53, in order to analyze the difference and similarity between these two cell lines. The samples of MCF-7 cells and T47D cells were combined and distinguished by p53 genotype. The sample clustering clearly showed two major subgroups which refer to samples of T47D cells and samples of MCF-7 cells, respectively. In line with sample clustering with each cell line separately, In T47D cells, condition"X1569+E2" is closer to condition "X15695"; while in MCF-7 cells, condition"X1569+E2" is much closer to condition" E2" (Figure 5.4A). The following PCA indicated samples can be clearly distinguished by p53 genotype. Samples expressed wild type p53 were more sensitive and easier to be distinguished to the given conditions, while samples expressed mutant p53 did not response to the given conditions and cannot be easily distinguished (Figure 5.4B).

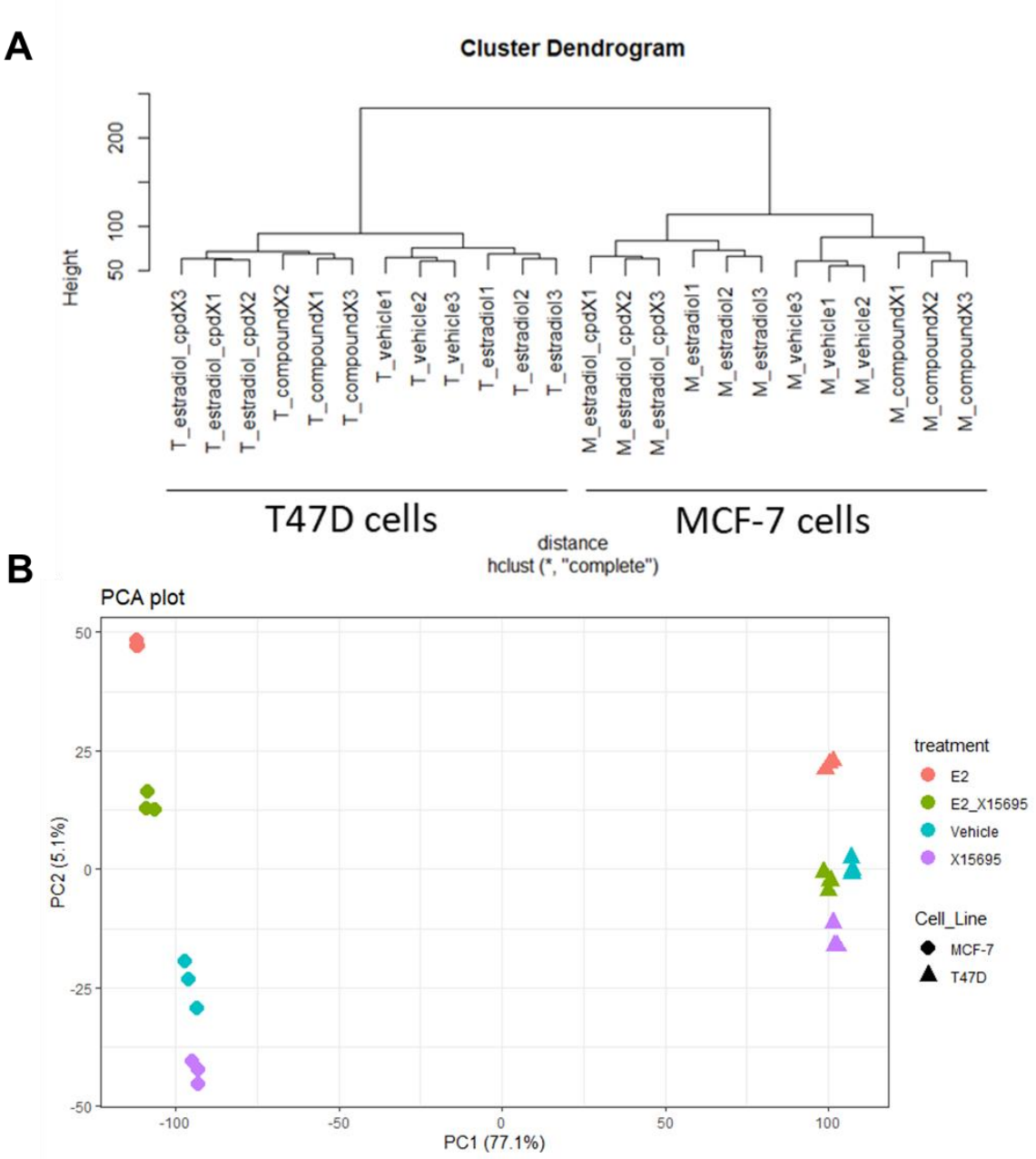

Figure 5. 4: **Sample clustering and PCA analysis of MCF-7 cells in combination with T47D cells.** (A). the clustering tree of 12 samples; (B). ggplot for Principal component 1 and Principal component 2.

References

Aggelis, V., and Johnston, S. R. D. (2019). Advances in Endocrine-Based Therapies for Estrogen Receptor-Positive Metastatic Breast Cancer. Drugs *79*, 1849-1866.

AlFakeeh, A., and Brezden-Masley, C. (2018). Overcoming endocrine resistance in hormone receptor-positive breast cancer. Curr Oncol *25*, S18-s27.

Allen, E., and Doisy, E. A. (1983). Landmark article Sept 8, 1923. An ovarian hormone. Preliminary report on its localization, extraction and partial purification, and action in test animals. By Edgar Allen and Edward A. Doisy. Jama *250*, 2681-2683.

Allen, K. E., Clark, E. R., and Jordan, V. C. (1980). Evidence for the metabolic activation of non-steroidal antioestrogens: a study of structure-activity relationships. Br J Pharmacol *71*, 83-91.

André, F., Ciruelos, E., Rubovszky, G., Campone, M., Loibl, S., Rugo, H. S., Iwata, H., Conte, P., Mayer, I. A., Kaufman, B.*, et al.* (2019). Alpelisib for PIK3CA-Mutated, Hormone Receptor-Positive Advanced Breast Cancer. N Engl J Med *380*, 1929-1940.

Arao, Y., and Korach, K. S. (2018). The F domain of estrogen receptor α is involved in species-specific, tamoxifen-mediated transactivation. J Biol Chem *293*, 8495-8507.

Arpino, G., De Angelis, C., Giuliano, M., Giordano, A., Falato, C., De Laurentiis, M., and De Placido, S. (2009). Molecular mechanism and clinical implications of endocrine therapy resistance in breast cancer. Oncology *77 Suppl 1*, 23-37.

Barraclough, D. L., Platt-Higgins, A., de Silva Rudland, S., Barraclough, R., Winstanley, J., West, C. R., and Rudland, P. S. (2009). The metastasis-associated anterior gradient 2 protein is correlated with poor survival of breast cancer patients. Am J Pathol *175*, 1848-1857.

Baselga, J., Campone, M., Piccart, M., Burris, H. A., 3rd, Rugo, H. S., Sahmoud, T., Noguchi, S., Gnant, M., Pritchard, K. I., Lebrun, F.*, et al.* (2012). Everolimus in postmenopausal hormone-receptor-positive advanced breast cancer. N Engl J Med *366*, 520-529.

Beham, A., Marin, M. C., Fernandez, A., Herrmann, J., Brisbay, S., Tari, A. M., Lopez-Berestein, G., Lozano, G., Sarkiss, M., and McDonnell, T. J. (1997). Bcl-2 inhibits p53 nuclear import following DNA damage. Oncogene *15*, 2767-2772.

Bennesch, M. A., and Picard, D. (2015). Minireview: Tipping the balance: ligand-independent activation of steroid receptors. Mol Endocrinol *29*, 349-363.

Bergh, J., Norberg, T., Sjögren, S., Lindgren, A., and Holmberg, L. (1995). Complete sequencing of the p53 gene provides prognostic information in breast cancer patients, particularly in relation to adjuvant systemic therapy and radiotherapy. Nat Med *1*, 1029-1034.

Berns, E. M., Foekens, J. A., Vossen, R., Look, M. P., Devilee, P., Henzen-Logmans, S. C., van Staveren, I. L., van Putten, W. L., Inganäs, M., Meijer-van Gelder, M. E.*, et al.* (2000). Complete sequencing of TP53 predicts poor response to systemic therapy of advanced breast cancer. Cancer Res *60*, 2155-2162.

Berry, N. B., Fan, M., and Nephew, K. P. (2008). Estrogen receptor-alpha hinge-region lysines 302 and 303 regulate receptor degradation by the proteasome. Mol Endocrinol *22*, 1535-1551.

Bertheau, P., Lehmann-Che, J., Varna, M., Dumay, A., Poirot, B., Porcher, R., Turpin, E., Plassa, L. F., de Roquancourt, A., Bourstyn, E.*, et al.* (2013). p53 in breast cancer subtypes and new insights into response to chemotherapy. Breast *22 Suppl 2*, S27-29.

Björnström, L., and Sjöberg, M. (2005). Mechanisms of estrogen receptor signaling: convergence of genomic and nongenomic actions on target genes. Mol Endocrinol *19*, 833-842.

Black, A. R., Black, J. D., and Azizkhan-Clifford, J. (2001). Sp1 and krüppel-like factor family of transcription factors in cell growth regulation and cancer. J Cell Physiol *188*, 143-160.

Boér, K. (2017). Fulvestrant in advanced breast cancer: evidence to date and place in therapy. Ther Adv Med Oncol *9*, 465-479.

Borlado, L. R., and Méndez, J. (2008). CDC6: from DNA replication to cell cycle checkpoints and oncogenesis. Carcinogenesis *29*, 237-243.

Brauch, H., Mürdter, T. E., Eichelbaum, M., and Schwab, M. (2009). Pharmacogenomics of tamoxifen therapy. Clin Chem *55*, 1770-1782.

Bray, F., Ferlay, J., Soerjomataram, I., Siegel, R. L., Torre, L. A., and Jemal, A. (2018). Global cancer statistics 2018: GLOBOCAN estimates of incidence and mortality worldwide for 36 cancers in 185 countries. CA Cancer J Clin *68*, 394-424.

Briand, P., and Lykkesfeldt, A. E. (1984). Effect of estrogen and antiestrogen on the human breast cancer cell line MCF-7 adapted to growth at low serum concentration. Cancer Res *44*, 1114-1119.

Brimmell, M., Burns, J. S., Munson, P., McDonald, L., O'Hare, M. J., Lakhani, S. R., and Packham, G. (1999). High level expression of differentially localized BAG-1 isoforms in some oestrogen receptor-positive human breast cancers. Br J Cancer *81*, 1042-1051.

Butt, A. J., McNeil, C. M., Musgrove, E. A., and Sutherland, R. L. (2005). Downstream targets of growth factor and oestrogen signalling and endocrine resistance: the potential roles of c-Myc, cyclin D1 and cyclin E. Endocr Relat Cancer *12 Suppl 1*, S47-59.

Cailleau, R., Olivé, M., and Cruciger, Q. V. (1978). Long-term human breast carcinoma cell lines of metastatic origin: preliminary characterization. In Vitro *14*, 911-915.

Carroll, J. S., Liu, X. S., Brodsky, A. S., Li, W., Meyer, C. A., Szary, A. J., Eeckhoute, J., Shao, W., Hestermann, E. V., Geistlinger, T. R.*, et al.* (2005). Chromosome-wide mapping of estrogen receptor binding reveals long-range regulation requiring the forkhead protein FoxA1. Cell *122*, 33-43.

Cato, A. C., and Mink, S. (2001). BAG-1 family of cochaperones in the modulation of nuclear receptor action. J Steroid Biochem Mol Biol *78*, 379-388.

Cato, L., Neeb, A., Sharp, A., Buzón, V., Ficarro, S. B., Yang, L., Muhle-Goll, C., Kuznik, N. C., Riisnaes, R., Nava Rodrigues, D.*, et al.* (2017). Development of Bag-1L as a therapeutic target in androgen receptor-dependent prostate cancer. Elife *6*.doi:10.7554/eLife.27159.

Chang, H. Y., Levasseur, M., and Jones, K. T. (2004). Degradation of APCcdc20 and APCcdh1 substrates during the second meiotic division in mouse eggs. J Cell Sci *117*, 6289-6296.

Cheang, M. C., Voduc, D., Bajdik, C., Leung, S., McKinney, S., Chia, S. K., Perou, C. M., and Nielsen, T. O. (2008). Basal-like breast cancer defined by five biomarkers has superior prognostic value than triple-negative phenotype. Clin Cancer Res *14*, 1368-1376.

Chen, G., Liu, Z., Zhang, Y., Shan, X., Jiang, L., Zhao, Y., He, W., Feng, Z., Yang, S., and Liang, G. (2013). Synthesis and Anti-inflammatory Evaluation of Novel Benzimidazole and Imidazopyridine Derivatives. ACS Med Chem Lett *4*, 69-74.

Chen, J. (2016). The Cell-Cycle Arrest and Apoptotic Functions of p53 in Tumor Initiation and Progression. Cold Spring Harb Perspect Med *6*, a026104.doi:10.1101/cshperspect.a026104.

Chernov, M. V., Ramana, C. V., Adler, V. V., and Stark, G. R. (1998). Stabilization and activation of p53 are regulated independently by different phosphorylation events. Proc Natl Acad Sci U S A *95*, 2284-2289.

Coates, A. S., Millar, E. K., O'Toole, S. A., Molloy, T. J., Viale, G., Goldhirsch, A., Regan, M. M., Gelber, R. D., Sun, Z., Castiglione-Gertsch, M.*, et al.* (2012). Prognostic interaction between expression of p53 and estrogen receptor in patients with node-negative breast cancer: results from IBCSG Trials VIII and IX. Breast Cancer Res *14*, R143. doi:10.1186/bcr3348.

Cocce, K. J., Jasper, J. S., Desautels, T. K., Everett, L., Wardell, S., Westerling, T., Baldi, R., Wright, T. M., Tavares, K., Yllanes, A.*, et al.* (2019). The Lineage Determining Factor GRHL2 Collaborates with FOXA1 to Establish a Targetable Pathway in Endocrine Therapy-Resistant Breast Cancer. Cell Rep *29*, 889-903.e810. doi:10.1016/j.celrep.2019.09.032.

Condorelli, R., and Vaz-Luis, I. (2018). Managing side effects in adjuvant endocrine therapy for breast cancer. Expert Rev Anticancer Ther *18*, 1101-1112.

Cutress, R. I., Townsend, P. A., Sharp, A., Maison, A., Wood, L., Lee, R., Brimmell, M., Mullee, M. A., Johnson, P. W., Royle, G. T.*, et al.* (2003). The nuclear BAG-1 isoform, BAG-1L, enhances oestrogen-dependent transcription. Oncogene *22*, 4973-4982.

D'Souza, A., Spicer, D., and Lu, J. (2018). Overcoming endocrine resistance in metastatic hormone receptor-positive breast cancer. J Hematol Oncol *11*, 80.doi:10.3747/c0.25.3575.

Dahiya, V., Agam, G., Lawatscheck, J., Rutz, D. A., Lamb, D. C., and Buchner, J. (2019). Coordinated Conformational Processing of the Tumor Suppressor Protein p53 by the Hsp70 and Hsp90 Chaperone Machineries. Mol Cell *74*, 816-830.e817.doi:10.1016/j.molcel.2019.03.026.

Damghani, T., Moosavi, F., Khoshneviszadeh, M., Mortazavi, M., Pirhadi, S., Kayani, Z., Saso, L., Edraki, N., and Firuzi, O. (2021). Imidazopyridine hydrazone derivatives exert antiproliferative effect on lung and pancreatic cancer cells and potentially inhibit receptor tyrosine kinases including c-Met. Sci Rep *11*, 3644.doi:10.1038/s41598-021-83069-4.

Darbre, P. D., and Daly, R. J. (1990). Transition of human breast cancer cells from an oestrogen responsive to unresponsive state. J Steroid Biochem Mol Biol *37*, 753-763.

Di Leo, A., Jerusalem, G., Petruzelka, L., Torres, R., Bondarenko, I. N., Khasanov, R., Verhoeven, D., Pedrini, J. L., Smirnova, I., Lichinitser, M. R.*, et al.* (2010). Results of the CONFIRM phase III trial comparing fulvestrant 250 mg with fulvestrant 500 mg in postmenopausal women with estrogen receptor-positive advanced breast cancer. J Clin Oncol *28*, 4594-4600.

Dnistrian, A. M., Schwartz, M. K., Greenberg, E. J., Smith, C. A., and Schwartz, D. C. (1991). Evaluation of CA M26, CA M29, CA 15-3 and CEA as circulating tumor markers in breast cancer patients. Tumour Biol *12*, 82-90.

Donepudi, M. S., Kondapalli, K., Amos, S. J., and Venkanteshan, P. (2014). Breast cancer statistics and markers. J Cancer Res Ther *10*, 506-511.

Doong, H., Vrailas, A., and Kohn, E. C. (2002). What's in the 'BAG'?--A functional domain analysis of the BAG-family proteins. Cancer Lett *188*, 25-32.

Dorssers, L. C., Van der Flier, S., Brinkman, A., van Agthoven, T., Veldscholte, J., Berns, E. M., Klijn, J. G., Beex, L. V., and Foekens, J. A. (2001). Tamoxifen resistance in breast cancer: elucidating mechanisms. Drugs *61*, 1721-1733.

Dowsett, M., Nicholson, R. I., and Pietras, R. J. (2005). Biological characteristics of the pure antiestrogen fulvestrant: overcoming endocrine resistance. Breast Cancer Res Treat *93 Suppl 1*, S11-18.doi:10.107/s10549-005-9037-3.

Drăgănescu, M., and Carmocan, C. (2017). Hormone Therapy in Breast Cancer. Chirurgia (Bucur) *112*, 413-417.

Early Breast Cancer Trialists' Collaborative, G. (2005). Effects of chemotherapy and hormonal therapy for early breast cancer on recurrence and 15-year survival: an overview of the randomised trials. Lancet *365*, 1687-1717.

Early Breast Cancer Trialists' Collaborative, G. (2015). Aromatase inhibitors versus tamoxifen in early breast cancer: patient-level meta-analysis of the randomised trials. Lancet *386*, 1341-1352.

El-Awady, R. A., Semreen, M. H., Saber-Ayad, M. M., Cyprian, F., Menon, V., and Al-Tel, T. H. (2016). Modulation of DNA damage response and induction of apoptosis mediates synergism between doxorubicin and a new imidazopyridine derivative in breast and lung cancer cells. DNA Repair (Amst) *37*, 1-11.

el-Deiry, W. S., Tokino, T., Velculescu, V. E., Levy, D. B., Parsons, R., Trent, J. M., Lin, D., Mercer, W. E., Kinzler, K. W., and Vogelstein, B. (1993). WAF1, a potential mediator of p53 tumor suppression. Cell *75*, 817-825.

Elledge, R. M., and Allred, D. C. (1998). Prognostic and predictive value of p53 and p21 in breast cancer. Breast Cancer Res Treat *52*, 79-98.

Elledge, R. M., Green, S., Howes, L., Clark, G. M., Berardo, M., Allred, D. C., Pugh, R., Ciocca, D., Ravdin, P., O'Sullivan, J.*, et al.* (1997). bcl-2, p53, and response to tamoxifen in estrogen receptor-positive metastatic breast cancer: a Southwest Oncology Group study. J Clin Oncol *15*, 1916-1922.

Elwakeel, A. (2022). Abrogating the Interaction Between p53 and Mortalin (Grp75/HSPA9/mtHsp70) for Cancer Therapy: The Story so far. Front Cell Dev Biol *10*, 879632.

Endoori, S., Gulipalli, K. C., Bodige, S., Ravula, P., and Seelam, N. (2021). Design, synthesis, anticancer activity, and in silico studies of novel imidazo[1,2-a]pyridine based 1H-1,2,3-triazole derivatives. Journal of Heterocyclic Chemistry *58*, 1311-1320.

Ennis, H. L., and Lubin, M. (1964). CYCLOHEXIMIDE: ASPECTS OF INHIBITION OF PROTEIN SYNTHESIS IN MAMMALIAN CELLS. Science *146*, 1474-1476.

Enthammer, M., Papadakis, E. S., Salomé Gachet, M., Deutsch, M., Schwaiger, S., Koziel, K., Ashraf, M. I., Khalid, S., Wolber, G., Packham, G.*, et al.* (2013). Isolation of a novel thioflavin S-derived compound that inhibits BAG-1-mediated protein interactions and targets BRAF inhibitor-resistant cell lines. Mol Cancer Ther *12*, 2400-2414.

Esser, C., Alberti, S., and Höhfeld, J. (2004). Cooperation of molecular chaperones with the ubiquitin/proteasome system. Biochim Biophys Acta *1695*, 171-188.

Fackenthal, J. D., and Olopade, O. I. (2007). Breast cancer risk associated with BRCA1 and BRCA2 in diverse populations. Nat Rev Cancer *7*, 937-948.

Fan, M., Park, A., and Nephew, K. P. (2005). CHIP (carboxyl terminus of Hsc70-interacting protein) promotes basal and geldanamycin-induced degradation of estrogen receptor-alpha. Mol Endocrinol *19*, 2901-2914.

Fan, Y., Wang, X., and Li, Y. (2021). IFI30 expression predicts patient prognosis in breast cancer and dictates breast cancer cells proliferation via regulating autophagy. Int J Med Sci *18*, 3342-3352.

Fawell, S. E., White, R., Hoare, S., Sydenham, M., Page, M., and Parker, M. G. (1990). Inhibition of estrogen receptor-DNA binding by the "pure" antiestrogen ICI 164,384 appears to be mediated by impaired receptor dimerization. Proc Natl Acad Sci U S A *87*, 6883-6887.

Feng, L., Lin, T., Uranishi, H., Gu, W., and Xu, Y. (2005). Functional analysis of the roles of posttranslational modifications at the p53 C terminus in regulating p53 stability and activity. Mol Cell Biol *25*, 5389-5395.

Ferrandina, G., Scambia, G., Bardelli, F., Benedetti Panici, P., Mancuso, S., and Messori, A. (1997). Relationship between cathepsin-D content and disease-free survival in node-negative breast cancer patients: a meta-analysis. Br J Cancer *76*, 661-666.

Figueroa-Magalhães, M. C., Jelovac, D., Connolly, R., and Wolff, A. C. (2014). Treatment of HER2-positive breast cancer. Breast *23*, 128-136.

Fisher, B., Costantino, J. P., Redmond, C. K., Fisher, E. R., Wickerham, D. L., and Cronin, W. M. (1994). Endometrial cancer in tamoxifen-treated breast cancer patients: findings from the National Surgical Adjuvant Breast and Bowel Project (NSABP) B-14. J Natl Cancer Inst *86*, 527-537.

Fisher, B., Costantino, J. P., Wickerham, D. L., Cecchini, R. S., Cronin, W. M., Robidoux, A., Bevers, T. B., Kavanah, M. T., Atkins, J. N., Margolese, R. G.*, et al.* (2005). Tamoxifen for the prevention of breast cancer: current status of the National Surgical Adjuvant Breast and Bowel Project P-1 study. J Natl Cancer Inst *97*, 1652-1662.

Flanagan, J., Qian, Y., Gough, S., Andreoli, M., Bookbinder, M., Cadelina, G., Bradley, J., Rousseau, E., Willard, R., Pizzano, J.*, et al.* (2019). Abstract P5-04-18: ARV-471, an oral estrogen receptor PROTAC degrader for breast cancer. Cancer Research *79*, P5-04-18-P05-04-18.

Froesch, B. A., Takayama, S., and Reed, J. C. (1998). BAG-1L protein enhances androgen receptor function. J Biol Chem *273*, 11660-11666.

Fu, X., Jeselsohn, R., Pereira, R., Hollingsworth, E. F., Creighton, C. J., Li, F., Shea, M., Nardone, A., De Angelis, C., Heiser, L. M.*, et al.* (2016). FOXA1 overexpression mediates endocrine resistance by altering the ER transcriptome and IL-8 expression in ER-positive breast cancer. Proc Natl Acad Sci U S A *113*, E6600-e6609.

Fuentes, N., and Silveyra, P. (2019). Estrogen receptor signaling mechanisms. Adv Protein Chem Struct Biol *116*, 135-170.

Gabizon, R., Brandt, T., Sukenik, S., Lahav, N., Lebendiker, M., Shalev, D. E., Veprintsev, D., and Friedler, A. (2012). Specific recognition of p53 tetramers by peptides derived from p53 interacting proteins. PLoS One *7*, e38060.doi:10.1371/journal.pone.0038060.

Gennari, A., Sormani, M. P., Pronzato, P., Puntoni, M., Colozza, M., Pfeffer, U., and Bruzzi, P. (2008). HER2 status and efficacy of adjuvant anthracyclines in early breast cancer: a pooled analysis of randomized trials. J Natl Cancer Inst *100*, 14-20.

Giannakakou, P., Sackett, D. L., Ward, Y., Webster, K. R., Blagosklonny, M. V., and Fojo, T. (2000). p53 is associated with cellular microtubules and is transported to the nucleus by dynein. Nat Cell Biol *2*, 709-717.

Gillesby, B. E., and Zacharewski, T. R. (1999). pS2 (TFF1) levels in human breast cancer tumor samples: correlation with clinical and histological prognostic markers. Breast Cancer Res Treat *56*, 253-265.

Goetz, M. P., Rae, J. M., Suman, V. J., Safgren, S. L., Ames, M. M., Visscher, D. W., Reynolds, C., Couch, F. J., Lingle, W. L., Flockhart, D. A.*, et al.* (2005). Pharmacogenetics of tamoxifen biotransformation is associated with clinical outcomes of efficacy and hot flashes. J Clin Oncol *23*, 9312-9318.

Goldhirsch, A., Winer, E. P., Coates, A. S., Gelber, R. D., Piccart-Gebhart, M., Thürlimann, B., and Senn, H. J. (2013). Personalizing the treatment of women with early breast cancer: highlights of the St Gallen International Expert Consensus on the Primary Therapy of Early Breast Cancer 2013. Ann Oncol *24*, 2206-2223.

Gompel, A., Somaï, S., Chaouat, M., Kazem, A., Kloosterboer, H. J., Beusman, I., Forgez, P., Mimoun, M., and Rostène, W. (2000). Hormonal regulation of apoptosis in breast cells and tissues. Steroids *65*, 593-598.

Gottardis, M. M., Robinson, S. P., Satyaswaroop, P. G., and Jordan, V. C. (1988). Contrasting actions of tamoxifen on endometrial and breast tumor growth in the athymic mouse. Cancer Res *48*, 812-815.

Green, S., Kumar, V., Krust, A., Walter, P., and Chambon, P. (1986). Structural and functional domains of the estrogen receptor. Cold Spring Harb Symp Quant Biol *51 Pt 2*, 751-758.

Gu, W., and Roeder, R. G. (1997). Activation of p53 sequence-specific DNA binding by acetylation of the p53 C-terminal domain. Cell *90*, 595-606.

Gudmundsson, K. S., Boggs, S. D., Catalano, J. G., Svolto, A., Spaltenstein, A., Thomson, M., Wheelan, P., and Jenkinson, S. (2009). Imidazopyridine-5,6,7,8-tetrahydro-8-quinolinamine derivatives with potent activity against HIV-1. Bioorg Med Chem Lett *19*, 6399-6403.

Guiochon-Mantel, A., Milgrom, E., and Schaison, G. (1999). [Estrogen biosynthesis and receptors]. Ann Endocrinol (Paris) *60*, 381-391.

Guzey, M., Takayama, S., and Reed, J. C. (2000). BAG1L enhances trans-activation function of the vitamin D receptor. J Biol Chem *275*, 40749-40756.

Haider, K., Rehman, S., Pathak, A., Najmi, A. K., and Yar, M. S. (2021). Advances in 2-substituted benzothiazole scaffold-based chemotherapeutic agents. Arch Pharm (Weinheim) *354*, e2100246.doi:10.1002/ardp.202100246.

Haines, C. N., Klingensmith, H. D., Komara, M., and Burd, C. J. (2020). GREB1 regulates PI3K/Akt signaling to control hormone-sensitive breast cancer proliferation. Carcinogenesis *41*, 1660-1670.

Hanker, A. B., Sudhan, D. R., and Arteaga, C. L. (2020). Overcoming Endocrine Resistance in Breast Cancer. Cancer Cell *37*, 496-513.

Hao, Z., Zhang, H., and Cowell, J. (2012). Ubiquitin-conjugating enzyme UBE2C: molecular biology, role in tumorigenesis, and potential as a biomarker. Tumour Biol *33*, 723-730.

Höhfeld, J., and Jentsch, S. (1997). GrpE-like regulation of the hsc70 chaperone by the anti-apoptotic protein BAG-1. Embo j *16*, 6209-6216.

Horwitz, K. B., Mockus, M. B., and Lessey, B. A. (1982). Variant T47D human breast cancer cells with high progesterone-receptor levels despite estrogen and antiestrogen resistance. Cell *28*, 633-642.

Hou, Y. F., Yuan, S. T., Li, H. C., Wu, J., Lu, J. S., Liu, G., Lu, L. J., Shen, Z. Z., Ding, J., and Shao, Z. M. (2004). ERbeta exerts multiple stimulative effects on human breast carcinoma cells. Oncogene *23*, 5799-5806.

Hu, J., Hu, B., Wang, M., Xu, F., Miao, B., Yang, C. Y., Wang, M., Liu, Z., Hayes, D. F., Chinnaswamy, K.*, et al.* (2019). Discovery of ERD-308 as a Highly Potent Proteolysis Targeting Chimera (PROTAC) Degrader of Estrogen Receptor (ER). J Med Chem *62*, 1420-1442.

Hu, X. F., Veroni, M., De Luise, M., Wakeling, A., Sutherland, R., Watts, C. K., and Zalcberg, J. R. (1993). Circumvention of tamoxifen resistance by the pure anti-estrogen ICI 182,780. Int J Cancer *55*, 873-876.

Huovinen, M., Loikkanen, J., Myllynen, P., and Vähäkangas, K. H. (2011). Characterization of human breast cancer cell lines for the studies on p53 in chemical carcinogenesis. Toxicol In Vitro *25*, 1007-1017.

Iosefson, O., and Azem, A. (2010). Reconstitution of the mitochondrial Hsp70 (mortalin)-p53 interaction using purified proteins--identification of additional interacting regions. FEBS Lett *584*, 1080-1084.

Iqbal, M. A., Husain, A., Alam, O., Khan, S. A., Ahmad, A., Haider, M. R., and Alam, M. A. (2020). Design, synthesis, and biological evaluation of imidazopyridine-linked thiazolidinone as potential anticancer agents. Arch Pharm (Weinheim) *353*, e2000071.doi:10.1002/ardp.202000071.

Iwase, H., Zhang, Z., Omoto, Y., Sugiura, H., Yamashita, H., Toyama, T., Iwata, H., and Kobayashi, S. (2003). Clinical significance of the expression of estrogen receptors alpha and beta for endocrine therapy of breast cancer. Cancer Chemother Pharmacol *52 Suppl 1*, S34-38.

Jafari, R., Almqvist, H., Axelsson, H., Ignatushchenko, M., Lundbäck, T., Nordlund, P., and Martinez Molina, D. (2014). The cellular thermal shift assay for evaluating drug target interactions in cells. Nat Protoc *9*, 2100-2122.

Jänicke, F., Prechtl, A., Thomssen, C., Harbeck, N., Meisner, C., Untch, M., Sweep, C. G., Selbmann, H. K., Graeff, H., and Schmitt, M. (2001). Randomized adjuvant chemotherapy trial in high-risk, lymph node-negative breast cancer patients identified by urokinase-type plasminogen activator and plasminogen activator inhibitor type 1. J Natl Cancer Inst *93*, 913-920.

Jeselsohn, R., Buchwalter, G., De Angelis, C., Brown, M., and Schiff, R. (2015). ESR1 mutations—a mechanism for acquired endocrine resistance in breast cancer. Nat Rev Clin Oncol *12*, 573-583.

Jia, Y., Zhou, J., Luo, X., Chen, M., Chen, Y., Wang, J., Xiong, H., Ying, X., Hu, W., Zhao, W.*, et al.* (2018). KLF4 overcomes tamoxifen resistance by suppressing MAPK signaling pathway and predicts good prognosis in breast cancer. Cell Signal *42*, 165-175.

Jiang, Y., Yang, L., Yang, X., Yin, S., Zhuang, F., Liu, Z., Wang, Y., Liang, G., and Qian, J. (2020). The imidazopyridine derivative X22 prevents diabetic kidney dysfunction through inactivating NF-κB signaling. Biochem Biophys Res Commun *525*, 877-882.

Jin, K., Park, S., Teo, W. W., Korangath, P., Cho, S. S., Yoshida, T., Győrffy, B., Goswami, C. P., Nakshatri, H., Cruz, L. A.*, et al.* (2015). HOXB7 Is an ERα Cofactor in the Activation of HER2 and Multiple ER Target Genes Leading to Endocrine Resistance. Cancer Discov *5*, 944-959.

Johnson, M. D., Zuo, H., Lee, K. H., Trebley, J. P., Rae, J. M., Weatherman, R. V., Desta, Z., Flockhart, D. A., and Skaar, T. C. (2004). Pharmacological characterization of 4-hydroxy-N-desmethyl tamoxifen, a novel active metabolite of tamoxifen. Breast Cancer Res Treat *85*, 151-159.

Jordan, V. C. (1988). The development of tamoxifen for breast cancer therapy: a tribute to the late Arthur L. Walpole. Breast Cancer Res Treat *11*, 197-209.

Jordan, V. C., Collins, M. M., Rowsby, L., and Prestwich, G. (1977). A monohydroxylated metabolite of tamoxifen with potent antioestrogenic activity. J Endocrinol *75*, 305-316.

Kalaitzidis, D., and Gilmore, T. D. (2005). Transcription factor cross-talk: the estrogen receptor and NF-kappaB. Trends Endocrinol Metab *16*, 46-52.

Kastan, M. B., Zhan, Q., el-Deiry, W. S., Carrier, F., Jacks, T., Walsh, W. V., Plunkett, B. S., Vogelstein, B., and Fornace, A. J., Jr. (1992). A mammalian cell cycle checkpoint pathway utilizing p53 and GADD45 is defective in ataxia-telangiectasia. Cell *71*, 587-597.

Kaul, S. C., Reddel, R. R., Mitsui, Y., and Wadhwa, R. (2001). An N-terminal region of mot-2 binds to p53 in vitro. Neoplasia *3*, 110-114.

Kaula, S. C., Reddelb, R. R., Sugiharac, T., Mitsuia, Y., and Wadhwac, R. (2000). Inactivation of p53 and life span extension of human diploid fibroblasts by mot-2. FEBS Lett *474*, 159-164.

Kereh, D. S., Pieter, J., Hamdani, W., Haryasena, H., Sampepajung, D., and Prihantono, P. (2021). Correlation of AGR2 expression with the incidence of metastasis in luminal breast cancer. Breast Dis *40*, S103-s107.

Kharb, R., Haider, K., Neha, K., and Yar, M. S. (2020). Aromatase inhibitors: Role in postmenopausal breast cancer. Arch Pharm (Weinheim) *353*, e2000081. doi:10.1002/ardp.20200081.

Khatun, S., Singh, A., Bader, G. N., and Sofi, F. A. (2021). Imidazopyridine, a promising scaffold with potential medicinal applications and structural activity relationship (SAR): recent advances. J Biomol Struct Dyn, 1-24.

Kikuchi, R., Noguchi, T., Takeno, S., Funada, Y., Moriyama, H., and Uchida, Y. (2002). Nuclear BAG-1 expression reflects malignant potential in colorectal carcinomas. Br J Cancer *87*, 1136-1139.

Kilbas, P. O., Akcay, I. M., Doganay, G. D., and Arisan, E. D. (2019). Bag-1 silencing enhanced chemotherapeutic drug-induced apoptosis in MCF-7 breast cancer cells affecting PI3K/Akt/mTOR and MAPK signaling pathways. Mol Biol Rep *46*, 847-860.

Kim, H., Abd Elmageed, Z. Y., Davis, C., El-Bahrawy, A. H., Naura, A. S., Ekaidi, I., Abdel-Mageed, A. B., and Boulares, A. H. (2014). Correlation between PDZK1, Cdc37, Akt and breast cancer malignancy: the role of PDZK1 in cell growth through Akt stabilization by increasing and interacting with Cdc37. Mol Med *20*, 270-279.

King, F. W., Wawrzynow, A., Höhfeld, J., and Zylicz, M. (2001). Co-chaperones Bag-1, Hop and Hsp40 regulate Hsc70 and Hsp90 interactions with wild-type or mutant p53. Embo j *20*, 6297-6305.

Kizilboga, T., Baskale, E. A., Yildiz, J., Akcay, I. M., Zemheri, E., Can, N. D., Ozden, C., Demir, S., Ezberci, F., and Dinler-Doganay, G. (2019). Bag-1 stimulates Bad phosphorylation through activation of Akt and Raf kinases to mediate cell survival in breast cancer. BMC Cancer *19*, 1254.doi:10.1186/s12885-019-6477-4.

Klinge, C. M. (2001). Estrogen receptor interaction with estrogen response elements. Nucleic Acids Res *29*, 2905-2919.

Klinge, C. M., Jernigan, S. C., Mattingly, K. A., Risinger, K. E., and Zhang, J. (2004). Estrogen response element-dependent regulation of transcriptional activation of estrogen receptors alpha and beta by coactivators and corepressors. J Mol Endocrinol *33*, 387-410.

Knapp, R. T., Steiner, A., Schmidt, U., Hafner, K., Holsboer, F., and Rein, T. (2012). BAG-1 diversely affects steroid receptor activity. Biochem J *441*, 297-303.

Krajewska, M., Turner, B. C., Shabaik, A., Krajewski, S., and Reed, J. C. (2006). Expression of BAG-1 protein correlates with aggressive behavior of prostate cancers. Prostate *66*, 801-810.

Kullmann, M., Schneikert, J., Moll, J., Heck, S., Zeiner, M., Gehring, U., and Cato, A. C. (1998). RAP46 is a negative regulator of glucocorticoid receptor action and hormone-induced apoptosis. J Biol Chem *273*, 14620-14625.

Kumar, A., Takada, Y., Boriek, A. M., and Aggarwal, B. B. (2004). Nuclear factor-kappaB: its role in health and disease. J Mol Med (Berl) *82*, 434-448.

Kumar, V., Green, S., Stack, G., Berry, M., Jin, J. R., and Chambon, P. (1987). Functional domains of the human estrogen receptor. Cell *51*, 941-951.

Kuznik, N. C., Solozobova, V., Jung, N., Gräßle, S., Lei, Q., Lewandowski, E. M., Munuganti, R., Zoubeidi, A., Chen, Y., Bräse, S., and Cato, A. C. B. (2021). Development of a Benzothiazole Scaffold-Based Androgen Receptor N-Terminal Inhibitor for Treating Androgen-Responsive Prostate Cancer. ACS Chem Biol *16*, 2103-2108.

Kuznik, N. C., Solozobova, V., Lee, II, Jung, N., Yang, L., Nienhaus, K., Ntim, E. A., Rottenberg, J. T., Muhle-Goll, C., Kumar, A. R.*, et al.* (2022). A chemical probe for BAG1 targets androgen receptor-positive prostate cancer through oxidative stress signaling pathway. iScience *25*, 104175. doi:10.1016/j.isci.2022.104175.

Laemmli, U. K. (1970). Cleavage of structural proteins during the assembly of the head of bacteriophage T4. Nature *227*, 680-685.

Lannigan, D. A. (2003). Estrogen receptor phosphorylation. Steroids *68*, 1-9.

Le Dily, F., and Beato, M. (2018). Signaling by Steroid Hormones in the 3D Nuclear Space. Int J Mol Sci *19*.doi:10.3390/ijms19020306.

Leznicki, P., Roebuck, Q. P., Wunderley, L., Clancy, A., Krysztofinska, E. M., Isaacson, R. L., Warwicker, J., Schwappach, B., and High, S. (2013). The association of BAG6 with SGTA and tail-anchored proteins. PLoS One *8*, e59590.doi:10.1371/journal.pone.0059590.

Liang, S. H., and Clarke, M. F. (1999). A bipartite nuclear localization signal is required for p53 nuclear import regulated by a carboxyl-terminal domain. J Biol Chem *274*, 32699-32703.

Liang, S. H., and Clarke, M. F. (2001). Regulation of p53 localization. Eur J Biochem *268*, 2779-2783.

Lippman, M. E., and Bolan, G. (1975). Oestrogen-responsive human breast cancer in long term tissue culture. Nature *256*, 592-593.

Liu, H., Lu, S., Gu, L., Gao, Y., Wang, T., Zhao, J., Rao, J., Chen, J., Hao, X., and Tang, S. C. (2014). Modulation of BAG-1 expression alters the sensitivity of breast cancer cells to tamoxifen. Cell Physiol Biochem *33*, 365-374.

Liu, R., Takayama, S., Zheng, Y., Froesch, B., Chen, G. Q., Zhang, X., Reed, J. C., and Zhang, X. K. (1998). Interaction of BAG-1 with retinoic acid receptor and its inhibition of retinoic acid-induced apoptosis in cancer cells. J Biol Chem *273*, 16985-16992.

Liu, S., Ren, B., Gao, H., Liao, S., Zhai, Y. X., Li, S., Su, X. J., Jin, P., Stroncek, D., Xu, Z.*, et al.* (2017). Over-expression of BAG-1 in head and neck squamous cell carcinomas (HNSCC) is associated with cisplatin-resistance. J Transl Med *15*, 189.doi:10.1186/s12967-017-1289-2.

Liu, W., Ip, M. M., Podgorsak, M. B., and Das, G. M. (2009). Disruption of estrogen receptor alpha-p53 interaction in breast tumors: a novel mechanism underlying the anti-tumor effect of radiation therapy. Breast Cancer Res Treat *115*, 43-50.

Liu, W., Konduri, S. D., Bansal, S., Nayak, B. K., Rajasekaran, S. A., Karuppayil, S. M., Rajasekaran, A. K., and Das, G. M. (2006). Estrogen receptor-alpha binds p53 tumor suppressor protein directly and represses its function. J Biol Chem *281*, 9837-9840.

Lonard, D. M., Nawaz, Z., Smith, C. L., and O'Malley, B. W. (2000). The 26S proteasome is required for estrogen receptor-alpha and coactivator turnover and for efficient estrogen receptor-alpha transactivation. Mol Cell *5*, 939-948.

Lu, R., Hu, X., Zhou, J., Sun, J., Zhu, A. Z., Xu, X., Zheng, H., Gao, X., Wang, X., Jin, H.*, et al.* (2016). COPS5 amplification and overexpression confers tamoxifen-resistance in ERα-positive breast cancer by degradation of NCoR. Nat Commun *7*, 12044.doi:10.1038/ncomms12044.

Ludmir, E. B., McCaw, Z. R., Kim, D. H., Tian, L., and Wei, L. J. (2020). Fulvestrant plus capivasertib for metastatic breast cancer. Lancet Oncol *21*, e233. doi:10.1016/s1470-2045(20)30228-X.

Lv, J., Zhang, F., Zhai, C., Wang, G., and Qu, Y. (2019). Bag-1 Silence Sensitizes Non-Small Cell Lung Cancer Cells To Cisplatin Through Multiple Gene Pathways. Onco Targets Ther *12*, 8977-8989.

Maddalo, D. (2009). Growth inhibitory action of distinct sequences derived from the co-chaperone Bag-1L. PhD Thesis. KIT,Karlsruhe,Germany. doi:10.5445/IR/1000016567.

Maggi, A. (2011). Liganded and unliganded activation of estrogen receptor and hormone replacement therapies. Biochim Biophys Acta *1812*, 1054-1060.

Magnani, L., Frige, G., Gadaleta, R. M., Corleone, G., Fabris, S., Kempe, M. H., Verschure, P. J., Barozzi, I., Vircillo, V., Hong, S. P.*, et al.* (2017). Acquired CYP19A1 amplification is an early specific mechanism of aromatase inhibitor resistance in ERα metastatic breast cancer. Nat Genet *49*, 444-450.

Mariotto, E., Viola, G., Zanon, C., and Aveic, S. (2020). A BAG's life: Every connection matters in cancer. Pharmacol Ther *209*, 107498. doi:10.1016/j.pharmthera.2020.107498.

Marsaud, V., Gougelet, A., Maillard, S., and Renoir, J. M. (2003). Various phosphorylation pathways, depending on agonist and antagonist binding to endogenous estrogen receptor alpha (ERalpha), differentially affect ERalpha extractability, proteasome-mediated stability, and transcriptional activity in human breast cancer cells. Mol Endocrinol *17*, 2013-2027.

Martinez Molina, D., Jafari, R., Ignatushchenko, M., Seki, T., Larsson, E. A., Dan, C., Sreekumar, L., Cao, Y., and Nordlund, P. (2013). Monitoring drug target engagement in cells and tissues using the cellular thermal shift assay. Science *341*, 84-87.

McDonnell, D. P., and Wardell, S. E. (2010). The molecular mechanisms underlying the pharmacological actions of ER modulators: implications for new drug discovery in breast cancer. Curr Opin Pharmacol *10*, 620-628.

McFall, T., McKnight, B., Rosati, R., Kim, S., Huang, Y., Viola-Villegas, N., and Ratnam, M. (2018). Progesterone receptor A promotes invasiveness and metastasis of luminal breast cancer by suppressing regulation of critical microRNAs by estrogen. J Biol Chem *293*, 1163-1177.

Meiller, A., Alvarez, S., Drané, P., Lallemand, C., Blanchard, B., Tovey, M., and May, E. (2007). p53-dependent stimulation of redox-related genes in the lymphoid organs of gamma-irradiated--mice identification of Haeme-oxygenase 1 as a direct p53 target gene. Nucleic Acids Res *35*, 6924-6934.

Mock, J. Y., Chartron, J. W., Zaslaver, M., Xu, Y., Ye, Y., and Clemons, W. M., Jr. (2015). Bag6 complex contains a minimal tail-anchor-targeting module and a mock BAG domain. Proc Natl Acad Sci U S A *112*, 106-111.

Molinari, A. M., Bontempo, P., Schiavone, E. M., Tortora, V., Verdicchio, M. A., Napolitano, M., Nola, E., Moncharmont, B., Medici, N., Nigro, V.*, et al.* (2000). Estradiol induces functional inactivation of p53 by intracellular redistribution. Cancer Res *60*, 2594-2597.

Moll, U. M., Riou, G., and Levine, A. J. (1992). Two distinct mechanisms alter p53 in breast cancer: mutation and nuclear exclusion. Proc Natl Acad Sci U S A *89*, 7262-7266.

Montemurro, F., Aglietta, M., and Del Mastro, L. (2009). Aromatase inhibitors as adjuvant therapy for breast cancer. J Clin Oncol *27*, 2566-2567.

Moon, S., and Lee, B. H. (2018). Chemically Induced Cellular Proteolysis: An Emerging Therapeutic Strategy for Undruggable Targets. Mol Cells *41*, 933-942.

Moriyama, T., Littell, R. D., Debernardo, R., Oliva, E., Lynch, M. P., Rueda, B. R., and Duska, L. R. (2004). BAG-1 expression in normal and neoplastic endometrium. Gynecol Oncol *94*, 289-295.

Nagata, S. (1996). Fas-mediated apoptosis. Adv Exp Med Biol *406*, 119-124.

Nakano, K., and Vousden, K. H. (2001). PUMA, a novel proapoptotic gene, is induced by p53. Mol Cell *7*, 683-694.

Narashimamurthy, J., Rao, A. R., and Sastry, G. N. (2004). Aromatase inhibitors: a new paradigm in breast cancer treatment. Curr Med Chem Anticancer Agents *4*, 523-534.

Nathan, M. R., and Schmid, P. (2017). A Review of Fulvestrant in Breast Cancer. Oncol Ther *5*, 17-29.

Nawata, H., Bronzert, D., and Lippman, M. E. (1981). Isolation and characterization of a tamoxifen-resistant cell line derived from MCF-7 human breast cancer cells. J Biol Chem *256*, 5016-5021.

Nayar, U., Cohen, O., Kapstad, C., Cuoco, M. S., Waks, A. G., Wander, S. A., Painter, C., Freeman, S., Persky, N. S., Marini, L.*, et al.* (2019). Acquired HER2 mutations in ER(+) metastatic breast cancer confer resistance to estrogen receptor-directed therapies. Nat Genet *51*, 207-216.

Nelson, L. R., and Bulun, S. E. (2001). Estrogen production and action. J Am Acad Dermatol *45*, S116-124.

Nguyen, P., Hess, K., Smulders, L., Le, D., Briseno, C., Chavez, C. M., and Nikolaidis, N. (2020). Origin and Evolution of the Human Bcl2-Associated Athanogene-1 (BAG-1). Int J Mol Sci *21*. doi:10.3390/ijms21249701.

Ni, E., Zhao, L., Yao, N., Zhu, X., Cao, H., Sun, S., and Zhu, W. (2019). The PXXP domain is critical for the protective effect of BAG3 in cardiomyocytes. Clin Exp Pharmacol Physiol *46*, 435-443.

Nigam, N., Grover, A., Goyal, S., Katiyar, S. P., Bhargava, P., Wang, P. C., Sundar, D., Kaul, S. C., and Wadhwa, R. (2015). Targeting Mortalin by Embelin Causes Activation of Tumor Suppressor p53 and Deactivation of Metastatic Signaling in Human Breast Cancer Cells. PLoS One *10*, e0138192.doi:10.1371/journal.pone.0138192.

Nilsson, S., and Koehler, K. F. (2005). Oestrogen receptors and selective oestrogen receptor modulators: molecular and cellular pharmacology. Basic Clin Pharmacol Toxicol *96*, 15-25.

Nourashrafeddin, S., Aarabi, M., Modarressi, M. H., Rahmati, M., and Nouri, M. (2015). The Evaluation of WBP2NL-Related Genes Expression in Breast Cancer. Pathol Oncol Res *21*, 293-300.

Nunez, A. M., Jakowlev, S., Briand, J. P., Gaire, M., Krust, A., Rio, M. C., and Chambon, P. (1987). Characterization of the estrogen-induced pS2 protein secreted by the human breast cancer cell line MCF-7. Endocrinology *121*, 1759-1765.

O'Lone, R., Frith, M. C., Karlsson, E. K., and Hansen, U. (2004). Genomic targets of nuclear estrogen receptors. Mol Endocrinol *18*, 1859-1875.

O'Malley, T., Alling, T., Early, J. V., Wescott, H. A., Kumar, A., Moraski, G. C., Miller, M. J., Masquelin, T., Hipskind, P. A., and Parish, T. (2018). Imidazopyridine Compounds Inhibit Mycobacterial Growth by Depleting ATP Levels. Antimicrob Agents Chemother *62*.

Olivier, M., Hollstein, M., and Hainaut, P. (2010). TP53 mutations in human cancers: origins, consequences, and clinical use. Cold Spring Harb Perspect Biol *2*, a001008.doi:10.1101/cshperspect.a001008.

Olivier, M., Langerød, A., Carrieri, P., Bergh, J., Klaar, S., Eyfjord, J., Theillet, C., Rodriguez, C., Lidereau, R., Bièche, I.*, et al.* (2006). The clinical value of somatic TP53 gene mutations in 1,794 patients with breast cancer. Clin Cancer Res *12*, 1157-1167.

Osborne, C. K., Bardou, V., Hopp, T. A., Chamness, G. C., Hilsenbeck, S. G., Fuqua, S. A., Wong, J., Allred, D. C., Clark, G. M., and Schiff, R. (2003). Role of the estrogen receptor coactivator AIB1 (SRC-3) and HER-2/neu in tamoxifen resistance in breast cancer. J Natl Cancer Inst *95*, 353-361.

Paeshuyse, J., Chezal, J. M., Froeyen, M., Leyssen, P., Dutartre, H., Vrancken, R., Canard, B., Letellier, C., Li, T., Mittendorfer, H.*, et al.* (2007). The imidazopyrrolopyridine analogue AG110 is

a novel, highly selective inhibitor of pestiviruses that targets the viral RNA-dependent RNA polymerase at a hot spot for inhibition of viral replication. J Virol *81*, 11046-11053.

Pakdel, F., Le Goff, P., and Katzenellenbogen, B. S. (1993). An assessment of the role of domain F and PEST sequences in estrogen receptor half-life and bioactivity. J Steroid Biochem Mol Biol *46*, 663-672.

Papadakis, E. S., Reeves, T., Robson, N. H., Maishman, T., Packham, G., and Cutress, R. I. (2017). BAG-1 as a biomarker in early breast cancer prognosis: a systematic review with meta-analyses. Br J Cancer *116*, 1585-1594.

Patel, H. K., and Bihani, T. (2018). Selective estrogen receptor modulators (SERMs) and selective estrogen receptor degraders (SERDs) in cancer treatment. Pharmacol Ther *186*, 1-24.

Pearson, A., Proszek, P., Pascual, J., Fribbens, C., Shamsher, M. K., Kingston, B., O'Leary, B., Herrera-Abreu, M. T., Cutts, R. J., Garcia-Murillas, I.*, et al.* (2020). Inactivating NF1 Mutations Are Enriched in Advanced Breast Cancer and Contribute to Endocrine Therapy Resistance. Clin Cancer Res *26*, 608-622.

Penault-Llorca, F., and Radosevic-Robin, N. (2017). Ki67 assessment in breast cancer: an update. Pathology *49*, 166-171.

Perey, L., Paridaens, R., Hawle, H., Zaman, K., Nolé, F., Wildiers, H., Fiche, M., Dietrich, D., Clément, P., Köberle, D.*, et al.* (2007). Clinical benefit of fulvestrant in postmenopausal women with advanced breast cancer and primary or acquired resistance to aromatase inhibitors: final results of phase II Swiss Group for Clinical Cancer Research Trial (SAKK 21/00). Ann Oncol *18*, 64-69.

Perou, C. M., Sørlie, T., Eisen, M. B., van de Rijn, M., Jeffrey, S. S., Rees, C. A., Pollack, J. R., Ross, D. T., Johnsen, H., Akslen, L. A.*, et al.* (2000). Molecular portraits of human breast tumours. Nature *406*, 747-752.

Pettersson, M., and Crews, C. M. (2019). PROteolysis TArgeting Chimeras (PROTACs) - Past, present and future. Drug Discov Today Technol *31*, 15-27.

Pham, M. Q., Tran, T. H. V., Pham, Q. L., and Gairin, J. E. (2019). In silico analysis of the binding properties of solasonine to mortalin and p53, and in vitro pharmacological studies of its apoptotic and cytotoxic effects on human HepG2 and Hep3b hepatocellular carcinoma cells. Fundam Clin Pharmacol *33*, 385-396.

Pratt, W. B., and Toft, D. O. (1997). Steroid receptor interactions with heat shock protein and immunophilin chaperones. Endocr Rev *18*, 306-360.

Pusztai, L., Krishnamurti, S., Perez Cardona, J., Sneige, N., Esteva, F. J., Volchenok, M., Breitenfelder, P., Kau, S. W., Takayama, S., Krajewski, S.*, et al.* (2004). Expression of BAG-1 and BcL-2 proteins before and after neoadjuvant chemotherapy of locally advanced breast cancer. Cancer Invest *22*, 248-256.

Rasha, F., Sharma, M., and Pruitt, K. (2021). Mechanisms of endocrine therapy resistance in breast cancer. Mol Cell Endocrinol *532*, 111322.doi:10.1016/j.mce.2021.111322.

Ravdin, P. M., Green, S., Dorr, T. M., McGuire, W. L., Fabian, C., Pugh, R. P., Carter, R. D., Rivkin, S. E., Borst, J. R., Belt, R. J., and et al. (1992). Prognostic significance of progesterone receptor levels in estrogen receptor-positive patients with metastatic breast cancer treated with tamoxifen: results of a prospective Southwest Oncology Group study. J Clin Oncol *10*, 1284-1291.

Ravdin, P. M., Tandon, A. K., Allred, D. C., Clark, G. M., Fuqua, S. A., Hilsenbeck, S. H., Chamness, G. C., and Osborne, C. K. (1994). Cathepsin D by western blotting and immunohistochemistry: failure to confirm correlations with prognosis in node-negative breast cancer. J Clin Oncol *12*, 467-474.

Razavi, P., Chang, M. T., Xu, G., Bandlamudi, C., Ross, D. S., Vasan, N., Cai, Y., Bielski, C. M., Donoghue, M. T. A., Jonsson, P.*, et al.* (2018). The Genomic Landscape of Endocrine-Resistant Advanced Breast Cancers. Cancer Cell *34*, 427-438.e426.

Recanatini, M., and Cavalli, A. (1998). Comparative molecular field analysis of non-steroidal aromatase inhibitors: an extended model for two different structural classes. Bioorg Med Chem *6*, 377-388.

Reid, G., Hübner, M. R., Métivier, R., Brand, H., Denger, S., Manu, D., Beaudouin, J., Ellenberg, J., and Gannon, F. (2003). Cyclic, proteasome-mediated turnover of unliganded and liganded ERalpha on responsive promoters is an integral feature of estrogen signaling. Mol Cell *11*, 695-707.

Ringnér, M. (2008). What is principal component analysis? Nat Biotechnol *26*, 303-304.

Roberts, C. G., Millar, E. K., O'Toole, S. A., McNeil, C. M., Lehrbach, G. M., Pinese, M., Tobelmann, P., McCloy, R. A., Musgrove, E. A., Sutherland, R. L., and Butt, A. J. (2011). Identification of PUMA as an estrogen target gene that mediates the apoptotic response to tamoxifen in human breast cancer cells and predicts patient outcome and tamoxifen responsiveness in breast cancer. Oncogene *30*, 3186-3197.

Robertson, J. F., Lindemann, J. P., Llombart-Cussac, A., Rolski, J., Feltl, D., Dewar, J., Emerson, L., Dean, A., and Ellis, M. J. (2012). Fulvestrant 500 mg versus anastrozole 1 mg for the first-line treatment of advanced breast cancer: follow-up analysis from the randomized 'FIRST' study. Breast Cancer Res Treat *136*, 503-511.

Romano, A., Adriaens, M., Kuenen, S., Delvoux, B., Dunselman, G., Evelo, C., and Groothuis, P. (2010). Identification of novel ER-alpha target genes in breast cancer cells: gene- and cell-selective co-regulator recruitment at target promoters determines the response to 17beta-estradiol and tamoxifen. Mol Cell Endocrinol *314*, 90-100.

Rorke, S., Murphy, S., Khalifa, M., Chernenko, G., and Tang, S. C. (2001). Prognostic significance of BAG-1 expression in nonsmall cell lung cancer. Int J Cancer *95*, 317-322.

Ryan, J. J., Prochownik, E., Gottlieb, C. A., Apel, I. J., Merino, R., Nuñez, G., and Clarke, M. F. (1994). c-myc and bcl-2 modulate p53 function by altering p53 subcellular trafficking during the cell cycle. Proc Natl Acad Sci U S A *91*, 5878-5882.

Saito, Y., Matsuda, S., Ohnishi, N., Endo, K., Ashitani, S., Ohishi, M., Ueno, A., Tomita, M., Ueda, K., Soga, T., and Muthuswamy, S. K. (2022). Polarity protein SCRIB interacts with SLC3A2 to

regulate proliferation and tamoxifen resistance in ER+ breast cancer. Commun Biol *5*, 403.doi:10.38/s42003-022-03363-3.

Saji, S., Hirose, M., and Toi, M. (2005). Clinical significance of estrogen receptor beta in breast cancer. Cancer Chemother Pharmacol *56 Suppl 1*, 21-26.

Samavat, H., and Kurzer, M. S. (2015). Estrogen metabolism and breast cancer. Cancer Lett *356*, 231-243.

Sane, S., Abdullah, A., Boudreau, D. A., Autenried, R. K., Gupta, B. K., Wang, X., Wang, H., Schlenker, E. H., Zhang, D., Telleria, C.*, et al.* (2014). Ubiquitin-like (UBX)-domain-containing protein, UBXN2A, promotes cell death by interfering with the p53-Mortalin interactions in colon cancer cells. Cell Death Dis *5*, e1118.doi:10.1038/cddis.2014.100.

Sari, A. N., Elwakeel, A., Dhanjal, J. K., Kumar, V., Sundar, D., Kaul, S. C., and Wadhwa, R. (2021). Identification and Characterization of Mortaparib(Plus)-A Novel Triazole Derivative That Targets Mortalin-p53 Interaction and Inhibits Cancer-Cell Proliferation by Wild-Type p53-Dependent and -Independent Mechanisms. Cancers (Basel) *13*.doi:10.3390/cancers13040835.

Sauerbrei, W., and Haeussler, T. (2018). Comment on 'BAG-1 as a biomarker in early breast cancer prognosis: a systematic review with meta-analyses'. Br J Cancer *118*, 1152-1153.

Schiff, R., Massarweh, S. A., Shou, J., Bharwani, L., Mohsin, S. K., and Osborne, C. K. (2004). Cross-talk between estrogen receptor and growth factor pathways as a molecular target for overcoming endocrine resistance. Clin Cancer Res *10*, 331s-336s.

Shaaban, A. M., O'Neill, P. A., Davies, M. P., Sibson, R., West, C. R., Smith, P. H., and Foster, C. S. (2003). Declining estrogen receptor-beta expression defines malignant progression of human breast neoplasia. Am J Surg Pathol *27*, 1502-1512.

Shatkina, L., Mink, S., Rogatsch, H., Klocker, H., Langer, G., Nestl, A., and Cato, A. C. (2003). The cochaperone Bag-1L enhances androgen receptor action via interaction with the NH2-terminal region of the receptor. Mol Cell Biol *23*, 7189-7197.

Shindoh, M., Adachi, M., Higashino, F., Yasuda, M., Hida, K., Nishioka, T., Ono, M., Takayama, S., Reed, J. C., Imai, K.*, et al.* (2000). BAG-1 expression correlates highly with the malignant potential in early lesions (T1 and T2) of oral squamous cell carcinoma. Oral Oncol *36*, 444-449.

Sondermann, H., Scheufler, C., Schneider, C., Hohfeld, J., Hartl, F. U., and Moarefi, I. (2001). Structure of a Bag/Hsc70 complex: convergent functional evolution of Hsp70 nucleotide exchange factors. Science *291*, 1553-1557.

Soule, H. D., Vazguez, J., Long, A., Albert, S., and Brennan, M. (1973). A human cell line from a pleural effusion derived from a breast carcinoma. J Natl Cancer Inst *51*, 1409-1416.

Stein, Y., Rotter, V., and Aloni-Grinstein, R. (2019). Gain-of-Function Mutant p53: All the Roads Lead to Tumorigenesis. Int J Mol Sci *20*.doi:10.3390/ijms20246197.

Takayama, S., Krajewski, S., Krajewska, M., Kitada, S., Zapata, J. M., Kochel, K., Knee, D., Scudiero, D., Tudor, G., Miller, G. J.*, et al.* (1998). Expression and location of Hsp70/Hsc-binding anti-

apoptotic protein BAG-1 and its variants in normal tissues and tumor cell lines. Cancer Res *58*, 3116-3131.

Takayama, S., and Reed, J. C. (2001). Molecular chaperone targeting and regulation by BAG family proteins. Nat Cell Biol *3*, E237-241.

Takayama, S., Sato, T., Krajewski, S., Kochel, K., Irie, S., Millan, J. A., and Reed, J. C. (1995). Cloning and functional analysis of BAG-1: a novel Bcl-2-binding protein with anti-cell death activity. Cell *80*, 279-284.

Takayama, S., Xie, Z., and Reed, J. C. (1999). An evolutionarily conserved family of Hsp70/Hsc70 molecular chaperone regulators. J Biol Chem *274*, 781-786.

Tang, D., Chen, X., Kang, R., and Kroemer, G. (2021). Ferroptosis: molecular mechanisms and health implications. Cell Res *31*, 107-125.

Tang, S. C. (2002). BAG-1, an anti-apoptotic tumour marker. IUBMB Life *53*, 99-105.

Tang, S. C., Beck, J., Murphy, S., Chernenko, G., Robb, D., Watson, P., and Khalifa, M. (2004). BAG-1 expression correlates with Bcl-2, p53, differentiation, estrogen and progesterone receptors in invasive breast carcinoma. Breast Cancer Res Treat *84*, 203-213.

Tang, S. C., Shehata, N., Chernenko, G., Khalifa, M., and Wang, X. (1999). Expression of BAG-1 in invasive breast carcinomas. J Clin Oncol *17*, 1710-1719.

Tateishi, Y., Kawabe, Y., Chiba, T., Murata, S., Ichikawa, K., Murayama, A., Tanaka, K., Baba, T., Kato, S., and Yanagisawa, J. (2004). Ligand-dependent switching of ubiquitin-proteasome pathways for estrogen receptor. Embo j *23*, 4813-4823.

Thress, K., Henzel, W., Shillinglaw, W., and Kornbluth, S. (1998). Scythe: a novel reaper-binding apoptotic regulator. Embo j *17*, 6135-6143.

Thress, K., Song, J., Morimoto, R. I., and Kornbluth, S. (2001). Reversible inhibition of Hsp70 chaperone function by Scythe and Reaper. Embo j *20*, 1033-1041.

Tonetti, D. A., Rubenstein, R., DeLeon, M., Zhao, H., Pappas, S. G., Bentrem, D. J., Chen, B., Constantinou, A., and Craig Jordan, V. (2003). Stable transfection of an estrogen receptor beta cDNA isoform into MDA-MB-231 breast cancer cells. J Steroid Biochem Mol Biol *87*, 47-55.

Torre, L. A., Siegel, R. L., Ward, E. M., and Jemal, A. (2016). Global Cancer Incidence and Mortality Rates and Trends--An Update. Cancer Epidemiol Biomarkers Prev *25*, 16-27.

Torres-Arzayus, M. I., Zhao, J., Bronson, R., and Brown, M. (2010). Estrogen-dependent and estrogen-independent mechanisms contribute to AIB1-mediated tumor formation. Cancer Res *70*, 4102-4111.

Townsend, P. A., Dublin, E., Hart, I. R., Kao, R. H., Hanby, A. M., Cutress, R. I., Poulsom, R., Ryder, K., Barnes, D. M., and Packham, G. (2002). BAG-i expression in human breast cancer: interrelationship between BAG-1 RNA, protein, HSC70 expression and clinico-pathological data. J Pathol *197*, 51-59.

Toy, W., Weir, H., Razavi, P., Lawson, M., Goeppert, A. U., Mazzola, A. M., Smith, A., Wilson, J., Morrow, C., Wong, W. L*., et al.* (2017). Activating ESR1 Mutations Differentially Affect the Efficacy of ER Antagonists. Cancer Discov *7*, 277-287.

Wadhwa, R., Takano, S., Robert, M., Yoshida, A., Nomura, H., Reddel, R. R., Mitsui, Y., and Kaul, S. C. (1998). Inactivation of tumor suppressor p53 by mot-2, a hsp70 family member. J Biol Chem *273*, 29586-29591.

Wadhwa, R., Yaguchi, T., Hasan, M. K., Mitsui, Y., Reddel, R. R., and Kaul, S. C. (2002). Hsp70 family member, mot-2/mthsp70/GRP75, binds to the cytoplasmic sequestration domain of the p53 protein. Exp Cell Res *274*, 246-253.

Wakeling, A. E. (1989). The potential for a novel pure anti-oestrogen. Horm Res *32 Suppl 1*, 257-259; discussion 260.

Wakeling, A. E., and Bowler, J. (1992). ICI 182,780, a new antioestrogen with clinical potential. J Steroid Biochem Mol Biol *43*, 173-177.

Wakeling, A. E., Dukes, M., and Bowler, J. (1991). A potent specific pure antiestrogen with clinical potential. Cancer Res *51*, 3867-3873.

Walker, C., Böttger, S., and Low, B. (2006). Mortalin-based cytoplasmic sequestration of p53 in a nonmammalian cancer model. Am J Pathol *168*, 1526-1530.

Wang, H. G., Takayama, S., Rapp, U. R., and Reed, J. C. (1996). Bcl-2 interacting protein, BAG-1, binds to and activates the kinase Raf-1. Proc Natl Acad Sci U S A *93*, 7063-7068.

Wang, L., Zeng, Y., Liu, Y., Hu, X., Li, S., Wang, Y., Li, L., Lei, Z., and Zhang, Z. (2014). Fucoxanthin induces growth arrest and apoptosis in human bladder cancer T24 cells by up-regulation of p21 and down-regulation of mortalin. Acta Biochim Biophys Sin (Shanghai) *46*, 877-884.

Wijayaratne, A. L., and McDonnell, D. P. (2001). The human estrogen receptor-alpha is a ubiquitinated protein whose stability is affected differentially by agonists, antagonists, and selective estrogen receptor modulators. J Biol Chem *276*, 35684-35692.

Wu, B., Peng, Y., Eggert, J., and Alexov, E. (2019). Novel Genetic Markers for Early Detection of Elevated Breast Cancer Risk in Women. Int J Mol Sci *20*. doi:10.3390/ijms20194828.

Xie, C., Powell, C., Yao, M., Wu, J., and Dong, Q. (2014). Ubiquitin-conjugating enzyme E2C: a potential cancer biomarker. Int J Biochem Cell Biol *47*, 113-117.

Yan, W., and Chen, X. (2006). GPX2, a direct target of p63, inhibits oxidative stress-induced apoptosis in a p53-dependent manner. J Biol Chem *281*, 7856-7862.

Yan, Z., DeGregori, J., Shohet, R., Leone, G., Stillman, B., Nevins, J. R., and Williams, R. S. (1998). Cdc6 is regulated by E2F and is essential for DNA replication in mammalian cells. Proc Natl Acad Sci U S A *95*, 3603-3608.

Yang, X., Chernenko, G., Hao, Y., Ding, Z., Pater, M. M., Pater, A., and Tang, S. C. (1998). Human BAG-1/RAP46 protein is generated as four isoforms by alternative translation initiation and overexpressed in cancer cells. Oncogene *17*, 981-989.

Yang, X., Hao, Y., Ferenczy, A., Tang, S. C., and Pater, A. (1999). Overexpression of anti-apoptotic gene BAG-1 in human cervical cancer. Exp Cell Res *247*, 200-207.

Yao, H., Li, P., Venters, B. J., Zheng, S., Thompson, P. R., Pugh, B. F., and Wang, Y. (2008). Histone Arg modifications and p53 regulate the expression of OKL38, a mediator of apoptosis. J Biol Chem *283*, 20060-20068.

Yaşar, P., Ayaz, G., User, S. D., Güpür, G., and Muyan, M. (2017). Molecular mechanism of estrogen-estrogen receptor signaling. Reprod Med Biol *16*, 4-20.

Yoon, C. I., Ahn, S. G., Cha, Y. J., Kim, D., Bae, S. J., Lee, J. H., Ooshima, A., Yang, K. M., Park, S. H., Kim, S. J., and Jeong, J. (2021). Metastasis Risk Assessment Using BAG2 Expression by Cancer-Associated Fibroblast and Tumor Cells in Patients with Breast Cancer. Cancers (Basel) *13*.doi:10.3390/cancers13184654.

Yu, C. L., Driggers, P., Barrera-Hernandez, G., Nunez, S. B., Segars, J. H., and Cheng, S. (1997). The tumor suppressor p53 is a negative regulator of estrogen receptor signaling pathways. Biochem Biophys Res Commun *239*, 617-620.

Yu, S., Kim, T., Yoo, K. H., and Kang, K. (2017). The T47D cell line is an ideal experimental model to elucidate the progesterone-specific effects of a luminal A subtype of breast cancer. Biochem Biophys Res Commun *486*, 752-758.

Yue, X., Zhao, Y., Huang, G., Li, J., Zhu, J., Feng, Z., and Hu, W. (2016). A novel mutant p53 binding partner BAG5 stabilizes mutant p53 and promotes mutant p53 GOFs in tumorigenesis. Cell Discov *2*, 16039. doi:10.1038/celldisc.2016.39.

Yun, C. O., Bhargava, P., Na, Y., Lee, J. S., Ryu, J., Kaul, S. C., and Wadhwa, R. (2017). Relevance of mortalin to cancer cell stemness and cancer therapy. Sci Rep *7*, 42016. doi:10.1038/srep42016.

Zhao, Q., Howard, E. W., Parris, A. B., Ma, Z., Xing, Y., and Yang, X. (2019). Bisphenol AF promotes estrogen receptor-positive breast cancer cell proliferation through amphiregulin-mediated crosstalk with receptor tyrosine kinase signaling. PLoS One *14*, e0216469. doi:10.1371/journal.pone.0216469.

Zimmermann, M., and Meyer, N. (2011). Annexin V/7-AAD staining in keratinocytes. Methods Mol Biol *740*, 57-63.